UNIVERSIDAD DE MÁLAGA

**FACULTAD DE CIENCIAS**

**DEPARTAMENTO DE INGENIERÍA QUÍMICA**


**PhD Thesis**


**NEEDLELESS ELECTROSPUN POLYACRYLONITRILE NANOFIBER MATS – PREPARATION, STABILIZATION, CARBONIZATION AND COMPOSITE FORMATION**

Author: Lilia Sabantina

Director: Prof. Dr. D. Tomás Cordero Alcántara

Prof. Dr. D. José Rodríguez Mirasol

Programa de Doctorado: Química y Tecnologías Químicas.

Materiales y Nanotecnología


Málaga, November 2018

AUTOR: Lilia Sabantina

http://orcid.org/0000-0002-1822-7954

D. TOMÁS CORDERO ALCÁNTARA, Catedrático de Ingeniería Química de la Universidad de Málaga,

D. JOSÉ RODRÍGUEZ MIRASOL, Catedrático de Ingeniería Química de la Universidad de Málaga,

CERTIFICAN: Que el trabajo de investigación recogido en la presente Memoria ha sido realizado bajo su dirección en el Departamento de Ingeniería Química de la Universidad de Málaga por Dª Lilia Sabantina, y reúne, a su juicio, contenido científico suficiente y las condiciones necesarias para ser presentado y defendido ante el Tribunal correspondiente para optar al Grado de Doctor en la Universidad de Málaga.

Málaga, Noviembre de 2018

Fdo.: Dr. D. Tomás Cordero Alcántara

Fdo.: Dr. D. José Rodríguez Mirasol

UNIVERSIDAD
DE MÁLAGA

D. TOMÁS CORDERO ALCÁNTARA, Catedrático de Ingeniería Química de la Universidad de Málaga,

D. JOSÉ RODRÍGUEZ MIRASOL, Catedrático de Ingeniería Química de la Universidad de Málaga,

CERTIFICAN: Que el trabajo de investigación recogido en la presente Memoria ha sido realizado bajo su dirección y que reúne los requisitos necesarios para ser presentado como Tesis Doctoral por compendio de publicaciones. Así mismo informamos de que las publicaciones que avalan está Tesis Doctoral no han sido utilizadas en Tesis anteriores.

Málaga, Noviembre de 2018

Fdo.: Dr. D. Tomás Cordero Alcántara

Fdo.: Dr. D. José Rodríguez Mirasol

# TABLE OF CONTENTS

UNIVERSIDAD
DE MÁLAGA

## LIST OF FIGURES

# LIST OF TABLES

## LIST OF ABBREVIATIONS

| | |
|---|---|
| AA | Acetic acid |
| AV | Aloe vera |
| CA | Cellulose acetate |
| CHO-DP12 | Chinese hamster ovary strain DP12 |
| CLSM | Confocal Laser Scanning Microscope |
| CNF | Carbon nanofibers |
| CNT | Carbon nanotubes |
| CS | Chitosan |
| $\Delta a*$ | Color value – difference in red/green axis |
| $\Delta b*$ | Color value – difference in yellow/blue axis |
| DCM | Dichloromethane |
| $\Delta E*$ | Color value – total difference in color value |
| $\Delta L*$ | Color value – difference in lightness/darkness value |
| DMAA | Dimethylacetamide |
| DMAc | Dimethylacetamide |
| DMF | Dimethylformamide |
| DMSO | Dimethyl sulfoxide |
| DSC | Differential Scanning Calorimetry |
| DSSC | Dye-Sensitized Solar Cells |
| EDTA | Ethylenediaminetetraacetic acid |
| EVOH | Poly(ethylene-co-vinyl alcohol) |
| FTIR | Fourier Transform Infrared Spectroscopy |

| | |
|---|---|
| HFIP | 1,1,1,3,3,3-Hexa Fluoro-2-Propanol |
| HOBt | Hydroxybenzotriazole |
| ISO | International Organization for Standardization |
| m-CNC | Magnetic nanocellulose |
| MgO | Magnesium oxide |
| MWCNT | Multi-Walled Carbon Nanotubes |
| PAN | Polyacrylonitrile |
| PBS | Polybutylene succinate |
| PC | Polycarbonate |
| PCL | Polycaprolactone |
| PEG | Poly(ethylenglycol) |
| PEO | Polyethylene oxide |
| PMMA | Polymethacrylate |
| PP | Polypropylene |
| PU | Polyurethane |
| PVA | Polyvinyl alcohole |
| SEM | Scanning Electron Microscope |
| SF | Silk fibroin |
| STP | Standard Temperature and Pressure |
| TFA | Trifluoroacetic acid |
| TFE | 2,2,2-Trifluoroethanol |
| TGA | Thermogravimetric Analysis |
| $TiNb_2O_7$ | Titanium Niobate |
| TPP | Tripolyphosphate |

XPS                              X-ray photoelectron spectroscopy

XRD                              X-ray diffraction

ZN                               Zein

ZnO                              Zinc oxide

# ACKNOWLEDGEMENTS

## SUMMARY

This dissertation deals with NEEDLELESS ELECTROSPUN POLYACRYLONITRILE NANOFIBER MATS - PREPARATION, STABILIZATION, CARBONIZATION AND COMPOSITE FORMATION and consists of a total of nine thematic chapters.

At the beginning of the work, the first chapter gives an overview of the research as well as short descriptions of important research results. In addition, theoretical frameworks of the work are presented and the state of the art is examined, with a focus on electrospinning technology and the influences of parameters in the electrospinning process. Subsequently, the oxidation and stabilization processes of nanofiber mats are presented.

The second chapter focuses on the methodology of the investigations and describes materials, devices and research methods used in this work. This chapter begins with an overview of the materials used. Then, the structure and principle of the needleless electrospinning machine is vividly illustrated. In addition, special attention is paid to the sample preparation and also to the fixing methods of nanofiber mats during the stabilization process. Several attempts to fix nanofibers during the stabilization process are illustrated and explained in more detail. In addition, experimental framework conditions for stabilization and carbonization parameters are presented and clearly described. This chapter concludes with various materials characterization methods that will be used during the research work in this dissertation.

The research results can be found in chapters three to eight, where they are presented as a compendium of publications. In total, these chapters are based on six publications that have already been published, accepted or submitted. The publications have been structured thematically, starting with basics such as the investigation of optimal electrospinning parameters for nanofiber mats. Subsequently, more complex topics such as the formation of composites such as the mixing of PAN with gelatin and experimental investigations of metal-carbon composites are carried out.

The following six publications, which have already been published, accepted or submitted, were used in this research work and form the core of this work.

For a better overview, the publications have been arranged in the same order as in chapters three to eight.

INVESTIGATION OF NEEDLELESS ELECTROSPUN PAN NANOFIBER MATS, L. Sabantina, J. Rodríguez-Mirasol, T. Cordero, K. Finsterbusch, A. Ehrmann, AIP Conference Proceedings 1952, 020085 (2018), doi.org/10.1063/1.5032047

WATER VAPOR PERMEABILITY THROUGH PAN NANOFIBER MAT WITH VARYING MEMBRANE-LIKE AREAS, L. Sabantina, L. Hes, J. Rodríguez-Mirasol, T. Cordero, A. Ehrmann, accepted for publication in No. 1/2019 of FIBERS & TEXTILES in Eastern Europe

INVESTIGATION OF STABILIZATION PARAMETERS FOR PAN NANOFIBER MATS NEEDLELESS-ELECTROSPUN FROM DMSO, L. Sabantina, M. Klöcker, M. Wortmann, J. Rodríguez-Mirasol, T. Cordero, K. Finsterbusch, A. Ehrmann, (submitted)

DEVELOPMENT OF CARBON NANOFIBERS FOR INTEGRATION IN 3D PRINTING FILAMENTS, L. Sabantina, K. Finsterbusch, A. Ehrmann, J. Rodríguez-Mirasol, T. Cordero, Aachen-Dresden-Denkendorf International Textile Conference, Stuttgart, November 30-31, 2017

STABILIZATION OF ELECTROSPUN PAN/GELATIN NANOFIBER MATS FOR CARBONIZATION, L. Sabantina, D. Wehlage, M. Klöcker, A. Mamun, T. Grothe, J. Rodríguez-Mirasol, T. Cordero, K. Finsterbusch, A. Ehrmann, Special Issue "Functional Nanomaterials for Energy Applications", Journal of Nanomaterials, Volume 2018, Article ID 6131085, 12 pages, doi.org/10.1155/2018/6131085

FIXING PAN NANOFIBER MATS DURING STABILIZATION FOR CARBONIZATION AND CREATING NOVEL METAL/CARBON COMPOSITES, L. Sabantina, M. Ángel Rodríguez-Cano, M. Klöcker, F. J. García-Mateos, J. J. Ternero-Hidalgo, A. Mamun, F. Beermann, M. Schwakenberg, A.-L. Voigt, J. Rodríguez Mirasol, T. Cordero, A. Ehrmann, Polymers 10, 735 (2018), doi.org/10.3390/polym1007073

Finally, the general conclusions are presented in chapter nine and provides some insights into the remaining and future work suggested as a research result of this dissertation.

CHAPTER 1


INTRODUCTION

# 1. INTRODUCTION

## 1.1 Overview of the thesis and objectives of the research

This dissertation deals with needleless electrospun polyacrylonitrile (PAN) nanofiber mats, which are electrospun with the non-toxic solvent dimethyl sulfoxide (DMSO). The motivation for this work is based on the fact that to the best of my knowledge neither PAN-nanofibers electrospun with needleless technology nor fibers electrospun from the low-toxic solvent DMSO have been investigated in the literature for optimal stabilization and carbonization properties. Recent studies typically use teratogenic solvents such as DMF (dimethylformamide) or DMAc (dimethylacetamide) as solvents. Studies on the transition between nanofiber mat and membrane with regard to water vapor permeability are also not to be found in the literature and are also investigated in this dissertation.

The blending of PAN with gelatin to produce highly porous nanofibers has been reported several times in the literature, but no attempts have yet been made to stabilize and carbonize these fibers. This dissertation will report on the first tests for stabilization of PAN/gelatin nanofibers, which show the influence of different stabilization temperatures and heating rates on the chemical properties and morphologies of the resulting nanofiber mats.

Furthermore, the problem of fiber fusing during stabilization and thus the prevention of the formation of separated straight carbon nanofibers (CNFs) after carbonization is often neglected or not studied in recent scientific literature. The dimensional change of nanofibers during the stabilization process and during carbonization in fixed and non-fixed nanofiber mats was additionally investigated in this dissertation.

Moreover, this study suggests a novel method to overcome the problem of insufficient fixing of the nanofiber mats during the stabilization process by electrospinning on an aluminum substrate on which the nanofiber mat adheres rigidly and retains its morphology during stabilization and carbonization processes. After the stabilization process, the nanofiber mats can be separated from the aluminum substrates to form pure carbon nanofibers after carbonization, or they can be carbonized together with aluminum substrates. In this case, new types of metal / carbon composites are being developed that can be widely used. The findings should make an important contribution to the field of metal/carbon composites.

This dissertation has the following main objectives:

(1) Investigation of spinning parameters for the needleless electrospinning process of PAN dissolved in DMSO and the resulting nanofiber mats and development of nearly impenetrable thin membranes by modifying the electrospinning parameters.

(2) Investigation of the influence of stabilization temperature and heating rates on the chemical properties as well as the morphologies of the resulting nanofiber mats from PAN and PAN/gelatin blends.

(3) Investigation of dimensional changes of nanofibers during the stabilization process and optimization of the fixing technology to prevent contraction and shrinkage of nanofibers and the resulting increase in diameter and undesirable bending.

To achieve these objectives, the following investigations will be performed:

– Studying the influence of spinning parameters on the resulting nanofiber mats

– Development of different ratios of nanofibers and membrane-like areas by varying electrospinning parameters

– Studying the impact of the mat morphology on the water vapor permeability through PAN nanofibers mats with different membrane-like areas

– Studying the influence of heating rates on the chemical properties as well as the morphologies of the resulting nanofiber mats from PAN and PAN/gelatin blends.

– Development of new fixation methods of nanofiber mats during stabilization

– Optimizing the balance between not burning the nanofibers and allowing a chemical reaction to proceed sufficiently fast to allow complete stabilization, i.e. investigation of optimal parameters during stabilization

– Investigation of PAN/gelatin blends during stabilization and carbonization

– Development of novel metal/carbon composites to overcome the undesired bending and conglutinations of the nanofibers in a mat

The investigations of needleless electrospun PAN nanofiber mats and nano-composites using DMSO as a solvent is of particular interest because it allows for using low-toxic solvents, enabling the use of the resulting nanofiber mats in applications like medicine or food packaging, and producing large-scale nanofiber mats, resulting in possible industrial-scale applications.

## 1.2 Electrospinning process background

Electrospinning has become increasingly important in recent years for many applications because of the large variety of many different polymers which can be processed by this technique. The importance of electrospun nanofibers can be determined by the regularly published numerous articles highlighting their importance in various fields of application with natural or synthetic polymers. Electrospinning is one of the most cost-effective techniques to create fibers on nano- to micrometer scales which is mainly used because of the ease of use and at the same time is susceptible to modifications. The fibers have diameters on the submicrometer scale ($10^{-2}$-10 μm) and have remarkable properties such as a high surface area to volume ratio [1].

## 1.3 Brief history

By electrospinning very thin fibers can be produced in an electric high-voltage field mainly from polymer solutions or polymer melts. The term ―electrospinning‖, derived from ―electrostatic spinning‖, can be traced back to more than 60 years ago.

The basis of the electrospinning process can be found in 1902 when C. F. Cooley and W. J. Morton patented electrospraying [2-3]. Farmhals patented the process of electrospinning in 1934 and re-patented his work in 1940 [4]. In the 1960's Taylor studied the shape formation of polymer droplet produced at the tip of the needle when the electric field is applied. This cone shape is known as a ―Taylor cone‖ [5-6]. In 1952, Vonnegut and Newbauer implemented a simple apparatus for electrical atomization [7]. In 1966, Simons patented an apparatus for the production of nonwovens for the production of ultrathin and very light fiber mats with various patterns using electric spinning [8]. In 1971, Baumgarten manufactured an apparatus for the electrospinning of acrylic fibers [9]. Since the 1980s, and especially in recent years, the electrospinning process has again attracted much attention due to the growing interest in nanotechnology and possibility to produce tailored ultrafine fibers or fibrous structures [10].

## 1.4 Electrospinning process and principles

The electrospinning technique is versatile and easily customizable [11]. With the following variants of technique such as needleless electrospinning, melt electrospinning, co-axial electrospinning, emulsion electrospinning and co-electrospinning a variety of nano-architectures such as core-shell, tube-in-tube, porous, hollow, cross-linked and particle-encapsulated structures can be obtained [12-15].

The typical construction of an electrospinning apparatus is illustrated in Fig. 1.1 Basically, an electrospinning system consists of the following three main components: a high voltage power supply, a spinneret and a grounded collector plate [16-17].. A syringe pump provides a polymer solution to the spinneret.
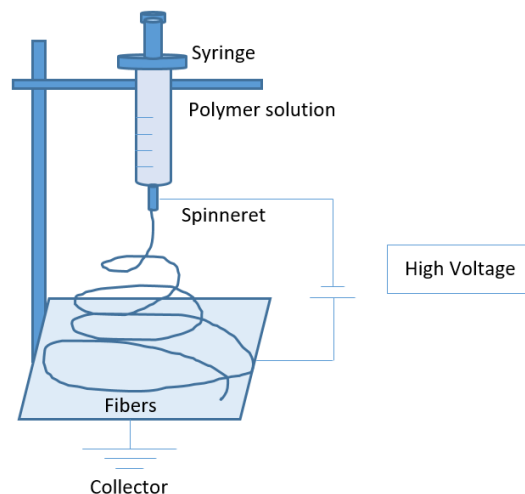


Fig. 1.1 A basic electrospinning apparatus.

The solution-electrospinning process involves the following steps: a polymer is dissolved in a solvent to form a polymer solution. This polymer solution is pressed through a nozzle (in case of needle-electrospinning), the solution is then stretched in a high voltage field and thus forms nanofibers which are deposited on the counter electrode as a random web in most cases [10]. The stretching of fibers takes place in milliseconds from the initial jet [18-19].

When the electric field is applied, a polymer solution of drops is positively charged. The droplet begins to deform and is attracted to the negative polarity counter electrode. The drop takes a spherical shape. When the critical stress of surface tension is exceeded, a polymer jet is produced in the direction of the collecting

electrode, also called "Taylor cone". At the same time, the evaporation of the solvent takes place, the polymer hardens and fine nanofibers are collected on the surface of the counter electrode. In this case, the polymer solution is metered onto an electrode and drawn off and accelerated by an electric field. As a result, very thin nanoscale fibers are formed as a nanofiber mats. With the evaporation of solvent dry or semidry nanofibers can be formed on the collector [1]. Needleless electrospinning process and principle will be explained in more detail in chapter 2.2.

## 1.5 Influence of parameters in electrospinning process

Electrospinning parameters such as charge density, viscosity and surface tension of the polymer solution as well as polymer solution properties, processing parameters and ambient conditions play a major role in the morphology of the fibers and their diameters [20-23]. Several factors affect the morphology of nanofibers. These factors can be classified as solution, processing and ambient parameters. In Table 1.1 the effects of spinning parameters on the fiber morphology are shown.

Table 1.1 Effect of spinning parameters on resulting fiber morphology.

| Parameters | | Effects on fiber morphology | Reference |
|---|---|---|---|
| Solution parameters | | | |
| Viscosity | ↑ | Fiber diameters increase (forming beads – beaded fibers – uniform fibers) | (Jiang et al. 2004, Huang et al. 2001, Zhao et al. 2005, Zhang et al. 2005a), [24-27] |
| Polymer concentration | ↑ | Fiber diameter increase | (Kim et al. 2005, Son et al. 2004, Jun et al. 2003), [28-31] |
| Molecular weight of polymer | ↑ | Reduction in the number of beads and droplet | (Chen and Ma 2004, Demir et al. 2002, Gupta et al. 2005), [32-34] |
| Solution conductivity | ↑ | Fiber diameters decrease | (Koski et al. 2004, Jun et al. 2003, Jiang et al., 2004), [35], [30], [24] |

| Parameter | | Effect | References |
|---|---|---|---|
| Surface tension | ↑ | Beaded fibers and beads increase | (Hohman et al. 2001, Zuo et al. 2005, Zhang et al. 2005, Mit-Uppatham et al. 2004), [36-37],[26], [38] |

| Applied voltage | ↑ | Fiber diameters increase (formation of beads) | (Demir et al. 2002, Jun et al. 2003, Kim et al. 2005, Still and Recum 2004, Deitzel et al. 2001, Haider et al. 2015), [32], [30], [17], [39]. [6] |
| Distance between tip and collector | ↑ | Fiber diameters decrease, (forming beaded morphologies with too short or too large distance, minimum distance required for uniform fibers) | (Ki et al. 2005, Geng et al. 2005, Buchko et al. 1999, Zhao et al. 2005, Megelski et al. 2002, Shamim et al.2012, Matabola and Moutloali 2013, Wang and Kumar 2006, Haider et al. 2015), [40-47], [6] |
| Feed rate/flow rate | ↑ | Increase in fiber diameter with increase of flow rate, increase of pore size (beaded fibers and ribbon-like structures with too high flow rate) | (Sill and Recum 2008, Zuo et al. 2005, Zhang et al. 2005, Haider et al. 2015), [17], [37], [43], [6] |

| | | Ambient parameters | |

| Temperature | ↑ | Fiber diameters decrease | (Reneker and Chun 1996, Mit-Uppatham et al. 2004), [18], [38], |
| Humidity | ↑ | Fiber diameters decrease (forming pores on fiber surfaces), then fiber decrease | (Li and Wang 2013, Mit-Uppatham et al. 2004, Pelipenko et al. 2013, Park and Lee 2010, Haider et al.2015), [48]., [37], [49-50], [6] |

↑ - means "increase in"

The solution parameters include viscosity, polymer concentration, molecular weight of polymer, solution conductivity and surface tension. Amongst the processing parameters, the applied voltage, the distance between tip and collector and the flow

rate play a key role. Humidity and temperature belong to the ambient parameters. Therefore, understanding the electrospinning technique and fabrication of nanofibers is essential for gaining the knowledge about dependency of parameters to obtain tailored nanofibers. Numerous research groups have studied the effects of electrospinning parameters on the morphology of nanofibers [51-52].

## 1.6 Fiber morphology

Electrospun nanofibers can show different morphologies and fiber architectures such as round cross-sections, bead-on-string structures or individual beads. The beads are typical for lower polymer concentration and lower applied voltages [50] and usually undesired. But occasionally these beads are preferable in some applications where they could be helpful to avoid fiber slippage in a resin matrix for improving mechanical strength of composites. Wong et al. (2018) studied the tribological properties of electrospun polymer-based microbeads made of polyvinylpyrrolidone, zinc oxide and multi-walled carbon nanotubes (MWCNTs) with electrospinning technique [53]. Xu et al. (2015) manufactured La-doped ZnO nanofibers with unique bead-like structures that were facilely produced [54]. These La-doped ZnO nanostructures can be a promising material for acetone sensors. Another approach for the beads as a potential drug delivery system was investigated by Supramaniam et al. (2018). They manufactured magnetic nanocellulose alginate hydrogel beads from the assembly of alginate and magnetic nanocellulose (m-CNCs) [55].

Fig. 1.2 depicts electrospun nanofibers with 14 % polyacrylonitrile (PAN) dissolved in dimethylsulfoxide (DMSO) with bead-on-string structure and uniform PAN nanofiber structures electrospun with 16 % PAN. By increasing the polymer solution viscosity, the conglutinations and beads were avoided.

The morphology of nanofibers is also changing during stabilization (Fig. 1.2 c and carbonization process as can be seen in Fig. 1.2 d).
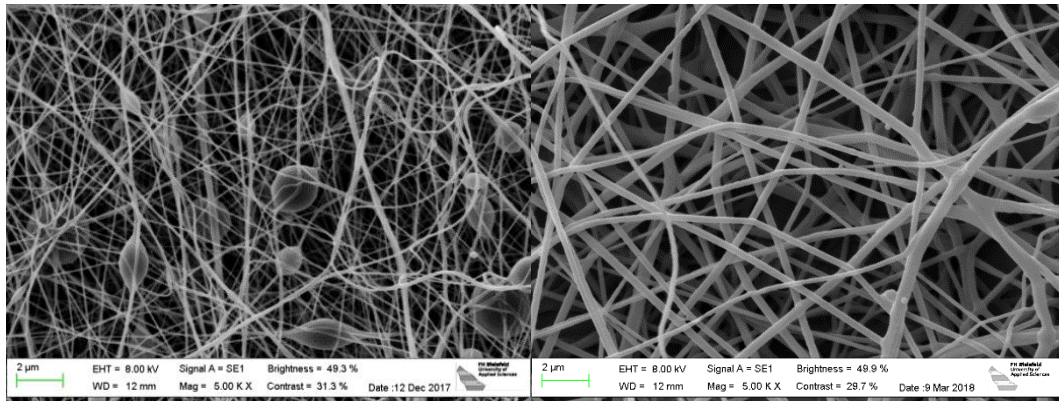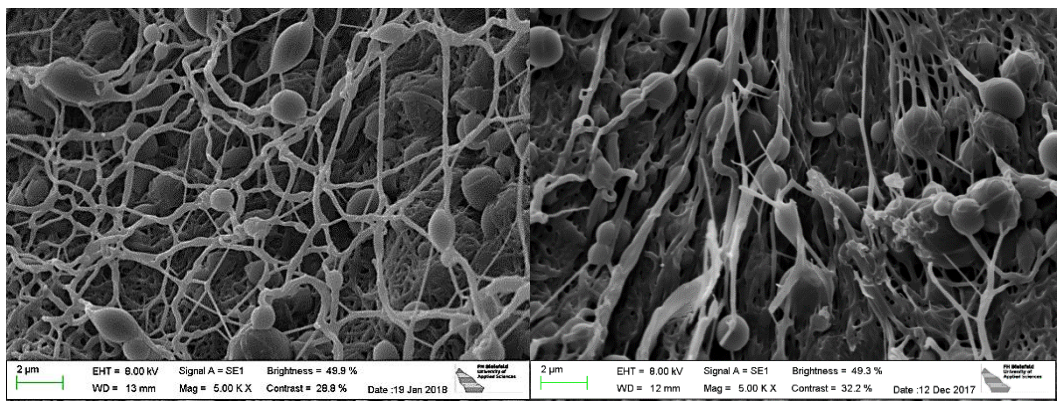
Fig. 1.2 SEM images showing bead-on-string structure morphology of polyacrylonitrile (PAN) nanofibers with 14 % (a) and without beads with 16 % of PAN dissolved in DMSO (b). The morphology of PAN nanofiber mats with 14 % of PAN after stabilization at 280 °C for 1 hour (c) and carbonization at 800 °C for 1 hour at the final temperature. The scale bars indicate 2 μm.

The morphology is also changing during stabilization and carbonization process. As can be seen in Fig. 1.2, the fibers shrink during stabilization and form interconnected structures. After the carbonizations process, the dimensions of PAN nanofibers are reduced even further. Nanofibers can be fixed to prevent the shrinkage of fibers.

The fiber surface morphology could be significantly affected by the following factors: polymer concentration, solution conductivity and viscosity, surface tension as well solvent properties are forming different fiber architectures [31], [48], [1]. Non-conductive solutions cannot be electrospun because without electric charge to the droplet surface no fibers can be created. Moreover, if the solution is highly conductive the extra charge cannot be affected to the droplet surface because of the small stretching force. Therefore, the solution for electrospinning should ideally be in the semi-conducting range. The polymer concentration plays a key role because it affects other properties such as surface tension, viscosity and conductivity [1].

Depending on the solvent used, the distance between electrodes or in case of high humidity during the needleless electrospinning process, sometimes nanofibers accumulate not only towards the counter electrode as in the normal case, but parts of the nanofibers strive in opposite direction and form artefacts with different shapes, as can be seen in Fig. 1.3.



Fig. 1.3 Examples of different artefacts occurring by needleless electrospinning process during this PhD project.

Usually by needleless electrospinning the nanofibers are collected regularly below the counter electrode on a polypropylene (PP) substrate, but in this case the artefacts are growing between high voltage electrode and substrate.

Moreover, the fibers collected in the middle of substrate are wet. This is one possible effect leading to nano-membrane formation with just a few fiber areas included. On the border of the spinning area, the nanofibers have more time to dry and can thus form uniform nanofiber with small membrane areas. An example of interconnected web structure of wet nanofibers and corresponding morphology can be seen in Fig. 1.4(b). Here EVOH fibers show strong thickened parts and form coherent networks.
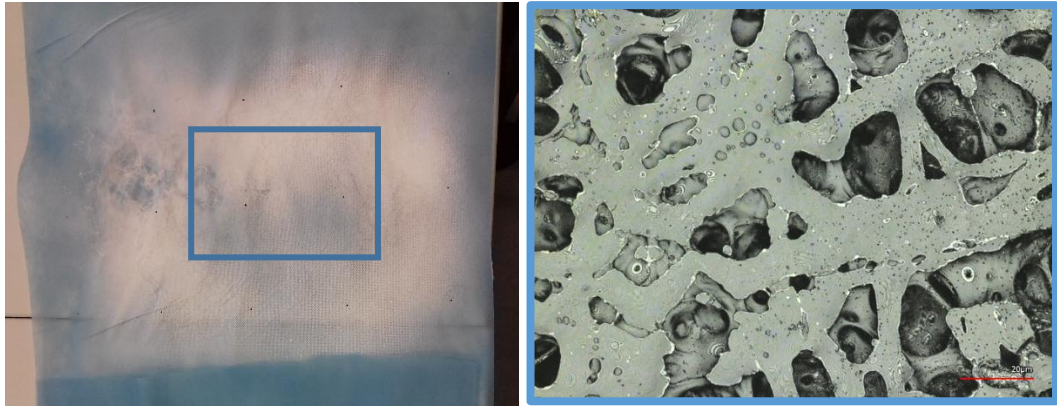
(a)                                    (b)

Fig. 1.4 EVOH nanofiber mat on polypropylene (PP) substrate (blue color) with wet area in the middle (a) and fibers interconnections (b). The scale bar in (b) indicates 20 μm.

The formation of artifacts in needleless electrospinning usually happened with increased humidity, addition of acetone and sometimes for other reasons.

Fig. 1.5 shows CLSM images of a comparison between fiber architecture of EVOH polymer dissolved in DMSO by adding acetone. Acetone has high volatility and is an important reagent for the chemical experiments [54].

EVOH nanofiber mats electrospun without acetone have relatively regular straight fibers with some beads-on-string structures and small membrane areas (Fig. 1.5 a). By adding 10 % of acetone the morphology of the nanofiber mats changes strongly and the nanofiber diameters increase while the nanofibers show interconnections (Fig. 1.5 b).
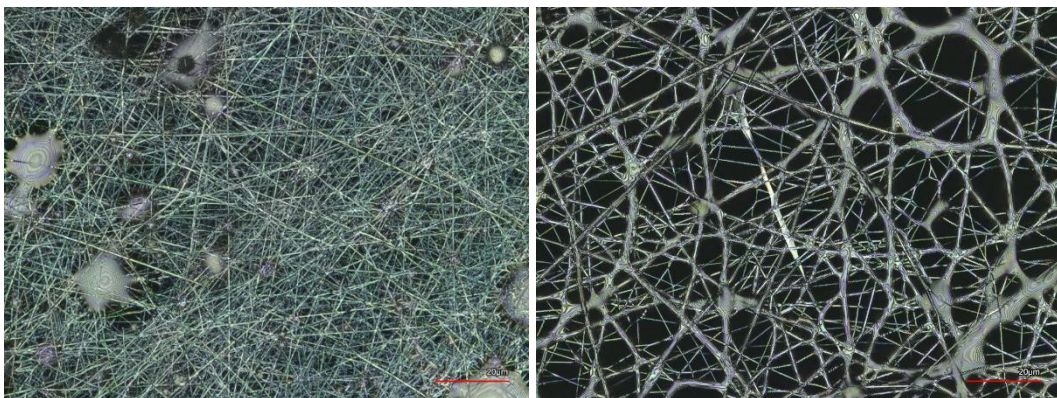




(a)                                    (b)

Fig. 1.5 CLSM images of 20% EVOH dissolved in DMSO without acetone (a), and  with 10% of acetone (b). The scale bar in (b) indicates 20 μm.

Solvents have an enormous influence on fiber morphology and evaporation process taking time [31]. If the solvents evaporate quickly then dry fiber will be collected. When it comes to a solvent with low volatility, wet fibers with interconnected web structure will be obtained [56]. The wet nanofibers form interconnections, beads and membrane-like areas.

One of the reasons for the formation of bead-on-string structures could be related to the low concentration of the polymer solution. Haider et al. (2013) and Pillay et al. (2013) determined that at low concentrations of polymer solution, entangled polymer chains break up into fragments before they reach the collector through the action of applied electric fields and surface tension [57-58]. For some polymers a high concentration of polymer solution favored the bead formation. In this case, the polymer solution conductivity could be increased by adding additives such as inorganic salts, surfactants and polymers and uniform nanofibers could be obtained. Hereby increasing the concentration of additives reduces the fiber diameter [1].

## 1.7 Polymers and solvents

Many different polymers with both synthetic and natural origin are used for the preparation of electrospun nanofibers (Table 1.2). Most of them are prepared with solvent or melt spinning [6]. A variety of materials could be spun, including natural and synthetic polymers, preceramic polymers, metals, and oxides [59]. By adding other substances such as carbon nanotubes (CNTs), silver or iron particles, nanoplates with promising properties can be produced that are of interest in biotechnological and medical applications [60-62].

Table 1.2 Overview of polymers and solvents in electrospinning.

| Polymers | Solvent | Reference |
|---|---|---|
| PCL/collagen | TFE | Zhang et al. 2005, [27] |
| PVA | Water | Koski et al. 2004, [35] |
| PCL/AV_CS | TFE; AA and water | Miguel et al. 2017, [63], [64] |
| Chitosan/arginine-chitosan | TFA:DCM | Antunes et al. 2015, [65], [6], [61] |
| CS/SF | HFIP:TFA | Cai et al. 2010, [66] |
| CS/PVA | Deionized water for PVA;HOBt, TPP and EDTA for CS | Charernsriwilaiwat et al. 2014, [67] |
| Collagen | HFIP | Rho et al. 2006, [68] |
| Collagen/ZN | AA | Lin et al. 2012, [69] |
| Gelatin/PU | HFIP | Kim et al. 2009, [70] |
| PLACL/SF/AV | DCM: DMF | Suganya et al. 2014, [71] |

| Polymers | Solvent | Reference |
|---|---|---|
| SF | Formic acid | Min et al. 2004, [72] |
| Cellulose acetate | Acetone/DMAc | Deng et al. 2013, [73] |
| Silk fibroin | Formic acid | Hang et al. 2012, [74] |
| Gelatin | TFE/HFIP | Huang et al. 2004, [75] |
| Elastin | Water | Huang et al. 2000, [76] |
| CA | DMAC | Liu and Hsieh 2002, [77] |
| PC | THF/DMF | Lee et al. 2005, [78] |
| PAN | Dichloromethane | Gu et al. 2005, [79] |
| PMMA | Acetone | Piperno et al. 2006, [80] |
| EVOH | Alcohol/water | Kenawy et al. 2003, [81] |
| Chitin | HFIP/PBS | Holzwarth and Ma 2011, [82] |

AA: Acetic acid; AV: Aloe Vera; CA: Cellulose acetate; CS: Chitosan; DCM: Dichloromethane; DMF: Dimethylformamide; DMAC: N,N-Dimethylacetamide; EVOH: Poly(ethylene-co-vinyl alcohol); EDTA: Ethylenediaminetetraacetic acid; HFIP: 1,1,1,3,3,3-hexa fluoro-2-propanol; HOBt: Hydroxybenzotriazole; PVA: Polyvinyl alcohol; PC: Polycarbonate; PBS: Polybutylene succinate; PAN: Polyacrylonitrile; PMMA: Polymethacrylate; PCL: Polycaprolactone; PU: Polyurethane; SF: Silk fibroin; TFA: Trifluoroacetic acid; TFE: 2,2,2-Trifluoroethanol; TPP: Tripolyphosphate; ZN: Zein; ZnO: Zinc oxide.;

## 1.8 Application of electrospun nanofibers

Electrospinning enables the continuous production of nanofibers with controllable fiber diameter and morphology, which make them appropriate for a wide range of applications such as nanocatalysis, filtration, optical and chemical sensors, energy storage, protective clothing, defense and security [83-88].

Moreover, nanofibers have emerged in recent decades as advanced fibers with wide use and high potential in biomedical, biotechnological or medical applications such as filters, cell growth, wound healing or tissue engineering [89]. Electrospun nanofibers scaffolds provide a suitable environment to the cells which results in their better attachment and proliferation [64]. [90]. For example, collagen fibrils are known to support the interaction between cells and scaffolds [6], [10]. The cellular infiltration of CHO-DP12 (Chinese hamster ovary strain DP12) into a PAN/gelatin blend nanofiber structure can be seen in Fig. 1.6. Another similar approach of blending gelatin with collagen-coated poly(-caprolactone) (PCL) mesh to enhance the ability of cell migration into the PCL network has been reported by Zhang et al. (2005) [43]. Majidi and co-workers fabricated 3D microporous alginate/gelatin hydrogel nanofibers which offer superior cell adhesion and proliferation [91].



Fig. 1.6 CLSM images of CHO-DP12 (Chinese hamster ovary strain DP12) cells, colored with methylene blue on a PAN/gelatin blend nanofiber mat. The scale bar indicates 20 μm.

The porosity of electrospun nanofibers allows the use of nanofibers in large biomedical applications. Nanofibers can act as protective tissues in hospital environments against infectious agents or be used for biomedical applications as tissue scaffolds for drugs and cosmetics [92]. Other applications can be found in the

areas of drug delivery or for the production of tissue in the biomedical fields [93-94]. Nanofibers can have a therapeutic effect and significantly reduce microbial risks in wound healing or regeneration [95]. The high surface-to-volume ratio of nanofibers enables enhanced interaction with their environment, making them promising for wound care, drug delivery, and biotechnological filter applications [85]. The high surface- to-volume ratio and the ability to absorb large concentrations of antimicrobial and anti-inflammatory agents underline the importance of electrospun nanofibers. Therefore, nanofibers are ideal candidates for modern and efficient wound treatment and wound care.

Numerous synthetic and organic polymers are used to produce nanofibers. Grothe et al. (2017) reported about production of nanofiber mats with aloe vera that could be used as wound dressings in burns and other types of wounds [20]. Similarly, a crosslinked alginate may be used as a wound dressing with aloe vera. Furthermore, nano-spun alginate fiber mats can take up a large amount of water or wound fluid, thus assisting in the drying out of wounds. Besides alginate, chitosan is particularly interesting for biotechnological and medical applications because of its antibacterial, antifungal and other intrinsic physical and chemical properties [96]. Optimal settings for electrospinning of chitosan with PEO (polyethylene oxide) have been reported by Grothe et al. (2017) [97].

Besides biomedical applications, electrospun nanofibers have also found application in the protection of environment as affinity membrane for water and air filtration. Mahapatra and co-workers (2013) have synthesized alumina nanofibers by using an electrospinning method for removal of toxicants in waste water and drinking water by adsorption of such toxicants on the surface of functionalized nanofibers [98]. The obtained alumina nanofibers were used as adsorbents for the removal of chromium and fluoride ions from an aqueous system.

Positive properties of nanofiber mats for water filtration compared to known materials are shown in Fig. 1.7. A simple test compares the filter effect of a polypropylene (PP) nonwoven and a PAN nanofiber mat.

<div align="center">(a)           (b)</div>
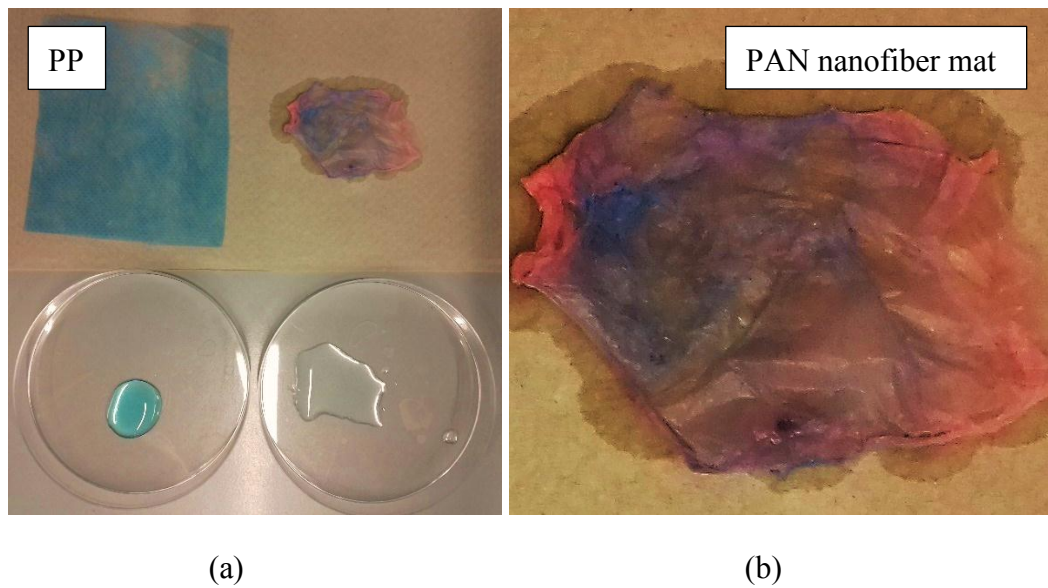
Fig. 1.7 Color Comparison of a polypropylene (PP) nonwoven and a PAN nanofiber mat filtering capability (a) and PAN nanofiber mats after filtration test with residues of dye (b).

Water was colored with methylene blue and then passed through a PP nonwoven and a PAN nanofiber mat. As can be seen in Fig. 1.7(b), the PAN nanofiber mat contains blue color particles and the water is relatively clear in contrast to PP nonwoven (Fig. 1.7(a)) where the filtered water still has a blue color. This finding confirms the assumption that nanofiber mats can be very well suited for water filtration.

In contrast to conventional filter fibers, nanofibers obtain much higher capability to capture particles due to the slip- flow effect around the nanofibers, leading to increased diffusion, interception and inertial impaction efficiency [99]. The slip-flow effect describes the air flow around a microfiber. The smaller the diameter of the fiber, the lower the flow resistance at the surface of the fiber. Because the nanofibers have very small diameters, they do not build a large flow resistance at the surface and can therefore capture more particles than conventional filter fibers [100].

In general, nanofibers are suitable for a wide range of applications in various areas such as health, protective clothing, aerospace, transportation, energy and environmental applications. Among others, nanofibers can find interesting applications in water and air purification. Nanofibers have many advantages over conventional fibers used in filtration. They have a high surface-to-volume ratio, are very light and can be manufactured on an industrial scale. By changing electrospinning parameters, it is possible to produce nanofibers, nanofibers with membranes or almost complete membranes.

Electrospinning thus enables a simple surface modification process and is a versatile technique for the production of highly porous nanofibers and nano-membranes. In addition, a large selection of different materials is available from which nanofibers and nanofibers membranes can be made [100-101].

These nanofiber membranes can offer good alternatives to conventional membranes. These membranes offer a relatively high porosity (typically about 80 %), open pore structures as well as controllable pore size distribution from micron to submicron range [102-104]. These nano-membranes offer high permeability and can be used, e.g., for water or air purification. In addition, electrospinning offers easy integration of the special functions of polymer nanofibers [105].

Huang et al. (2003) reported about electrospun nanofiber that can also be used for producing high-surface-area chemical and biological nanosensors [106]. In addition to chemical and biological sensors, highly sensitive polymeric nanofibers optical sensors have also been fabricated from fluorescent polymers by Lee et al. (2002) and Wang et al. (2002) [107-108].

Sahay et al. (2012) published a review article about nanofiber composite and their applications in various fields such as energy, filters, smart materials, sensors and biotechnology [12]. Jayaraman and co-workers (2014) reported about a novel $TiNb_2O_7$ nanofibrous material as anode material for fuel cell application [109].

## 1.9 Oxidation and stabilization of nanofiber mats

Polyacrylonitrile (PAN) and copolymers of PAN have been extensively studied for commercial and technological exploitation. PAN is valued for its important physical properties such as insolubility and resistance to swelling in common organic solvents. Mainly due to its high carbon yield, which is up to 56 %, PAN is the most commonly used polymer for the production of carbon nanofibers (CNFs). PAN can be dissolved in polar solvents like DMF, DMSO, DMAc, dimethyl sulfone, tetramethyl sulfide and aqueous solutions of ethylene carbonate and some minerals salts [110-111]. That makes PAN interesting for a wide range of applications.

Sabantina et al. (2018) investigated the production of polyacrylonitrile (PAN) nanofiber mats with a non-toxic solvent (DMSO, dimethyl sulfoxide) [21]. Unlike other biopolymers that can be spun from non-toxic solutions, PAN is water-resistant. This property makes PAN an interesting material for electrospinning of nanofiber webs, which can be used for biotechnological or medical applications such as filters, cell growth, wound healing or tissue engineering. In addition, PAN is a typical precursor for the production of carbon nanofibers [112].

In the processing of PAN, various solvents such as dimethylformamide (DMF), aqueous solution of sodium thiocyanate, dimethylacetamide (DMAA) and DMSO can be used which belong to the same class of aprotic solvents [111], [113]. PAN is mainly used for the production of carbon nanofibers by electrospinning because of its high carbonization rate and simple carbonization process.

The conversion of PAN nanofibers into carbon fibers takes place in a thermal process and is characterized by three main stages: electrospinning, oxidative stabilization and high-temperature carbonization [112], [114]. The graphitization of nanofibers takes place above 1000 °C. Fig. 1.8 shows a scheme of the conversion of PAN nanofibers into carbon nanofibers.

| Electrospinning | Stabilization in air 200-280°C (Ashad et al. 2011), [115]. | Carbonization >800°C in inert atmosphere (Rahaman et al. 2007), [116]. | Graphitization >1000°C [112] |

Fig. 1.8 Manufacturing process of carbon nanofibers from PAN.

Oxidative stabilization forms ladder structures that allow the stabilized precursor to be processed at higher temperatures. This step is usually carried out at a low temperature between 200-300 °C in air [112].

During this PhD project, color measurements were carried out on PAN nanofibers. The original white color of PAN nanofiber changes slowly from completely white to honey and turns brown (Fig. 1.9). From approx. 280 °C the color does not change anymore and remains dark brown even at higher stabilization temperatures.



| 180 °C | 200 °C | 220 °C | 250 °C | 300 °C |
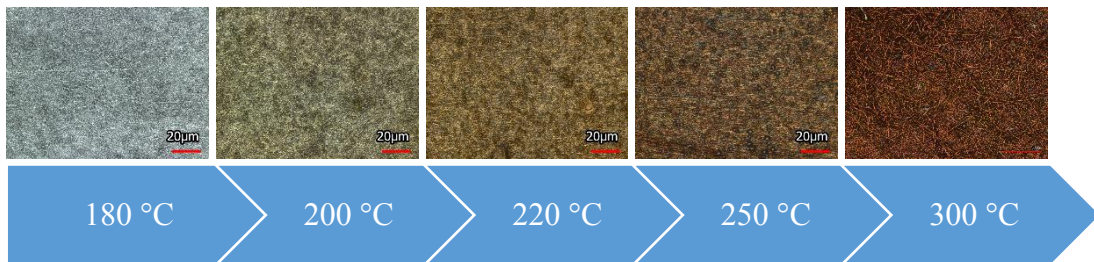
Fig. 1.9 Color change of PAN nanofibers during oxidative stabilization at different temperatures from white until deep brown color.

After oxidation, PAN is carbonized in an inert atmosphere up to 800 C [117], keeping non-carbon atoms such as hydrogen, nitrogen and oxygen away [112]. During carbonizing at 800 °C denitrogenation will occur and formation of a network structure will take place [112].
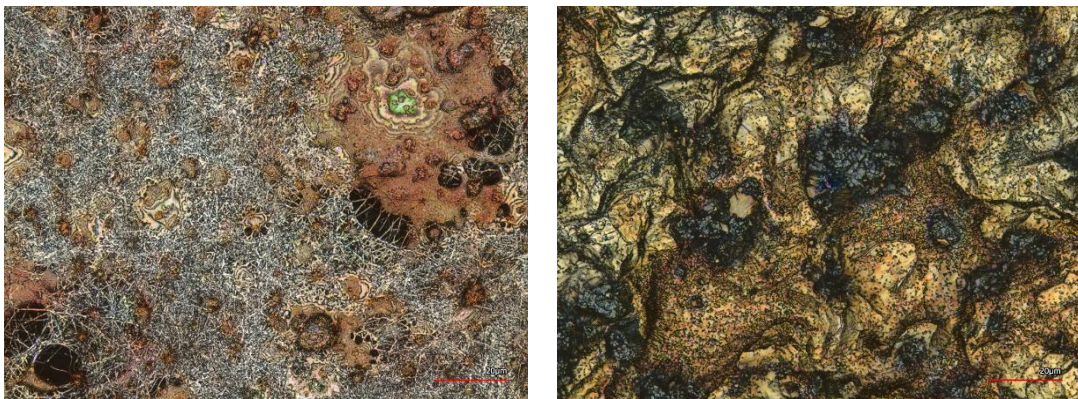


(a)                                                    (b)
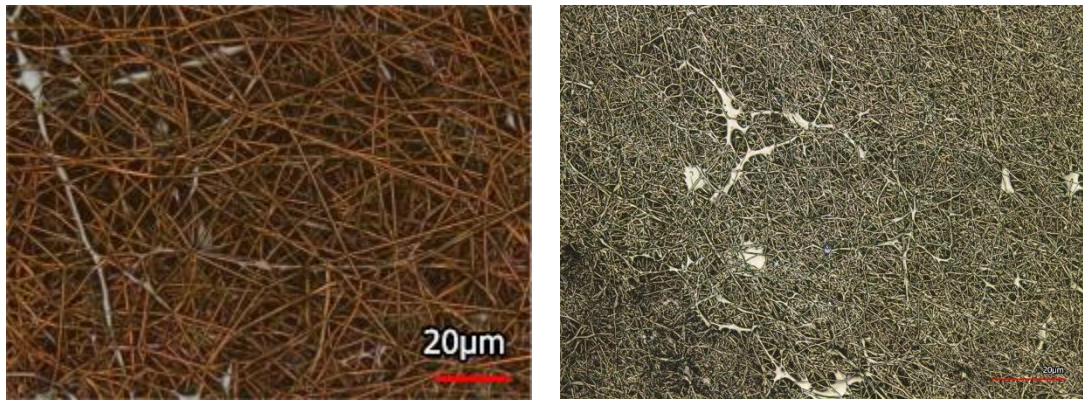
<div style="text-align:center">(c)             (d)</div>

Fig. 1.10 CLSM images of carbonized PAN/ferro-fluid (a) and PAN/ferro-fluid on aluminum foil (b) nanofiber mats and stabilized (c) and carbonized PAN/gelatin nanofiber mats (d). The scale bars indicate 20 µm.

The comparison of stabilized and carbonized PAN blended with gelatin and ferro-fluid nanofiber mats can be seen in Fig. 1.10.

During the carbonization process nanofibers shrink in diameter and loose approximately 50 % of their weight [114]. Fig. 1.11 shows the changes in sample size after carbonization.



<div style="text-align:center">(a)             (b)</div>

Fig. 1.11 Dimensional change of PAN and PAN/aluminum composites before (a) and after (b) carbonization process.

Graphitizing can be carried out afterwards by heating in an inert atmosphere up to 2000 °C to improve the stiffness of nanofibers which is significantly larger than the average stiffness of the surrounding amorphous carbon. [116].

## 1.10    References

1. T. Lin, X. Wang, 2014, Needleless electrospinning of nanofibers, technology and applications, Pan Stanfort Publishing Pte Ltd

2. J.F. Cooley, 1902, Apparatus for electrically dispersing fluids, US Patent Specification 692631

3- 115. W.J. Morton, 1997, Method of dispersing fluids, US Patent Specification 705691

4. K.J. Pawlowski, C.P. Barnes, E.D. Boland, G.E.Wnek, G.L. Bowlin, 2004, Biomedical nanoscience: electrospinning basic concepts, applications, and classroom demonstration, Mater Res Soc Symp Proc, 827, 17-28

5. G.I. Taylor, 1969, Electrically Driven Jets. Proc R Soc Lond, A Math Phys Sci, (1934–1990), 313, 453-75.

6. A. Haider, S. Haider, I-K. Kang, 2015, A comprehensive review summarizing the effect of electrospinning parameters and potential applications of nanofibers in biomedical and biotechnology, Arabian Journal of Chemistry

7. B. Vonnegut, R.L. Newbauer, 1952, Production of monodisperse liquid particles by electrical atomization, J Colloid Sci, 7, 616-622

8. H.L. Simons, 1966, Process and Apparatus for Producing Patterned Nonwoven Fabrics, US patent 3, 280, 229

9. P.K. Baumgarten, 19971, Electrostatic spinning of acrylic microfibers, J Colloid Interface Sci, 36, 71-79

10. N. Bhardwaj, S.C. Kundu, 2010, Electrospinning: A fascinating fiber fabrication technique, Biotechnology Advances, 28 (3), 325-347

11. S.H. Lee, N. Chen, S. Peng, L. Li, L. Tian, N. Thakor, S. Ramakrishna, 2018, Polymer-based composites by electrospinning: Preparation & functionalization with nanocarbons, Progress in Polymer Science, Vol. 86, 40-84

12. R. Sahay, P. Sureshkumar, R. Sridhar, J. Sundaramurthy, J. Venugopal, S.G. Mhaisalkar, S. Ramakrishna, 2012, Electrospun composite nanofibers and their multifaceted applications, J Mater Chem, 22, 12953-12971

13. A. Góra, R. Sahay, V. Thavasi, S. Ramakrishna, 2011, Melt-electrospun fibers for advances in biomedical engineering, clean energy, filtration, and separation, Polym Rev, 51, 265-287

14. P.S. Kumar, J. Sundaramurthy, S. Sundarrajan, V.J. Babu, G. Singh, S.I. Allakhverdiev, et al., 2014, Hierarchical electrospun nanofibers for energy harvesting, production and environmental remediation, Energy Environ Sci, 7, 3192-3222

15. S. Li, S. Peng, J.K.Y. Lee, D. Ji, M. Srinivasan, S. Ramakrishna, 2017, Electrospun hollow nanofibers for advanced secondary batteries, Nano Energy, 39, 111-139

16. D. Liang, B.S. Hsiao, B. Chu, 2007, Functional electrospun nanofibrous scaffolds for biomedical applications, Adv Drug Deliv Rev, 59, 1392-1412

17. T.J. Sill, H.A.V. Recum, 2008, Electrospinning: applications in drug delivery and tissue engineering, Biomaterials, 29, 1989-2006

18. D.H. Reneker, A.L. Yarin, H. Fong, S. Koombhongse, 2000, Bending instability of electrically charged liquid jets of polymer solutions ins electrospinning, Journal of Applied Physics, 87 (9, Pt.1), 4531-4547

19. Y. Dzenis, 2004, Material science: spinning continuous fibers for nanotechnology, Science (Washington, DC, United States), 304 (5679), 1971-1918

20. T. Grothe, D. Wehlage, T. Böhm, A. Remche, A. Ehrmann, 2017a, Needleless Electrospinning of PAN Nanofibre Mats, Tekstilec 60, 290-295

21. L. Sabantina, J. R. Mirasol, T. Cordero, K. Finsterbusch, A. Ehrmann, 2018, Investigation of Needleless Electrospun PAN Nanofiber Mats, AIP Conference Series 1952, 020085

22. J.C. Sy, A.S. Klemm, V.P. Shastri, 2009, Emulsion as a means of controlling electrospinning of polymers, Advanced Materials, 21, 1814-1819

23. M. Spasova, R. Mincheva, D. Paneva, N. Manolova, I. Rashkov, 2006, Perspectives on: Criteria for complex evaluation of the morphology and alignment of electrospun polymer nanofibers, Journal of Bioactive and Compatible Polymers, 21, 465-479

24. H.L. Jiang, D.F. Fang, B.S. Hsiao, B. Chu, W.L. Chen, 2004, Optimization and characterization of dextran membranes prepared by electrospinning, Biomacromolecules, 5, 326-333

25. L. Huang, K. Nagapudi, R.P. Apkarian, E.L. Chaikof, 2001, Engineered collagen-PEO nanofibers and fabrics, J Biomater Sci Polym Ed, 12, 979-993

26. Z.Z. Zhao, J.Q. Li, X.Y. Yuan, X. Li, Y.Y. Zhang, J. Sheng, 2005, Preparation and properties of electrospun poly (vinylidene fluoride) membranes, J Appl Polym Sci, 97, 466-474

27. C. Zhang, J. Venugopal, Z.M. Huang, C. T. Lim, S. Ramakrishna, 2005a, Characterization of the Surface Biocompatibility of the Electrospun PCL-Collagen Nanofibers Using Fibroblasts, Biomacromolecules, 6, 2583-2589

28. B. Kim, H. Park, S.H. Lee, W.M. Sigmund, 2005, Poly(acrylic acid) nanofibers by electrospinning, Mater Lett, 59, 829-832

29. W.K. Son, J.H. Youk, T.S. Lee, W.H. Park, 2004, The effects of solution properties and polyelectrolyte on electrospinning of ultrafine poly (ethylene oxide) fibers, Polymer, 45, 2959-2966

30. Z. Jiang, H. Hou, A. Schaper, J.H. Wendorff, A. Greiner, 2003, Poly-L-lactide nanofibers by electrospinning — influence of solution viscosity and electrical conductivity on fiber diameter and fiber morphology, e-Polym, 9, 1-9

31-30. J.H. Wendorff, S. Agarwal, A. Greiner, 2012, Electrospinning: Materials, Processing, and Applications, Wiley-VCH Verlag, Weinheim

32. V.J. Chen, P.X. Ma, 2004, Nano-fibrous poly (L -lactic acid) scaffolds with interconnected spherical macropores, Biomaterials, 25, 2065-2073

33. M.M. Demir, I. Yilgor, E. Yilgor, B. Erman, 2002, Electrospinning of polyurethane fibers, Polymer, 43, 3303-3309

34. P. Gupta, C. Elkins, T.E. Long, G.L. Wilkes, 2005, Electrospinning of linear homopolymers of poly (methylmethacrylate): exploring relationships between fiber formation, viscosity, molecular weight and concentration in a good solvent, Polymer, 46, 4799-4810

35. A. Koski, K. Yim, S. Shivkumar, 2004, Effect of molecular weight on fibrous PVA produced by electrospinning, Mater Lett, 58, 493-497

36. M.M. Hohman, M. Shin, G. Rutledge, M.P. Brenner, 2001, Electrospinning and electrically forced jets. II. Applications, Phys Fluids, 13, 2221-2236

37. W.W. Zuo, M.F. Zhu, W. Yang, H. Yu, Y.M. Chen, Y. Zhang, 2005, Experimental study on relationship between jet instability and formation of beaded fibers during electrospinning, Polym Eng Sci, 45, 704-709

38. C. Mit-Uppatham, M. Nithitanakul, P. Supaphol, 2004, Ultrafine electrospun polyamide-6 fibers: effect of solution conditions on morphology and average fiber diameter, Macromol Chem Phys, 205, 2327-2338

39. J.M. Deitzel, J. Kleinmeyer, D. Harris, N.C.B. Tan, 2001, The effect of processing variables on the morphology of electrospun nanofibers and textiles, Polymer, 42 (1), 261-272

40. C.S. Ki, D.H. Baek, K.D. Gang, K.H. Lee, I.C. Um, Y.H. Park, 2005, Characterization of gelatin nanofiber prepared from gelatin-formic acid solution, Polymer, 46, 5094-5102

41. X. Geng, O.H. Kwon, J. Jang, 2005, Electrospinning of chitosan dissolved in concentrated acetic acid solution, Biomaterials, 26, 5427-5432

42. C.J. Buchko, L.C. Chen, Y. Shen, D.C. Martin, 1999, Processing and microstructural characterization of porous biocompatible protein polymer thin films, Polymer, 40, 7397-7407

43. Y.Z. Zhang, X. Yuan, L. Wu, Y. Han, J. Sheng, 2005, Study on morphology of electrospun poly (vinyl alcohol) mats, Eur Polym J, 41, 423-432

44. S. Megelski, J.S. Stephens, D. Bruce Chase, J.F. Rabolt, 2002, Micro- and nanostructured surface morphology on electrospun polymer fibers, Macromolecules, 35 (22), 8456-8466

45. Z. Shamim, B. Saeed, T. Amir, R. Abo Saied, Damerchely Rogheih, 2012, The effect of flow rate on morphology and deposition area of electrospun nylon 6 nanofiber, J Eng Fabrics Fibers, 7 (4), 42

46. K.P. Matabola, R.M. Moutloali, 2013, The influence of electrospinning parameters on the morphology and diameter of poly(vinyledene fluoride) nanofibers-effect of sodium chloride, J Mater Sci, 48 (16), 5475

47. T. Wang, S. Kumar, 2006, Electrospinning of polyacrylonitrile nanofibers, J Appl Polym Sci, 102 (2), 1023-1029

48. Z. Li, C. Wang, 2013, One-dimensional nanostructures: Electrospinning technique and unique nanofibers, Springer, Heidelberg

49. J.Y. Park, I.-H. Lee, 2010, Relative humidity effect on the preparation of porous electrospun polystyrene fibers, J. Nanosci Nanotechnol, 10 (5), 3473-3477

50. J. Pelipenko, J. Kristl, B. Janković, S. Baumgartner, P. Kocbek, 2013, The impact of relative humidity during electrospinning on the morphology and mechanical properties of nanofibers, Int J Pharm, 456 (1), 125-134

51. T. Grothe, D. Wehlage, T. Böhm, A. Remche, A. Ehrmann, 2017, Needleless Electrospinning of PAN Nanofibre Mats, Tekstilec 60, 290-295 (2017)

52. J. Lasprilla-Botero, M. Álvarez-Láinez, J.M. Lagaron, 2018, The influence of electrospinning parameters and solvent selection on the morphology and diameter of polyimide nanofibers,, Materials Today Communications, Volume 14

53. D. Wong, J. Resendiz, P. Egberts, S. S. Park, 2018, Electrospinning of composite microbeads for tribological improvements, Journal of Manufacturing Process, 34 (A)

54. X.L. Xu, Y. Chen, S.Y. Ma, W.Q. Li, Y.Z. Mao, 2015, Excellent acetone sensor of La-doped ZnO nanofibers with unique bead-like structures, Sensors and Actuators B: Chemical, 213

55. J. Supramaniam, R. Adnan, N.H.M. Kaus, R. Bushra, 2018, Magnetic nanocellulose alginate hydrogel beads as potential drug delivery system, International Journal of Biological Macromolecules, 118, Part A

56. C.M. Hsu, S. Shivkumar, 2004, Nano-sized beads and porous fiber construstions of poly(vepsiln.-ceprolactone) produced by electrospinning, Journal of material Science, 39(9), 3003-3013

57. S. Haider, Y. Al-Zeghayer, F. Ahmed Ali, A. Haider, A. Mahmood, W. Al Masry, M. Imran, M. Aijaz, 2013, Highly aligned narrow diameter chitosan electrospun nanofibers, J Polym Res, 20 (4), 1-11

58. V. Pillay, C. Dott, Y.E. Choonara, C. Tyagi, L. Tomar, P. Kumar, L.C.du Toit, V.M.K. Ndesendo, 2013, A review of the effect of processing variables on the fabrication of electrospun nanofibers for drug delivery applications, J Nanomater, 22

59. D.J. Yang, L.-F. Zhang, L. Xu, C.-D. Xiong, J. Ding, Y.-Z. Wang, 2007, Fabrication and characterization of hydrophilic electrospun membranes made from the block copolymer of poly(ethylene glycol-co-lactide), J Biomed Mater Res, Part A, 82A (3), 680-688

60. M. Alaa, T.A. Osman, M.S. Toprak, M. Muhammed, A. Uheida, 2017, Surface functionalized composite nanofibers for efficient removal of arsenic from aqueous solutions, Chemosphere,180, 108-116

61. B. Duan, C. Dong, X. Yuan, K. Kangde Yao, 2004, Electrospinning of chitosan solutions in acetic acid with poly(ethylene oxide), Journal of Biomaterials Science, Polymer Edition, 15 (6), 795-803

62. P. Wang, L. Cheng, Y. Zhang, L. Zhang, 2017, Synthesis of SiC nanofibers with superior electromagnetic wave absorption performance by electrospinning, Journal of Alloys and Compounds, 716, 306-320

63. S.P. Miguel, M.P. Ribeiro, P. Couinho, I.J. Correia, 2017, Electrospun Polycaprolactone/Aloe Vera_Chitosan Nanofibrous Asymmetric Membranes Aimed for Wound Healing Applications, Polymers, 9, 183

64. A. Haider, K.C. Gupta, I.-K. Kang, 2014, PLGA/nHA hybrid nanofiber scaffold as a nanocargo carrier of insulin for accelerating bone tissue regeneration, Nanoscale Res. Lett., 9 (1), 314

65. B. Antunes, A. Moreira, V.M. Gaspar, I.J. Correia, 2015, Chitosan/arginine-chitosan polymer blends for assembly of nanofibrous membranes for wound regeneration, Carbohydr Polym, 130, 104-112

66. Z.X. Cai, X.M. Mo, K.H. Zhang, L.P. Fan, A.L. Yin, C.L. He, H.S.Wang, 2010, Fabrication of chitosan/silk fibroin composite nanofibers for Wound-dressing Applications, Int J Mol Sci, 11, 3529-3539

67. N. Charernsriwilaiwat, T. Rojanarata, T. Ngawhirunpat, P. Opanasopit, 2014, Electrospun chitosan/polyvinyl alcohol nanofibre mats for wound healing, Int Wound J, 11, 215-222

68. K.S. Rho, L. Jeong, G. Lee, B.M. Seo, Y.J. Park, S.D. Hong, S. Roh, J.J. Cho, W.H. Park, B.M. Min, 2006, Electrospinning of collagen nanofibers: Effects on the behavior of normal human keratinocytes and early-stage wound healing, Biomaterials, 27, 1452-1461

69. J. Lin, C. Li, Y. Zhao, J. Hu, L.M. Zhang, 2012, Co-electrospun nanofibrous membranes of collagen and zein for wound healing, ACS Appl Mater Interfaces, 4, 1050-1057

70. S.E. Kim, D.N. Heo, J.B. Lee, J.R. Kim, S.H. Park, S.H. Jeon, I.K. Kwon, 2009, Electrospun gelatin/polyurethane blended nanofibers for wound healing, Biomed Mater, 4, 044106

71. S. Suganya, J. Venugopal, S. Ramakrischna, B.S. Lakschmi, V.G.R. Dev, 2014, Naturally derived biofunctional nanofibrous scaffold for skin tissue regeneration, Int J Biol Macromol, 135-143

72. B.M. Min, G. Lee, S.H. Kim, Y.S. Nam, T.S. Lee, W.H. Park, 2004, Electrospinning of silk fibroin nanofibers and its effect on the adhesion and spreading of normal human keratinocytes and fibroblasts in vitro, Biomaterials, 25, 1289-1297

73. L. Deng, R.J. Young, I.A. Kinloch, Y. Zhu, S.J. Eichhorn, 2013, Carbon nanofibres produced from electrospun cellulose nanofibres, Carbon, 58, 66-75

74. Y. Hang, Y. Zhang, Y. Jin, H. Shao, X. Hu, 2012, Preparation of regenerated silk fibroin/silk sericin fibers by coaxial electrospinning, Int J Biol Macromol, 51 (5), 980-986

75. Z.M. Huang, Y. Zhang, S. Ramakrishna, C. Lim, 2004, Electrospinning and mechanical characterization of gelatin nanofibers, Polymer, 45 (15), 5361-5368

76. L. Huang, R.A. McMillan, R.P. Apkarian, B. Pourdeyhimi, V.P. Conticello, E.L. Chaikof, 2000, Generation of synthetic elastin-mimetic small diameter fibers and fiber networks, Macromolecules, 33 (8), 2989-2997

77. H. Liu, Y.L. Hsieh, 2002, Ultrafine fibrous cellulose membranes from electrospinning of cellulose acetate, J Polymer Science Part B: Polymer Physics, 40 (18), 2119-2129

78. J.K.Y. Lee, B. Lee, C. Kim, H. Kim, K. Kim, C. Nah, 2005, Stress-strain behavior of the electrospun thermoplastic polyurethane elastomer fiber mats, Macromolecular Research Field, 13 (5), 441-445

79. S.Y. Gu, Q.L. Wu, J. Ren, G. Vansco, G. Julius, 2005, Mechanical properties of a single electrospun fiber and its structures, Macromolecular Rapid Communications, 26 (9), 716-720

80. S. Piperno, L. Lozzi, R. Rastelli, M. Passacantando, S. Santucci, 2006, PMMA nanofibers production by electrospinning, Applied Surface Science, 252 (15), 5583-5586

81. E. Kenawy, J. Layman, J. Watkins, G. Bowlin, J. Matthews, D. Simpsons et al., 2003, Electrospinning of poly(ethylene-co- vinyl alcohol) fibers, Biomaterials, 24 (6), 907-913

82. J.M. Holzwarth, P.X. Ma, 2011, Biomimetic nanofibrous scaffolds for bone tissue engineering, Biomaterials, 32 (36), 9622-9629

83. Y.K. Luu, K. Kim, B.S. Hsiao, B. Chu, M. Hadjiargyrou, 2003, Development of a nanostructured DNA delivery scaffold via electrospinning of PLGA and PLA-PEG block copolymers, J Control Release, 89, 341–353

84. T. Subbiah, G.S. Bhat, R.W. Tock, S. Parameswaran, S.S. Ramkumar, 2005, Electrospinning of nanofibers, J Appl Polym Sci, 96, 557–69

85. S. Ramakrishna, K. Fujihara, W.E. Teo, T. Yong, Z. Ma, R. Ramaseshan, 2006, Electrospun nanofibers: solving global issues, Mater Today, 9, 40–50

86. W. Cui, S. Zhou, X. Li, J. Weng, 2006, Drug-loaded biodegradable polymeric nanofibers prepared by electrospinning, Tissue Eng, 12, 1070

87. C.P. Barnes, S.A. Sell, D.C. Knapp, B.H. Walpoth, D.D. Brand, G.L. Bowlin, 2007, Preliminary investigation of electrospun collagen and polydioxanone for vascular tissue engineering applications, Int J Electrospun Nanofibers Appl, 1, 73–87

88. A. Welle, M. Kroger, M. Doring, K. Niederer, E. Pindel, S. Chronakis, 2007, Electrospun aliphatic polycarbonates as tailored tissue scaffold materials. Biomaterials, 28, 2211–9

89. C. Großerhode, D. Wehlage, T. Grothe, N. Grimmelsmann, S. Fuchs, J. Hartmann, P. Mazur, V. Reschke, H. Siemens, A. Rattenholl, S.V. Homburg, A. Ehrmann, 2017, AIMS Bioengineering 4, 376-385

90. B. Ostrowska, J. Jaroszewicz, E. Zaczynska, W.Tomaszewski, W. Swieszkowski, K.J. Kurzydlowski, 2014, Evaluation of 3D hybrid microfiber/nanofiber scaffolds for bone tissue engineering, Bull Polish Acad Sci Tech Sci, 551-556

91. S.S. Majidi, P. Slemming-Adamsen, M. Hanif, Z. Zhang, Z. Wang, M. Chen, 2018, Wet electrospun alginate/gelatin hydrogel nanofibers for 3D cell culture, International Journal of Biological Macromolecul, in press

92. X. Sheng, L. Fan, C. He, K. Zhang, X. Mo, H. Wang, 2013, Vitamin E-loaded silk fibroin nanofibrous mats fabricated by green process for skin care application, Int J Biol Macromol, 56, 49-56

93. J. Panyam, V. Labhasetwar, 2003, Biodegradable nanoparticles for drug and gene delivery to cells and tissue, Adv Drug Deliv Rev, 55, 329-347

94. G. Mo, R. Zhang, Y. Wang, L. He, 2017, The interplay between gelation and phase separation in PAN/DMSO/H2O blends and the resulted critical gels, European Polymer Journal, 92, 2017, 40-50

95. A. Repanas, S. Andriopoulou, B. Glasmacher, 2016, The significance of electrospinning as a method to create fibrous scaffolds for biomedical engineering and drug delivery applications, Journal of Drug Delivery Science and Technology, 31, 137-146

96. M. Mohiti-Asli, E.G. Loboa, 2016, 23 - Nanofibrous smart bandages for wound care, Magnus S. Ågren (Ed.), Wound Healing Biomaterials, Woodhead Publishing, 483-499

97. T. Grothe, C. Großerhode, T. Hauser, P. Kern, K. Stute, A. Ehrmann, 2017b, Needleless electrospinning of PEO nanofiber mats, Advances in Engineering Research 102, 54-58

98. A. Mahapatra, B.G. Mishra, G. Hota, 2013, Electrospun Fe2O3–Al2O3 nanocomposite fibers as efficient adsorbent for removal of heavy metal ions from aqueous solution, Journal of Hazardous Materials, Vol. 258–259, 116-123

99. K. Kosmider, J. Scott, 2002, Polymeric nanofibers exibit an enhanced air filtration performance, Filtration Separation, 39 (6), 20-22

100. K. Graham, M. Ouyang, T. Reather, T. Grafe, B. McDonald, P. Knauf, 2002, Polymeric Nanofibers in Air Filtration Applications, Donaldson Co. Inc., Presented at the 15th Annual Technical Conference & Expo of the American Filtration and Separation Society, Galveston, Texas, April 9-12

101. X. Wang, B.S Hsiao,2016, Electrospun nanofiber membranes, Current Opinion in Chemical Engineering, Volume 12

102. R.S. Barhate, S. Ramakrishna, 2007, Nanofibrous filtering media: filtration problems and solutions from tiny materials, J Membr. Sci, 296

103. S. Kaur, S. Sundarrajan, D. Rana, R. Sridhar, R. Gopal, T. Matsuura, S. Ramakrishna, 2014, Review: the characterization of electrospun nanofibrous liquid filtration membranes, J. Mater. Sci, 49

104. S. Homaeigohar, M. Elbahri, 2016, Nanocomposite electrospun nanofiber membranes for environmental remediation, Materials, 7

105. S. Homaeigohar, M. Elbahri, 2014, Nanocomposite electrospun nanofiber membranes for environmental remediation, Materials, 7

106. Z.M. Huang, Y.Z. Zhang, M. Kotaki, S. Ramakrishna, 2003, review on polymer nanofibers by electrospinning and their applications in nanocomposites, Compos Sci Technol, 63 (15), 2223-2253

107. S.H. Lee, B.C. Ku, X. Wang, L.A. Samuelson, J. Kumar, 2002, Design, synthesis and electrospinning of a novel fluorescent polymer for optical sensor applications, Mater Res Soc Symp. – Pro., 403-408

108. X. Wang, C. Drew, S.H. Lee, K.J. Senecal, J. Kumar, L.A. Samuelson, 2002, Electrospun nanofibrous membranes for highly sensitive optical sensors, Nano Lett, 2 (11), 1273-1275

109. S. Jayaraman, V. Aravindan, P. Suresh Kumar, W.C. Ling, S. Ramakrishna, S. Madhavi, 2014, Exceptional performance of TiNb2O7 anode in all one-dimensional architecture by electrospinning, ACS Applied Materials and Interfaces, 6, 8660-8666

110. A. Khajuria, P. N. Balaguru,1992, Plastic shrinkage characteristics of fiber reinforced cement composites. In: Swamy RN, editor: Fibre reinforced cement composites, London, Routledge, Taylor & Francis, 82–90

111. M.M. Iovleva, V.N. Smirnova, G.A. Budnitskii, 2001, The solubility of poyacrylonitrile, Fibre Chemistry, 33, No. 4, 262

112. E. Cipriani, M. Zanetti, P. Bracco, V. Brunella, M.P. Luda, L. Costa, 2016, Crosslinking and carbonization processes in PAN films and nanofibers, Polymer Degradation and Stability, 123, 178-188

113. Y. Eom, B. C. Kim, 2014, Solubility parameter-based analysis of polyacrylonitrile solutions in N,N-dimethyl formamide and dimethyl sulfoxide, Polymer, 55 (10), 2570-2577

114. S.K. Nataraj, K.S. Yang, T.M. Aminabhavi, 2012, Polyacrylonitrile-based nanofibers—A state-of-the-art review, Progress in Polymer Science, 37, (3), 487-513

115. S.N. Arshad, M. Naraghi, I. Chasiotis, 2011, Strong carbon nanofibers from electrospun polyacrylonitrile, Carbon, 49, 1710-1719

116. M. Rahaman, A. Ismail, A. Mustafa, 2007, A review of heat treatment on polyacrylonitrile fiber, Polym Degrad Stab, 92, 1421–32

117. C. Song, T. Wang, Y. Qiu, J. Qiu, H. Cheng, 2009, Effect of carbonization atmosphere on the structure changes of PAN carbon membranes, J Porous Mater, 16, 197-203

CHAPTER 2

EXPERIMENTAL METHODOLOGY

## 2. EXPERIMENTAL METHODOLOGY

This section presents the general methodology used in the dissertation. The relevant aspects in terms of preparation and characterization of the investigated materials and methods as well as specific aspects will be explained in more detail here. The sections presented here contain only the key information, specific conditions, and experimental units used to prepare and characterize samples. If required, more detailed information and descriptions can be found in the respective chapters.

### 2.1 Materials and chemicals

For the investigations shown here, a PAN solution for electrospinning was prepared with 16 % solid content in low-toxic solvent DMSO (dimethyl sulfoxide) by stirring for 2 hours at room temperature. This concentration was found ideal in previous tests to avoid clogging of the nozzle as well as electrospraying instead of electrospinning.

- In this work, inexpensive PAN knitted yarn was used for the production of nanofiber mats.

- The solvent DMSO (dimethyl sulfoxide) (min. 99.9 % was purchased from S3 Chemicals, Germany) and was used for all electrospinning solutions.

- For preparation of PAN / gelatin nanofiber mats, gelatin was purchased from Abtei, Germany.

- As a substrate, household aluminum foil (from Rewe, Bielefeld, Germany) was used for creation of carbon-metal composites in addition to the common polypropylene (PP) substrate typically used in the electrospinning machine Nanospider.

## 2.2 Electrospinning set-up

For the electrospinning of nanofiber mats the wire-based nanospinning machine "Nanospider Lab" (Elmarco, Czech Republic) was used. This needleless electrospinning machine is well suited for experimental work and product development in academic research field, provides an effective production of small quantities of materials and the capability of spinning a variety of polymers. In addition, many of the process parameters can be changed and adjusted very easily. In Fig. 2.1 the needleless nanospinning machine is illustrated.
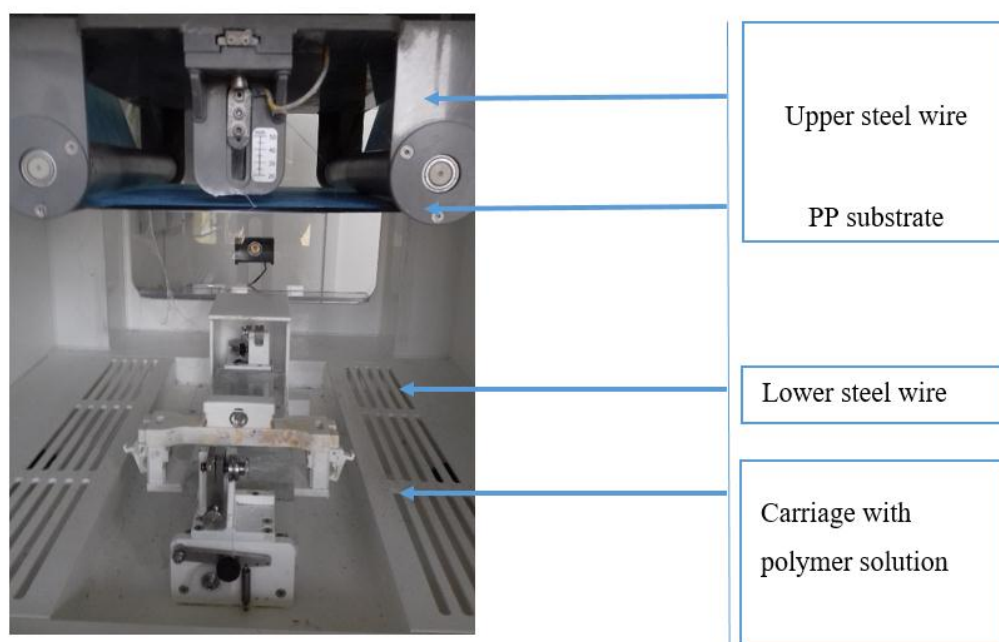


Fig. 2.1 Needleless nanospinning machine "Nanospider Lab" (Elmarco, Czech Republic).

The electrospinning process can be described as follows: two steel wires (upper and lower wire) are mounted in a high voltage field. The lower steel wire is coated with spinning solution which comes from a nozzle fixed on a movable carriage. The electric field pulls the solved polymer to the counter electrode which is shielded by a substrate. The nanofibers adhere to the substrate and can be easily removed after the spinning process is finished. The electrospinning machine can be used to produce nanofiber mats consistently and with consistent quality. In this work a polypropylene (PP) non-woven fabric (from Elmarco) was used as a substrate for the deposition of nanofibers by electrospinning process. Other substrates like cellulose, synthetics, fiberglass and foils are also possible to use. The technical data of the nanospinning machine are given below (see Table 2.1) [1].

Table 2.1 Technical data of wire-based nanospinning machine "Nanospider Lab" (Elmarco).

| Parameter | Range |
| --- | --- |
| Spinning voltage [kV] | 0-80 |
| Substrate speed [mm/min] | 0-500 |
| Spinning (Electrode-electrode) distance[mm] | 120-240 |
| Nozzle diameter [mm] | 0.6-1.5 |
| Carriage speed [mm/s] | 50-300 |
| Ground-substrate distance [mm] | 50-240 |
| Spinning duration [min] | 5-30 |
| Working temperature [°C] | 20-20 |
| Working humidity [% RH] | 20-40 |
| Process air flow [$m^3$/hour] | 30-250 |
| Polymer filling; batch mode – volume [ml] | 10-500 |
| Max substrate width [mm] | 550 |
| Max. diameter of substrate roll [m] Integrated unidirectional substrate unwind/rewind | 400 |

The following parameters were performed by the creating of PAN nanofiber mats by studying the influence of spinning parameters on the needleless electrospinning process: high voltage of 80 kV, a nozzle diameter of 0.9 mm and a carriage speed of 150 mm/s during a spinning time of 5 min. The carriage speed is the speed at which the carrier with the spinning nozzle drives along the electrode wire and coats it with solved polymer. The substrate speed was 20 mm/min. With substrate speed the rotation of the PP non-woven roll is meant where the nanofibers adhere in the electrospinning process. Later, the nanofibers can be easily removed from the PP substrate. The distance between the high voltage electrode and the middle of the substrate was varied between 120 mm and 240 mm (the maximum possible values). Detailed information and results from this series of experiments can be found in chapter 3.

Electrospinning of PAN/gelatin nanofiber mats was performed with the following spinning parameters: high voltage 70 kV, nozzle diameter 1.5 mm, carriage speed 100 mm/s, ground-substrate distance 240 mm, electrode-substrate distance 50 mm,

temperature in chamber 22 °C, relative humidity in chamber 33 %. See chapter 7 for more detailed information.

To create carbon-metal nanofiber mats (see chapter 8) the following spinning parameters were used: high voltage 60 kV, current approx. 0.04 mA, electrode–substrate distance 240 mm, nozzle diameter 0.8 mm, carriage speed 50 mm/s, substrate speed 50 mm/min, relative humidity 33 %, and temperature 22.0 °C. More detailed information of this series of experiments can be found in chapter 8.

## 2.3 Preparation of samples

For dimensional measurements samples were cut from the electrospun mats in dimensions of 50 mm x 50 mm. A frame of 40 mm x 40 mm was marked for dimension measurements while the "border" was used to fix some of the samples during stabilization. Afterwards the samples were weighed and labeled.

## 2.4 Fixation of nanofiber samples during stabilization

A problem which is less mentioned in the scientific literature is the dimension change of nanofibers during the stabilization process. In this work, fixed and unfixed nanofiber samples were compared during the stabilization process in order to find the differences in the morphology. To overcome the problem of undesired nanofiber dimensional change during the stabilization process, other research groups tried various techniques to minimize sample shrinkage. The tension during stabilization and carbonization influenced the tensile strength and Young modulus of carbon nanofibers [2]. A well-known problem in the stabilization of nanofibers is the contraction and shrinkage of nanofibers and the resulting increase in diameter and unwanted bending of nanofibers. Therefore, the fixation of the PAN nanofiber mats during the stabilization process is necessary to avoid contraction of the fibers, which is related to undesirable bending.

First, an attempt by preliminary tests was made to attach specimens to the grid in the oven using a paperclip stabilization process as can be seen in Fig. 2.2(a) and (b). It has been found that at higher temperatures above 250 °C, the samples are usually torn up from the grid because the tension was too strong. In addition, the samples stuck to the grid and it was not possible to remove them without losing small parts as

can be clearly seen in the Fig. 2.2(c) at the edges of sample that was stabilized by 250 °C. The electrospun PAN nanofiber mats are white in color and therefore relatively easy to label with ballpoint pens or permanent markers. In the stabilization process from nanofiber up to 220 °C, the labeling of samples was easy to read. With the increasing of the temperature in the stabilization process the color of samples changes from white to yellow and dark brown as can be seen in Fig. 2.2(c). Over 250 °C, the color of samples changes to dark brown and labeling on the samples is no longer visible.



<div align="center">(a)         (b)         (c)</div>
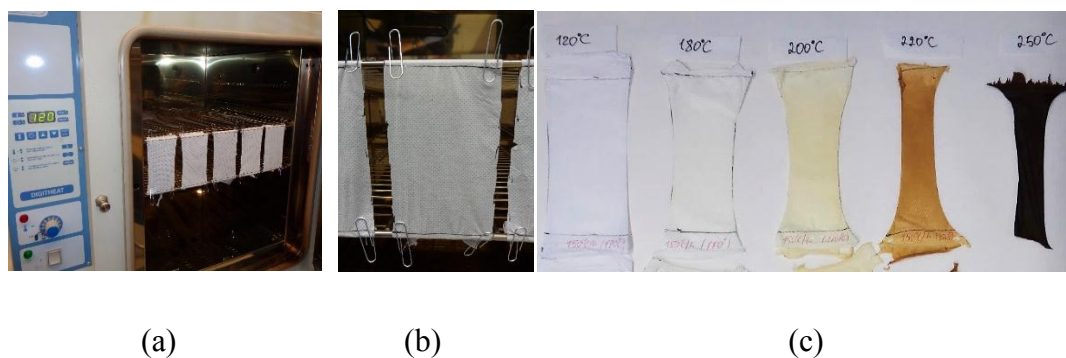
Fig. 2.2 (a) Fixed PAN nanofiber mats before stabilization, (b) fixing method with paperclips to prevent shrinkage of samples, (c) samples stabilized at 120 °C, 180 °C, 200 °C, 220 °C and 250 °C.

After this preliminary test, a fixing method with a metal frame was chosen because of the ease of use in this work. For dimensional measurements the samples were cut from the electrospun mats in defined dimensions and a frame was marked while the "border" was used to fix some of the samples during stabilization. For this, a metal frame of sufficient weight was applied to obtain the dimensions of the sample. In this method, the samples were also often torn from one side of the metal frame at temperatures over 250 °C but it was easier to prepare the samples without weight loss in comparison with fixation method in preliminary tests. It should be mentioned that fixing of samples with metal frame significantly reduces the effect of shrinkage and thickening of nanofibers, but this effect cannot be completely avoided. Furthermore, using PAN/gelatin blends as precursors for carbon nanofibers offers a new possibility to create long, straight fibers without many undesired conglutinations.

In addition, another attempt was made in this work to deal with the problem of undesired conglutinations of nanofiber suggesting a simple new approach to overcome this problem and to create a novel metal–carbon composite. Electrospun

PAN nanofiber mats on aluminum substrates offer an easy way to fix the nanofiber mats during the stabilization process without conglutinations of nanofibers. Moreover, at higher carbonization temperatures, aluminum-carbon composites can be formed which offer a promising application in many industrial fields. Moreover, using PAN/gelatin blends as precursors for carbon nanofibers offers a new possibility to create long, straight fibers without many undesired conglutinations.

## 2.5 Thermal treatment

Stabilizing of the first test PAN samples was performed in a drying and sterilizing oven ―Digitheat" (J. P. Selecta, Barcelona, Spain). Temperature was swept from 60 °C to 200 °C with a heating rate of 20 °C/h. Afterwards, isothermal treatment at 200 °C was performed. For carbonizing of nanofiber mats, the furnace CTF 12 / TZF 12 (Carbolite Gero Ltd., UK) was used. The stabilized samples as well as one original nanofiber mat were introduced before the furnace was evacuated and purged with nitrogen. The furnace was heated to 800 °C with a heating rate of 10 °C /min in a nitrogen flow of 150 mL/min (STP). The isothermal treatment was performed for 2 hours at 800 °C. The results of this test series can be found in the chapter 6.

In other series of experiments, a muffle furnace B150 (Nabertherm, Lilienthal, Germany) was used for the stabilization of nanofiber mats with heating rates of 0.5 °C/min, 1 °C/min, 2 °C min, 4°C/min, 8°C/min and 16 °C/min. In addition, samples were placed in the already heated oven. This resulted in a sudden decrease of the oven temperature by approximately 40 °C and a new increase to the desired temperature during approximately 2.5 - 3 minutes. This was done to test what happens when the samples are placed in a preheated oven. The values thus obtained are referred to as 16 °C/min in order to be able to represent them in the heating rate-dependent diagrams. More detailed information about stabilization parameters can be found in the chapter 5.

The samples of electrospun PAN / gelatin nanofiber mats were stabilized in a muffle furnace B150 (Nabertherm) with stabilization temperatures between 240 °C and 300 °C with heating rates between 0.5 °C/min, 1 °C/min, 2 °C/min and 4 °C/min. Afterwards an isothermal treatment was performed at the final temperature for 1 hour. For each combination of heating rate and temperature, the samples were stabilized. Here the difference between and unfixed samples was investigated. After

stabilization procedure carbonization of the PAN/gelatin nanofiber mats (see chapter 8) was performed using furnace CTF 12/TZF 12 (Carbolite Gero Ltd., Hope, UK). A thermal treatment was performed with a temperature of 800 °C with a heating rate of 10 °C/min in a nitrogen flow of 150 mL/min (STP), followed by isothermal treatment for 1 hour.

For the creation of carbon-metal nanofibers the samples of the electrospun nanofiber mats were stabilized in a muffle furnace B150 (Nabertherm, Lilienthal, Germany), approaching a typical stabilization temperature of 280 °C at a heating rate of 1 °C/min, followed by isothermal treatment at this maximum temperature for 1 hour. In this case the samples electrospun on aluminum were not separated from their aluminum substrate. Afterwards, carbon-metal nanofiber mats were carbonized using a furnace CTF 12/TZF 12 (Carbolite Gero Ltd., Hope, UK), approaching temperatures of 500 °C or 800 °C. As in other test series the heating rate was 10 °C/min, the nitrogen flow 150 mL/min (STP), followed by isothermal treatment for 1 hour.

## 2.6 Materials characterization

In this section, devices and methods that were used in this work are explained in detail.

Masses of the samples were taken using an analytical balance (VWR). The software ImageJ 1.51j8 (from National Institutes of Health, Bethesda, MD, USA) was applied to determine the nanofiber diameters from SEM images using 50 fibers per sample.

For the color measurements in this work the instrument sph900 by Color-Lite was used. Here the colors of the samples were investigated. During stabilization process, the nanofiber mats samples change their color from white to honey-colored and when reaching higher temperatures to dark brown or black. The color measurements indicate at what temperature the stabilization process has already been completed. With a spectrophotometer, colors can be compared with a reference standard regardless of the user, ambient lighting or time. A spectrophotometer has the following operation; colors are measured by illuminating the sample and analyzing diffuse light. The resulting sample spectrum is compared to the spectrum of a known, usually white, area. Subsequently, spectral properties of the measured surface are

calculated. Thereafter, this sample spectrum is evaluated with a standard type of light and also with a color spectral value function. Thus, three values X, Y and Z are determined which depend on the type of light used and also on the color matching function. Normally, three color values DL *, Da * and Db * are usually characterized or summarized in a single value (DE*- ―delta" E). Hereby DL* means a difference in lightness/darkness value. Da* is a difference on red/green axis. And Db* is a difference on yellow/blue axis. DE* means a total difference in color value [3].

Differential scanning calorimetry (DSC) is the measurement of the change of the difference in the heat flow rate between the reference sample and the sample while both samples are subjected to a defined temperature. Differential scanning calorimetry is used to determine glass transition temperatures, measurement points, crystallization points or heat formation for specific materials. Differential scanning calorimetry is a thermal analysis method for measuring the amount of heat flow released or absorbed by a sample during heating, cooling, or an isothermal process. Often, DSC is used to characterize materials such as polymers or composites to analyze the types of temperatures and stresses a material can tolerate [4]. In this work for the differential scanning calorimetry (DSC) measurements, a DSC Q100 (TA Instruments) was used.

Fourier Transformed Infrared Spectroscopy (FTIR) is useful for identifying chemicals that could be either organic or inorganic. It is a powerful tool for identifying types of chemical bonds (functional groups). The wavelength of the absorbed light is characteristic of the defined chemical bond. The evaluation of the recorded IR spectra is carried out via known comparison or sample spectra of known reference materials which are available in extensive "infrared libraries". The absorption bands occurring in the IR spectra are assigned to the vibrations of individual atomic groups (functional groups) [5]. For the present work the Fourier-Transform Infrared Spectroscopy (FTIR) measurements were performed with an Inc. Excalibur 3100 (Varian, Inc., Palo Alto, CA, USA).

The principle of the Scanning Electron Microscope (SEM) is based on the scanning of the object surface by means of a finely-collimated electron beam. To avoid interactions with atoms and molecules in the air, the complete process normally takes place in a high vacuum. In scanning electron microscopy only conductive surfaces can be displayed. Therefore, samples are sometimes specially prepared and the

surfaces of samples can be made conductive by vapor deposition of a metal film such as gold [6]. The nanofiber mats and composites were evaluated in this work by scanning electron microscopy (SEM) JSM-6490 LV, Jeol Ltd., Japan, as well as scanning electron microscopy (SEM) images were taken by a Zeiss 1450VPSE (Oberkochen, Germany) with a resolution of 5 nm or a JSM-840 microscope, respectively, using a nominal magnification of 5000 x.

Investigation of the nanofiber mat morphologies was performed by a confocal laser scanning microscope (CLSM) VK-9000 or VK-9700 (both by Keyence, Neu-Isenburg, Germany) with a nominal magnification of 2000 x, using three areas per sample. A Confocal Laser Scanning Microscope (CLSM) is a special light microscope in which a focused laser beam comes out of the lens and scans an object point by point and thus the assembled points form an image [6]. The software ImageJ 1.51j8 (from National Institutes of Health, Bethesda (MD), USA) was applied to determine the ratio of membrane / nanofiber areas in the CLSM images. Optical images of the nanofiber mats were taken using a confocal laser scanning microscope (CLSM) VK-100 with a nominal magnification of 2000×.

A PERMETEST (SKIN MODEL), built by Sensora Textile Measuring Instruments and Consulting, Czech Republic, was used in this work to measure the water vapor resistance on three areas per sample. This fast response measuring instrument (Skin Model) provides non-destructive determination of water-vapor and thermal resistance or permeability of textile fabrics, nonwovens, foils and paper sheets. The PERMETEST (SKIN MODEL) offers measurements very similar to ISO-11092 standard. The results are evaluated according to the same procedure as required in this ISO [7]. The ISO-11092 standard is the norm that deals with the comfort of clothing textiles. This ―Sweating guarded-hotplate" test method, often referred to as a ―skin model", aims to simulate the heat transport and mass transport processes that take place near the skin of a human. The water vapor transmission resistance, also referred to as ―breathability", is measured with the skin model. The water vapor transmission resistance here is a measure of the transport of vaporous vapor through the textile.

This test method is carried out as follows: an electrically heated porous metal plate is covered with a film which is permeable to water vapor but impermeable to liquid water. Water is supplied to this heated plate which passes through the film as water

vapor. Throughout the test, a constant temperature is maintained and conditioned air flows across a channel and parallel to the heated plate, as specified in this international standard. Here, the water vapor transmission resistance of a material is determined by subtracting the water vapor transmission resistance of the adhesive air layer above the surface of the measuring head from the resistance of the measuring sample plus the layer of adhesive air [8].

## 2.7 References

1. ELMARCO s.r.o. – EUROPE, 2018, http://www.elmarco.com/upload/soubory/dokumenty/159-1-ns-1s500u-profile-151118-72dpi.pdf, accessed on 01.08.2018

2. S. Ma, J. Liu, M. Qu, X. Wang, R. Huang, J. Liang, 2016, Effects of carbonization tension on the structural and tensile properties of continuous bundles of highly aligned electrospun carbon nanofibers, Mater Lett, 183, 369–373

3. ColorLight GmbH, 2018, https://www.colorlite.de/sites/default/files/artikelanhang/broschure_sph900_sph870_de.pdf, accessed on 01.06.2018

4. G. Höhne, W. Hemminger, H.-J. Flammersheim, 2010, Differential Scanning Calorimetr, second ed Springer, Berlin

5. B.C. Smith, 2011, Fundamentals of Fourier Transformed Infrared Spectroscopy, Second Edition, CRC Press

6. S.L. Flegler, J. W. Heckman, K. L. Klomparens, 2009, Elektronenmikroskopie - Grundlagen, Methoden, Anwendungen. Spektrum Akademischer Verlag, 1995, Handbook of Sample Preparation for Scanning Electron Microscopy and X-Ray Microanalysis, Patrick Echlin, Springer, New York

7. L. Hes, 2018, Sensora+Textile Measuring Instruments&Consulting, http://www.sensora.eu/permetest.html, accessed on 01.06.2018

8. DIN Deutsches Institut für Normung e. V, 2018, Textiles – Physiological effects – Measurement of thermal and water-vapour resistance under steady-state conditions (sweating guarded-hotplate test) (ISO 11092:2014); German version EN ISO 11092:2014

CHAPTER 3


INVESTIGATION OF NEEDLELESS ELECTROSPUN PAN
NANOFIBER MATS

## 3. INVESTIGATION OF NEEDLELESS ELECTROSPUN PAN NANOFIBER MATS

## 3.1 Abstract

Polyacrylonitrile (PAN) can be spun from a nontoxic solvent (DMSO, dimethyl sulfoxide) and is nevertheless waterproof, opposite to the biopolymers which are spinnable from aqueous solutions. This makes PAN an interesting material for electrospinning nanofiber mats which can be used for diverse biotechnological or medical applications, such as filters, cell growth, wound healing or tissue engineering. On the other hand, PAN is a typical base material for producing carbon nanofibers. Nevertheless, electrospinning PAN necessitates convenient spinning parameters to create nanofibers without too many membranes or agglomerations. Thus we have studied the influence of spinning parameters on the needleless electrospinning process of PAN dissolved in DMSO and the resulting nanofiber mats.

## 3.2 Introduction

Electrospinning is a method to create mats from fine fibers, usually in the diameter range of some hundred nanometers. The process can be subdivided into electrospinning using a syringe to extrude the polymer which is spun, and needleless electrospinning. Both methods can be used to spin fibers from a molten polymer mass or from a polymer solution, opening this technology for a broad range of polymer materials.

In electrospinning from a solution, a suitable solvent has to be found to dissolve the desired polymer. This requirement often results in the problem that toxic, corrosive or other dangerous solvents have to be used which are hard to handle, especially in academic environments. Besides biopolymers, several of which can be spun from aqueous solutions [1,2], polyacrylonitrile (PAN) is of high interest since it is spinnable from dimethyl sulfoxide (DMSO). This solvent has to be handled with care because it increases penetration of other materials through the surface of the skin, but it does not cause problems in medical or biotechnological applications [3].

This is why PAN is often used for electrospinning [4,5], often to created nanofiber mats which are afterwards carbonized in order to create carbon nanofibers [5-8].

PAN can also be used with embedded inorganic components like ZnO or MgO [9-11]. In spite of the technological relevance of this material, only few articles about the dependence of the nanofiber mat morphology on the spinning and material parameters can be found [12-14], none of which deals with needleless electrospinning. Previous investigations, however, have already shown the enormous influence of the polymer solution as well as the spinning conditions on the resulting nanofiber mats, with some parameters apparently having stronger effects than it was found in a previous systematic investigation of needleless electrospinning poly(ethylenglycol) (PEG) [15]. This is why our article depicts the results of systematic variations of different spinning parameters and the resulting changes in nanofiber mat morphologies.

## 3.3 Materials and Methods

For the investigation shown here, a PAN solution was prepared using 14 % PAN in DMSO by stirring for 2 hours at room temperature. This concentration was found ideal in previous tests – lower concentrations tended to electrospraying, i.e. forming droplets instead of fibers, while higher concentrations became too highly viscous to flow through the spinning nozzle continuously without clogging it.

For electrospinning, the needleless nanospinning machine "Nanospider Lab" (Elmarco, Czech Republic) was used. The spinning parameters, such as high voltage, electrode-substrate distance, carriage speed, etc. were varied as depicted in Table 3.1. All manually changed parameters are marked by a light-blue background. Some parameters slightly changed due to the spinning process, while others remained unaltered (cf. Table 3.1). It should be mentioned that all nanofiber mats were electrospun for 5 min so that the measured areal weights of the mats are proportional to the flow of the polymer from the electrode to the substrate.

Table 3.1 Electrospinning parameters. Manually changed parameters are marked light-blue.

| Parameter | Min. | Max. |
|---|---|---|
| Voltage [kV] | 30 | 80 |
| Current [mA] | 0.003 | 0.07 |
| Nozzle diameter [mm] | 0.6 | 1.5 |
| Carriage speed [mm/s] | 50 | 300 |
| Substrate speed [mm/min] | | 0 |
| Ground-substrate distance [mm] | | 50 |
| Electrode-electrode distance [mm] | 120 | 240 |
| Temperature in spinning chamber [°C] | 23.0 | 24.6 |
| Rel. humidity in spinning chamber [%] | 31 | 33 |
| Spinning duration [min] | | 5 |
| Air flow [m$^3$/hour] | | 120 |

A confocal laser scanning microscope (CLSM) VK-9000 (Keyence) with a nominal magnification of 2000 x was used to investigate the nanofiber mat morphologies. Further examinations by FTIR (Fourier-transform infrared spectroscopy), TGA (thermogravimetric analysis) and DSC (differential scanning calorimetry) did not reveal any differences in chemical composition or crystallinity of the samples, respectively, and are thus not depicted here. The software ImageJ 1.51j8 (from National Institutes of Health, Bethesda, MD, USA) was applied to determine the nanofiber diameters from CLSM images using 50 fibers per sample.

## 3.4 Results and Discussion

Firstly, the influence of the electrode-electrode distance on the nanofiber creation was examined. In an earlier investigation of needleless electrospinning PEG [15], an increasing electrode-substrate distance resulting in decreasing currents but did not show significant impact on the resulting nanofiber mats. Fig. 3.1 depicts the nanofiber diameter distribution as well as the areal weights of the nanofiber mats, using a high voltage of 80 kV, a nozzle diameter of 0.9 mm and a carriage speed of 150 mm/s.

While the fiber diameters stay relatively constant within measurement accuracy, the areal weight changes strongly with varied electrode distance. On the one hand, this finding can be attributed to placing the electrospun fibers more concentrated in the middle of the substrate for smaller electrode distances. On the other hand, reducing the electrode distance increased the electric field between both electrodes and thus the force dragging the solved polymer to the substrate.

Fig. 3.2 depicts CLSM images of nanofiber mats gained with the maximum and minimum electrode distances. Here it becomes visible that the nanofiber mats show significantly more irregularities and membrane-like areas for a reduced electrode-electrode distance. Apparently, a compromise must be found between producing higher areal weights in a given time and producing more constant nanofiber mats.



(a)                                    (b)
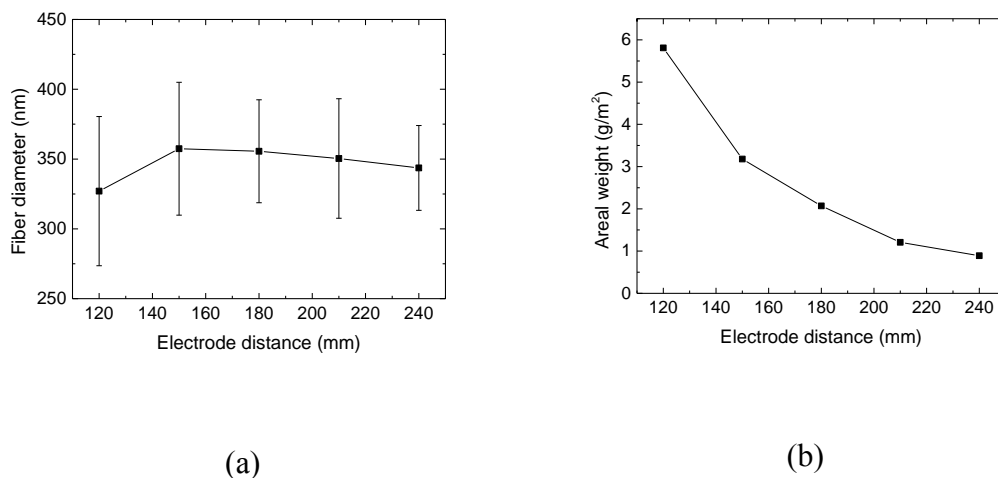
Fig. 3.1 Fiber diameters (a) and areal weights (b) of different PAN nanofiber mats as functions of the electrode-electrode distance.
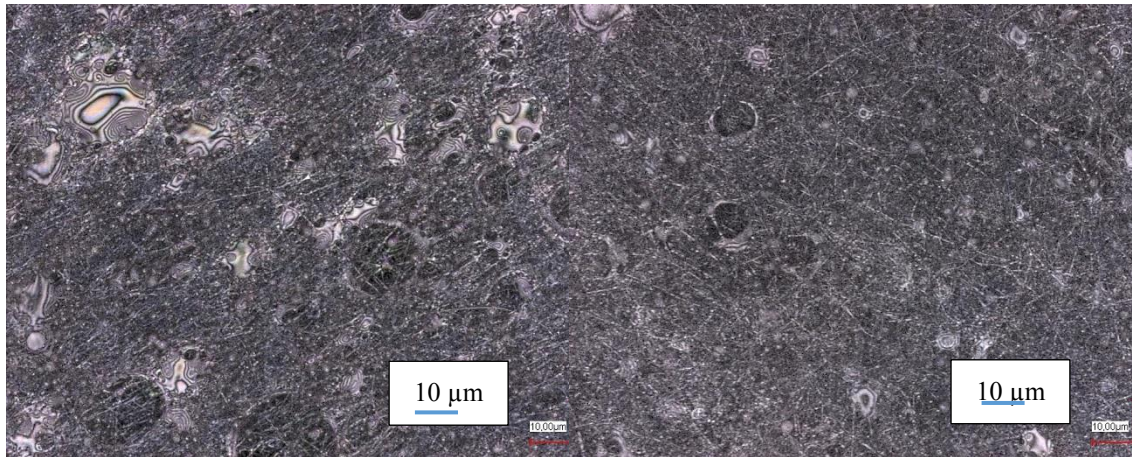
Fig. 3.2 PAN nanofiber mats, produced with 120 mm (a) and 240 mm (b) electrode-electrode distance, respectively.

In the next step, the high voltage was modified, using the maximum electrode distance of 240 mm, a nozzle diameter of 0.9 mm and a carriage speed of 150 mm/s. Fig. 3.3 depicts the resulting fiber diameters and areal weights.

While the fiber diameters show a slight tendency of decreasing with increasing voltage, opposite to previous results of electrospinning PEG which revealed no such dependency [15], the areal weight is approx. proportional to the high voltage. Spinning with 30 kV resulted in a nanofiber mat too fine to be removed from the substrate, impeding areal weight measurement. Extrapolating this graph to 30 kV, the areal weight can be assumed to be nearly 0.

The CLSM images of the resulting nanofiber mats, however, show more clearly the influence of the high voltage (Fig. 3.4). While higher voltages produce significantly denser nanofiber mats, lower voltages result in more linearly oriented fibers which are clearly differentiated from each other. Due to the strong correlation of the areal weight with the voltage, here again a compromise must be found between ―better" nanofibers and higher material output.

Additionally, it should be mentioned that lower voltages result in increased formation of beads along the fibers, a phenomenon which is nearly invisible for spinning at 80 kV (cf. Fig. 3.4). These beads are well-known for PAN and some other polymers and are attributed to too low solution viscosity [16,17] in the literature and resulting capturing of not yet completely solidified fibers on the substrate [18].
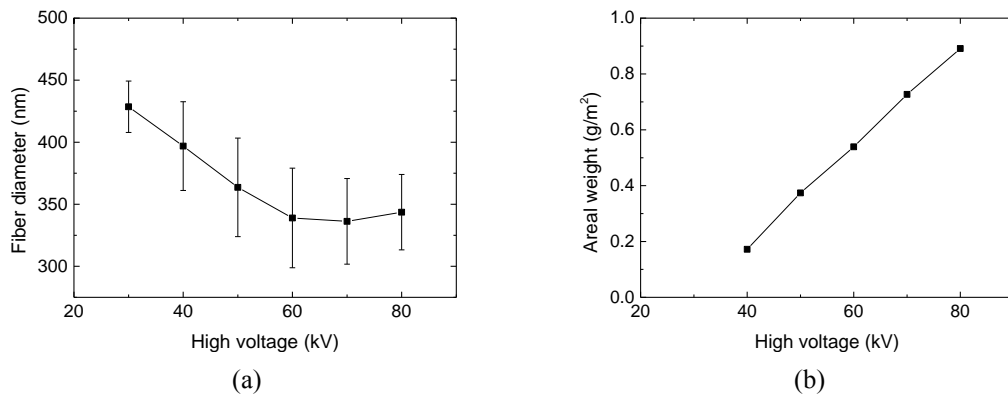
Fig. 3.3 Fiber diameters (a) and areal weights (b) of different PAN nanofiber mats as functions of the high voltage.



(a)                                                    (b)
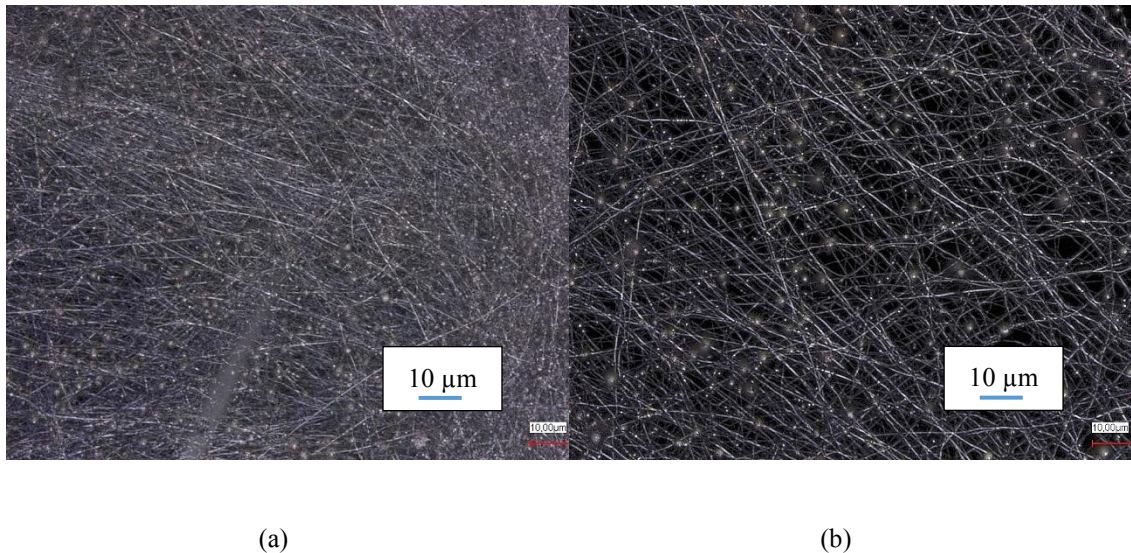
Fig. 3.4 PAN nanofiber mats, produced with high voltages 60 kV (a) and 30 kV (b), respectively.

In the next step, the carriage speed – i.e. the velocity with which the carrier with the spinning nozzle drives along the electrode wire and coats it with solved polymer – was modified. For the other spinning parameters, the maximum high voltage of 80 kV and the maximum electrode distance of 240 mm were chosen in combination with a nozzle diameter of 0.9 mm. The resulting fiber diameters and areal weights are depicted in Fig. 3.5. While no significant deviations of the fiber diameter with the carriage speed were measured, the areal weight decreases with increasing carriage speed. This finding was expected since a higher carriage speed should be correlated with a reduced polymer coating on the electrode wire.

The CLSM images of the nanofiber mats gained with maximum and minimum carriage speed are depicted in Fig. 3.6. Similarly, to the findings described above, the higher areal weight is again correlated with the lower fabric quality. For the lowest carriage speed, several membrane-like areas and inhomogeneities are visible, while the highest carriage speed results in a significantly more even nanofiber mat with more straight fibers.

Finally, the impact of the nozzle diameter was investigated, changing between two commercially available nozzles (0.6 mm and 0.9 mm) as well as one nozzle with manually increased diameter (1.5 mm). Again, the maximum high voltage of 80 kV, the maximum electrode distance of 240 mm and a carriage speed of 150 mm/s were used. The results are depicted in Fig. 3.7.



(a)                                                    (b)
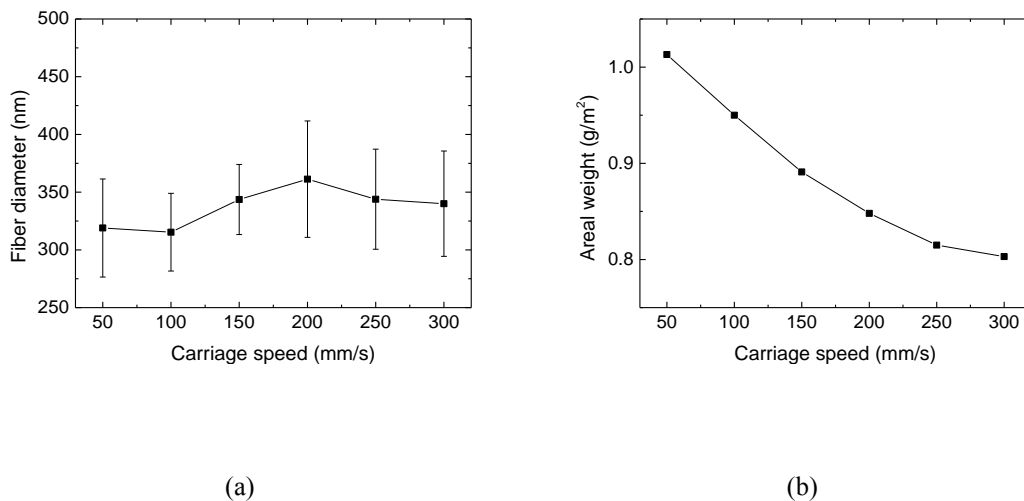
Fig. 3.5 Fiber diameters (a) and areal weights (b) of different PAN nanofiber mats as functions of the carriage speed.
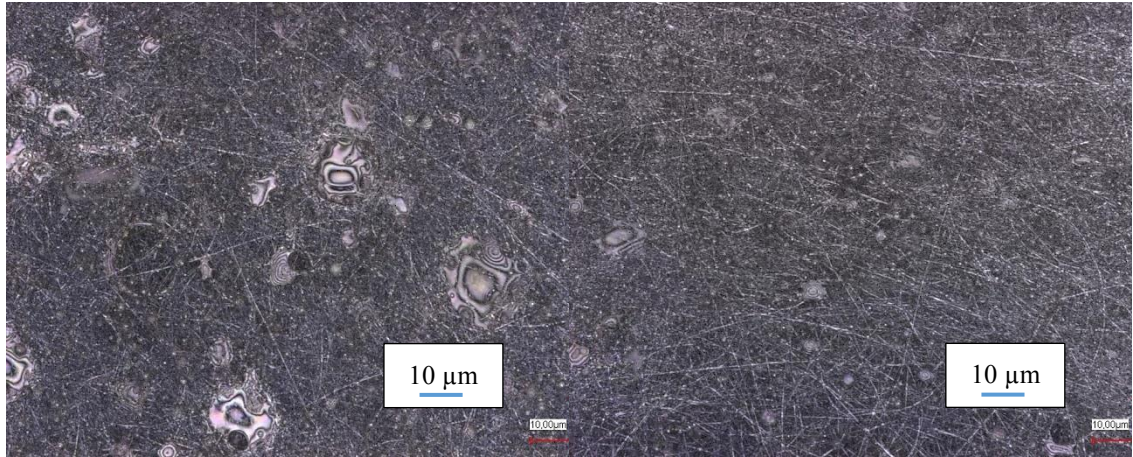
(a)                                                    (b)

Fig. 3.6 PAN nanofiber mats, produced with carriage speeds of 50 mm/s (a) and 300 mm/s (b), respectively.

As expected, the areal weight grows with increasing nozzle diameter, since through a larger nozzle more polymer solution can be coated on the electrode wire. On the other hand, no significant differences in the fiber diameter are visible.

Nevertheless, it should be mentioned that the nanofiber mat quality considerably changes with the nozzle diameter (Fig. 3.8). With the 0.6 mm nozzle, straighter fibers are produced than with the middle nozzle size of 0.9 mm (Fig 3.2). Increasing the nozzle size to 1.5 mm, the nanofiber mat becomes severely irregular, with several holes and membrane-like areas. It should be mentioned that this study was not performed with the aim of producing ideal nanofibers since other parameters, such as the spinning mechanism, the spinning chamber geometry, air flow through the chamber and especially the relative humidity in the spinning chamber significantly influence the nanofiber mat morphologies, necessitating that these ―ideal" conditions are defined for each spinning situation separately. Instead, this study aims at giving hints which parameters influence the fiber diameters, areal weights and last but not least the nanofiber mat morphologies in which ways.
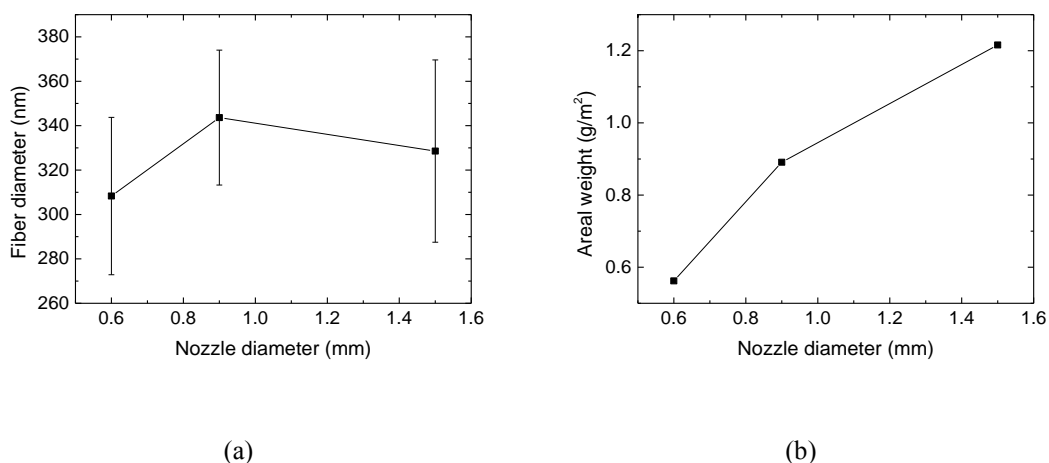
Fig. 3.7 Fiber diameters (a) and areal weights (b) of different PAN nanofiber mats as functions of the nozzle diameter.
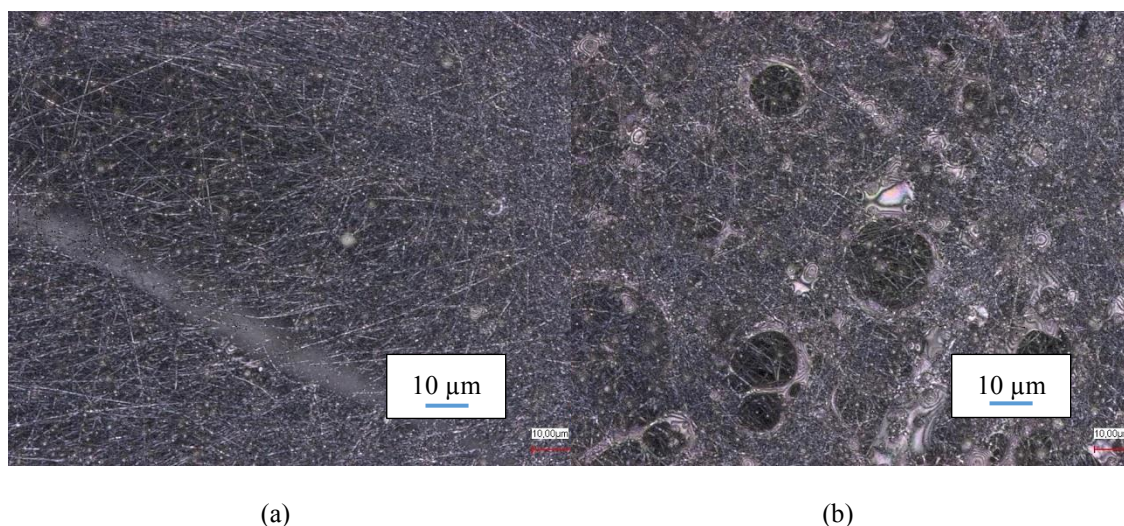


Fig. 3.8 Nanofiber mats, produced with nozzle diameters of 0.6 mm (a) and 1.5 mm (b), respectively.

## 3.5 Conclusions

To conclude, we have compared PAN nanofiber mats electrospun with different parameters. While the areal weights depend significantly on all parameters under investigation, the nanofiber diameters often show only weak trends or no deviations at all. Nevertheless, the nanofiber mat morphologies change severely with the electrode distance, the high voltage, the carriage speed and the nozzle diameter. Thus, for the production of high-quality nanofibers it is indispensable to examine the electrospun nanofiber mats by CLSM, scanning electron microscopy or other techniques which allow for investigating the nanofibers with sufficient resolution.

## 3.6 References

1. N. Grimmelsmann, S. V. Homburg, A. Ehrmann, IOP Conference Series: Materials Science and Engineering 213, 012007(2017).

2. T. Grothe, C. Großerhode, T. Hauser, P. Kern, K. Stute, A. Ehrmann, Advances in Engineering Research 102, 54-58 (2017).

3. C. Großerhode, D. Wehlage, T. Grothe, N. Grimmelsmann, S. Fuchs, J. Hartmann, P. Mazur, V. Reschke, H. Siemens, A. Rattenholl, S. V. Homburg, A. Ehrmann, AIMS Bioengineering 4, 376-385 (2017).

4. B. Maddah, M. Soltaninezha, K. Adib, M. Hasanzadeh, Separation Science and Technology 52, 700-711 (2017).

5. G. Panthi, S. J. Park, S. H. Chae, T. W. Kim, H. J. Chung, S. T. Hong, M. Park, H. Y. Kim, Journal of Industrial and Engineering Chemistry 45, 277-286 (2017).

6. R. E. Neisiany, J. K. Y. Lee, S. N. Khorasani, S. Ramakrishna, Journal of Applied Polymer Science 134, 44956 (2017).

7. G. H. Kim, S. H. Park, M. S. Birajdar, J. W. Lee, S. C. Hong, Journal of Industrial and Engineering Chemistry 52, 211-217 (2017).

8. J. Y. Guo, Q. J. Niu, Y. C. Yuan, I. Maitlo, J. Nie, G. P. Ma, Applied Surface Science 416, 118-123 (2017).

9. M. Kancheva, A. Toncheva, D. Paneva, N. Manolova, I. Rashkov, N. Markova, Journal of Inorganic and Organometallic Polymers and Materials 27, 912-922 (2017).

10. F. E. C. Othman, N. Yusof, H. Hasbullah, J. Jaafar, A. F. Ismail, N. Abdullah, N. A. H. M. Nordin, F. Aziz, W. N. W. Salleh, Journal of Industrial and Engineering Chemistry 51, 281-287 (2017).

11. I. Iatsunskyi, A. Vasylenko, R. Viter, M. Kempinski, G. Mowaczyk, S. Jurga, M. Bechelany, Applied Surface Science 411, 494-501 (2017).

12. H. T. Niu, X. G. Wang, T. Lin, Journal of Engineered Fibers and Fabrics 7, 17-22 (2012).

13. S. V. Lomos, K. Molnar, Express Polymer Letters 10, 25-35 (2016).

14. J. N. Zhang, M. Y. Song, D. W. Li, Z. P. Yang, J. H. Cao, Y. Chen, Y. Xu, Q. F. Wei, Fibers and Polymers 17, 1414-1420 (2016).

15. T. Grothe, J. Brikmann, H. Meissner, A. Ehrmann, Materials Science 23, 342-349 (2017).

16. H. Fong, I. Chun, D. H. Reneker, Polymer 40, 4585-4592 (1999).

17. Z.-M. Huang, Y.-Z. Zhang, M. Kotaki, S. Ramakrishna, Composites Science and Technology 63: 2223-2253 (2003).

18. E. Kostakova, M. Seps, P. Pokorny, D. Lukas, eXPRESS Polymer Letters 8, 554-564 (2014).

53

CHAPTER 4


WATER VAPOR PERMEABILITY THROUGH PAN NANOFIBER
MAT WITH VARYING MEMBRANE – LIKE AREAS

# 4. WATER VAPOR PERMEABILITY THROUGH PAN NANOFIBER MAT WITH VARYING MEMBRANE-LIKE AREAS

## 4.1 Abstract

Electrospinning can be used to produce nanofiber mats from diverse polymers which can be used as filters etc. Depending on the spinning parameters, also nano-membranes, i.e. non-fibrous mats, can be produced as well as mixtures between both morphologies. The ratio of membrane to fibrous areas can be tailored by the distance between the high voltage electrode and the substrate. Here, the impact of the mat morphology on the water vapor permeability through polyacrylonitrile nanofiber mats with different membrane-like areas is shown, allowing for tailoring the permeability between 0.1Pa·m²/W and more than 10 Pa·m²/W. In this way it is possible to create finest filters as well as nearly impenetrable thin membranes with the same technology.

## 4.2 Introduction

Electrospinning is a technology allowing for creation of fine fibers with diameters between some ten and several hundred nanometers, sometimes a few micrometers. The electrostatic forces in a strong electric field draw a molten or dissolved polymer to a substrate, at the same time stretching and drying the polymer so that finest fibers are formed and finally placed on the substrate. Diverse polymers, polymer blends and other materials can be used to create such nanofiber mats, [1-3] amongst them a broad variety of biopolymers, but also typical industrially used polymers such as polyacrylonitrile (PAN), polyamides, polyesters, etc.

Nanofibers created by electrospinning have round cross-sections in most cases whose diameters can be changed by modifying the polymer solid content in the solution / melt as well as other spinning and solution parameters. [4-5] Besides this typical form, it could be shown that flat ribbons can also be produced. [6-7] Pure droplets [8] or combinations of droplets and fibers are also possible results of the electrospinning process. [4,9]

Finally, it is possible to create mixtures between fibers and membranes or pure membranes. In a former project, the feasibility of creating mats with tailored fiber/membrane area ratios was investigated especially for chitosan/poly(ethylene

glycol) (PEG) blends, finding that the chitosan:PEG ratio was crucial for the mat morphology. [10,11] Another way to intentionally create membrane areas is adding surfactants to reduce the surface tension of the spinning solution and thus avoid fiber formation. [12]

An interesting material for the possible use in filters etc. is PAN which is not water-soluble and can thus be utilized without a further stabilization step. For PAN, it could be shown that by changing the distance between the high voltage electrode and the substrate, the morphology could be varied between pure nanofibers for large distances and pure membranes for small distances. [13] This finding can be attributed to the flight time of the fibers – if this time is reduced, the solvent is not completely evaporated before the substrate is reached, and the still partly dissolved fibers can unite to finally form a fine membrane instead of single fibers.

This effect means not only that the chosen distance between the high voltage electrode and the substrate is relevant for the resulting morphology, i.e. the ratio of membrane to nanofiber areas, but deviations from the middle of the substrate – where the distance to the high voltage electrode is smallest – to the borders can also be expected. However, in the scientific literature, only few reports about examinations of this effect can be found.

Niu *et al.*, e.g., calculated the influence of different fiber generator geometries, amongst which they also investigated cylinders with different diameters. They found that the electric field intensity in the middle area increased with decreasing cylinder diameter, i.e. should be highest for a thin wire, while at the same time the discrepancies along the whole substrate increased. [14] Wang *et al.* used a simulation to optimize the electric field in a series of modelled designs, starting from a cylindrical spinneret. [15] Fractal spinnerets were optimized by simulations and found to reach more homogeneous electric field distributions than recent needleless electrospinning technologies. [16] Earlier research concentrated on replacing the single needle technology – which results in the most non-uniform electrical field distribution – by a flat spinneret to gain more uniform nanofiber mats. [17] Other simulations revealed that even along a cylinder used as spinneret, the electric field was not constant but concentrated along the cylinder ends. [18]

Direct correlations between the position on the substrate and the nano-mat morphology, however, were not yet reported in the scientific literature to the best of our knowledge.

In this paper, the water vapor resistance of mats with varying morphologies between pure nanofibers and pure membranes is examined. Although this property is essential for many applications, especially for filtration, it is only scarcely investigated for nanofibers mats. Recently, two methods (dry cup method and tube method) of measuring water vapor diffusion through a polyurethane nanofiber mat were compared, without using these methods to examine the influence of spinning parameters on the water vapor permeability. [19] The water vapor permeability of an electrospun nanofiber mat was not significantly altered by a polyurethane coating. [20] For a membrane consisting of hollow fibers, water vapor permeability was investigated dependent on operating temperature and other operating parameters. [21] Linking the inter-fiber junction points after the spinning process by exposing a nanofiber mat to a solvent vapor was shown to not significantly reduce the water vapor permeability. [22] The effect of fluorination on water vapor permeation was studied for polyurethane nanofiber mats. [23] The influence of modification of the nanofiber web density on water resistance combined with water vapor and air permeability was investigated for layered fabric structures consisting of electrospun nanofiber mats and different substrates. [24] However, investigations of the transition between nanofiber mat and membrane in terms of water vapor permeability cannot be found in the literature.

## 4.3 Materials and Methods

The wire-based nanospinning machine "Nanospider Lab" (Elmarco, Czech Republic) was used for electrospinning, applying a high voltage of 80 kV, a nozzle diameter of 0.9 mm and a carriage speed of 150 mm/s during a spinning time of 5 min. The relative humidity in the spinning chamber was 32 % , air flow 120 m$^3$/hour and the temperature during spinning was 23 °C. Since the voltage strongly influences the nanofiber diameters and lengths, [13] it was kept constant to avoid possible modifications of the water vapor permeability due to modified pore diameters. Similarly, changing the nozzle diameter, carriages speed or spinning time would influence the nanofiber mat thickness and correspondingly again the water vapor

permeability which was avoided in this test series concentrating on the influence of membrane/nanofiber creation. The distance between the high voltage electrode and the middle of the substrate was varied between 120 mm and 240 mm (the maximum possible values).

The PAN solution for spinning was prepared with 14 % solid content in DMSO (dimethyl sulfoxide) by stirring for 2 hours at room temperature. This concentration was found ideal in previous tests to avoid clogging of the nozzle as well as electrospraying instead of electrospinning.

Investigation of the nanofiber mat morphologies was performed by a confocal laser scanning microscope (CLSM) VK-9000 (Keyence) with a nominal magnification of 2000 x, using three areas per sample.

A Permetest skin model (built by Sensora Textile Measuring Instruments and Consulting, Czech Republic) was used to measure the water vapor resistance [25] on three areas per sample.

The software ImageJ 1.51j8 (from National Institutes of Health, Bethesda (MD), USA) was applied to determine the ratio of membrane / nanofiber areas in the CLSM images using 50 fibers per sample.

## 4.4 Results and Discussion

Varying the distance between the electrodes results in nearly perfect nanofiber mats for the largest possible distance (Fig. 4.1a), nearly complete membranes without holes for the smallest possible distance (Fig. 4.1c) and diverse mixtures of both morphologies for intermediate distances (Fig. 4.1b). Apparently it is possible to tailor the desired fiber:membrane ratio by varying this parameter.

(a)
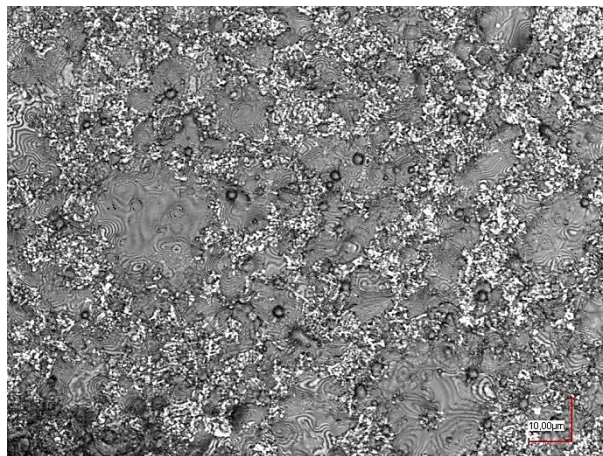


(b)
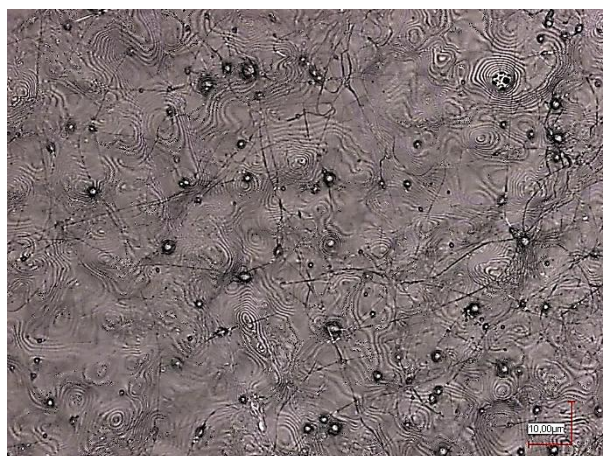


(c)

Fig. 4.1 Electrospun nanofiber mats prepared with approx. 2 % membrane ratio (a), 68 % (b) and 99.9 % membrane ratio (c). All scale bars have length 10 μm.

Fig. 4.2(a) depicts the influence of the electrode-substrate distance on the membrane ratio of the nanofiber mats. Besides measurements in the middle of the sample, i.e. on the direct line between both electrode wires, measurements along the borders were added for which the distances between substrate and high voltage electrode were calculated along the direct connection lines between the respective positions on the substrate and the wire. Although the newly formed nanofibers can be expected to impinge on the substrate under different angles and the electric fields are known to vary along the substrate area, combining all these measurements in one correlation works unexpectedly well.

An approximately linear decrease of the membrane ratio with increasing distance is visible until at ~ 230 cm distance the membrane areas vanish nearly completely. It should be mentioned that depending on the relative humidity in the spinning chamber and the solid content in the spinning solution, small membrane-like areas are often visible in ─pure" nanofiber mats (cf. Fig. 4.1a), so that the membrane area for a typical electrospinning situation is often not exactly zero.



(a)                                    (b)
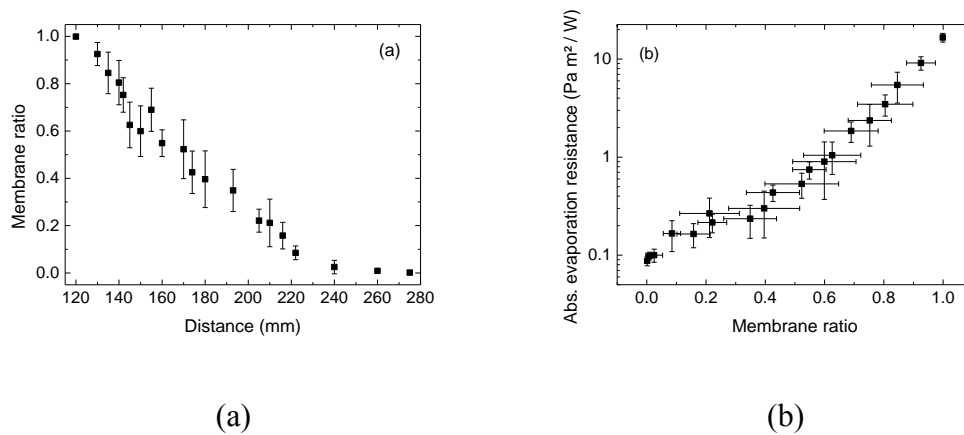
Fig. 4.2 Correlation between membrane ratio and electrode-substrate distance (a) and absolute evaporation resistance and membrane ratio (i.e. the membrane area divided by the whole area) in the PAN nanofiber mats (b).

Fig. 4.2(b) shows measurements of the absolute evaporation resistance and the membrane part of the nanofiber mats, as determined from 3 CLSM images per sample. Please note that the y-axis is scaled logarithmically. Generally, a linear correlation can be estimated in this graph, indicating an exponential correlation between absolute evaporation resistance and membrane ratio. Nevertheless, it must be mentioned that while the absolute evaporation resistance of most samples has

relatively small standard deviations, evaluations of the CLSM images with respect to the membrane ratios show partly large error bars, especially for membrane fractions around 0.2-0.8. This finding can be attributed to partly irregular nanofiber mats, exhibiting differing morphologies on the small dimensions visible in each CLSM image.

## 4.5 Conclusions

Concluding, PAN nanofiber mats with different ratios of nanofibers and membrane-like areas were prepared. The membrane: nanofiber ratio could be tailored by modifying the distance between the high voltage electrode and the substrate. Measuring the water vapor permeability showed an approximately exponential correlation between the absolute evaporation resistance and the membrane ratio. The water vapor permeability could be varied by more than two orders of magnitude, showing the possibilities to tailor this value by modifying the electrospinning parameters.

## 4.6 References

1. Kenawy, E. R., Layman, J. M., Watkins, J. R., Bowlin, G. L., Matthews, J. A., Simpson, D. G. and Wnek, G. E., 2003, Electrospinning of poly(ethylene-co-vinyl alcohol) fibers, Biomaterials, vol. 24(6), pp. 907-913.

2. Deitzel, J. M., Kleinmeyer, J. D., Hirvonen, J. K., and Beck Tan, N. C., 2001, Controlled deposition of electrospun poly(ethylene oxide) fibers, Polymer, vol. 42(19), pp. 8163-8170.

3. Reneker, D. H. and Chun, I., 1996, Nanometre diameter fibres of polymer, produced by electrospinning, Nanotechnology, vol. 7, pp. 216-223.

4. Larrondo, L., Manley R. S. J., 1981, Electrostatic fiber spinning from polymer melts. I. Experimental observations on fiber formation and properties, J Polym Sci Polym Phys Ed, vol. 19, pp. 909-920.

5. Grothe, T., Brikmann, J., Meissner, H., Ehrmann, A., 2017, Needleless electrospinning of poly(ethylene oxide) , Materials Science, vol. 23(4), pp. 342-349.

6. Koombhongse, S., Liu, W., Reneker, D. H., 2001, Flat ribbons and other shapes by electrospinning, J Polym Sci, Polym Phys Ed, vol. 39, pp. 2598-2606.

7. Frenot, A., Chronakis, I. S., 2003, Polymer nanofibers assembled by electrospinning, Current Opinion in Colloid and Interface Science, vol. 8, pp. 64-75.

8. Grothe T., Großerhode C., Hauser T., Kern P., Stute K., Ehrmann A., 2017, Needleless electrospinning of PEO nanofiber mats, Advances in Engineering Research, vol. 102, pp. 54-58.

9. Fong, H., Chun, I., Reneker, D. H., 1999, Beaded nanofibers formed during electrospinning, Polymer, vol. 40, pp. 4585-4592.

10. Grimmelsmann, N., Homburg, S. V., Ehrmann, A., 2017, Electrospinning chitosan blends for nonwovens with morphologies between nanofiber mat and membrane, IOP Conference Series: Materials Science and Engineering, vol. 213, no. 012007.

11. N. Grimmelsmann, S. V. Homburg, A. Ehrmann, 2017, Needleless electrospinning of pure and blended chitosan, IOP Conference Series: Materials Science and Engineering, vol. 225, no. 012098.

12. Yalcinkaya, F., Yalcinkaya, B., Jirsak, O., 2016, Dependent and Independent Parameters of Needleless Electrospinning, Electrospinning – Material, Techniques and Biomedical Applications, pp. 67-93.

13. Sabantina, L., Mirasol, J. R., Cordero, T., Finsterbusch, K., and Ehrmann, A., 2017, Investigation of Needleless Electrospun PAN Nanofiber Mats, AIP Conference Series, vol. 1952, no. 020085.

14. Niu, H. T., Wang, X. G., Lin, T., 2012, Needleless electrospinning: influences of fibre generator geometry, Journal of the Textile Institute, vol. 103, pp. 787-794.

15. Wang, W., Qiang, W, Dai, H. C., 2017, Impact Mechanisms of Needleless Electrospinning Spinneret Geometry on Electric Field Distribution Regularities, Chemical Journal of Chinese Universities, vol. 38, pp. 982-989.

16. Yang, W. X., Liu, Y. B., Zhang, L. G., Cao, H., Wang, Y., Yao, J. B., 2016, Optimal spinneret layout in Von Koch curves of fractal theory based needleless electrospinning process, AIP Advances, vol. 6, no. 065223.

17. Zhou, F.-L., Gong, R.-H., Porat, I., 2010, Needle and Needleless Electrospinning for Nanofibers, Journal of Applied Polymer Science, vol 115, pp. 2591-2598.

18. Niu, H. T., Lin, T., Wang, X. G., 2009, Needleless Electrospinning. I. A Comparison of Cylinder and Disk Nozzles, Journal of Applied Polymer Science, vol 114, pp. 3524-3530.

19. Cernohorsky, M., Semerak, P., Ticha, P., Havrlik, M., 2017, Measuring of Water Vapour Diffusion of Nanofibre Textiles, 8th International Conference on Nanomaterials – Research & Application, pp. 319-323.

20. Hong, K. A., Yoo, H. S., Kim, E., 2015, Effect of waterborne polyurethane coating on the durability and breathable waterproofing of electrospun nanofiber web-laminated fabrics, Text. Res. J., vol. 85(2), pp. 160-170.

21. Sun, A. C., Kosar, W., Zhang, Y. F., Feng, X. S., 2014, Vacuum membrane distillation for desalination of water using hollow fiber membranes, Journal of Membrane Science, vol. 455, pp. 131-142.

22. Huang, L., Manickam, S. S., McCutcheon, J. R., 2013, Increasing strength of electrospun nanofiber membranes for water filtration using solvent vapor, Journal of Membrane Science, vol. 436, pp. 213-220.

23. Shimada, N., Mori, T., Ito, A., Yamaguchi, S., Nakane, K., Haraguchi, M., Ozawa, M., Ogata, N., 2012, Structure and Physical Properties of Polyurethane/Fluorinated Hyper Branched Polymer Nanofiber Mat, Sen-I Gakkaishi, vol. 68(10), pp. 269-275.

24. Yoon, B., Lee, S., 2011, Designing Waterproof Breathable Materials Based on Electrospun Nanofibers and Assessing the Performance Characteristics, Fibers and Polymers, vol. 12(1), pp. 57-64.

25. Hes, L., Araujo, M., 2010, Simulation of the Effect of Air Gaps between the Skin and a Wet Fabric on Resulting Cooling Flow, Textile Research Journal, vol. 80, pp. 1488-1497.

CHAPTER 5

INVESTIGATION OF STABILIZATION PARAMETERS FOR PAN NANOFIBER MATS NEEDLELESS- ELECTROSPUN FROM DMSO

# 5. INVESTIGATION OF STABILIZATION PARAMETERS FOR PAN NANOFIBER MATS NEEDLELESS-ELECTROSPUN FROM DMSO

## 5.1 Abstract

Polyacrylonitrile (PAN) can be used as a base material for thermo-chemical conversion into carbon. Especially nanofiber mats, produced by electrospinning, are of interest to create carbon nanofibers. Optimal stabilization and carbonization parameters, however, strongly depend on the spatial features of the original material. While differences between nano- and microfibers are well-known, this paper shows that depending on the electrospinning method and the solvent used, severe differences between various nanofiber mats have to be taken into account for the optimization of the stabilization conditions. Here we examine for the first time PAN nanofiber mats, electrospun with wire-electrospinning from the low-toxic dimethyl sulfoxide (DMSO) as a solvent, instead of the typically used needle-electrospinning from the toxic dimethyl formamide (DMF). Additionally, we used inexpensive PAN from knitting yarn instead of highly-specialized material, tailored for carbonization. Our results show that by carefully controlling the maximum stabilization temperature and especially the heating rate, fully stabilized PAN fibers without undesired interconnections can be created as precursors for carbonization.

## 5.2 Introduction

Polyacrylonitrile (PAN) nanofibers are an interesting precursor for carbon nanofibers (CNFs) due to the small diameters of a few hundred nanometers which can be reached by this method, depending on the spinning and solution parameters. [1] Typically, such nanofibers contain only few structural imperfections and are highly oriented, [2] resulting in higher mechanical strength of the CNFs compared to common microfibers. Creating mechanically strong fibers, however, necessitates optimized stabilization and carbonization parameters. [3]

Additionally, nanofiber mats can be easily prepared by needle-electrospinning. Other variations of electrospinning, such as drum or wire electrospinning, can even be up-scaled to industrial production unambiguously. This allows for the production of CNFs applicable to increase the mechanical properties of composites, [4] the electrical properties of batteries [5-6] or super-capacitors, [7] etc.

Since PAN is a typical precursor for CNFs, several articles deal with the stabilization and carbonization process and describe the thermo-chemical conversion of PAN into carbon. Generally, the oxidative stabilization, i.e. the thermal treatment in air, is regarded as a combination of cyclization, dehydrogenation, oxidation, aromatization, and crosslinking reactions. [8] The ideal temperatures for these processes are widely discussed in the literature. Microfibers with diameters of approx. 10 μm are suggested to be stabilized in a temperature range between 200 °C and 300 °C, e.g. at 270 °C for high-performance carbon fibers, [9] while other publications mention temperatures of up to 400 °C. [10] Finding the optimal balance between not burning the fibers and chemical reaction to proceed sufficiently fast to allow complete stabilization is crucial even for microfibers.

For nanofibers, heat transfer processes are significantly faster. [11] This means on the one hand that shorter stabilization times and lower temperatures are required for stabilizing PAN nanofibers; on the other hand, the process parameters have to be adapted even more carefully.

Several approaches can be found in the literature. One of the most detailed examinations was performed by Mólnar *et al.* who prepared PAN nanofibers with a rotating electrode from DMF, working with a fixed heating rate of 5 °C/min and isothermal treatment at the maximum temperature for 1 h. [12] They concluded that all nitrile groups were eliminated, and full structural conversion has been reached at 265 °C, while DSC and color change investigations revealed that the stabilization process was completed below 280 °C since all available exothermic heat was released and all color changes were set.

Another detailed test series was performed by Gu *et al.* who used the typical needle-electrospinning from DMF and tested stabilization temperatures between 200 and 270 °C, reached with a heating rate of 2 °C/min. [13] They concluded that stabilization has already been completed at 250 °C due to Fourier-transform infrared spectroscopy (FTIR) and X-ray diffraction (XRD) data. Additionally, this paper is one of the few which explicitly mention the undesired conglutinations between overlapping fibers, starting at a temperature of 250 °C and becoming strongly visible at 270 °C.

Both aforementioned papers do not take into account the influence of the heating rate. Different heating rates between 1 °C/min and 4 °C/min in combination with different end temperatures between 180 °C and 270 °C were investigated by Rafiei *et al.* who also prepared PAN nanofiber mats by needle-electrospinning from DMF. [14] They found heating rates above 2 °C/min resulting in brittle products and defined 270 °C as the ideal end temperature with a dwell time of 1-2 hours. Here, no undesired fiber conglutinations are visible for an end temperature of 270 °C approached with a heating rate of 1 °C/min.

Other groups stabilize electrospun PAN nanofibers with similar, but not identical parameters. The following examples are all based on needle-electrospinning from DMF. Gergin *et al.* found 250 °C to be the optimum temperature in combination with isothermal treatment for 3 h, while even 300 °C was insufficient to eliminate all C≡N triple bonds. [15] Similar to Alarifi *et al.* who performed stabilization at 270 °C for one hour, no heating rate is given. [16] In the latter paper, however, fiber interconnections are visible in the SEM images after carbonization. This is also the case in the study of Arbab *et al.* who used a heating rate of 5 °C/min to approach final temperatures between 240 °C and 300 °C; for a temperature of 270 °C, the undesired conglutinations are also visible here. [17] The same effect is visible in the paper by Dhakate *et al.*, stabilizing at temperatures between 250 °C and 320 °C and showing molten fibers after stabilization at 275 °C. [18]

Interestingly, this was not reported by Arshad *et al.*, using stabilization for 1 h at 300 °C after approaching the maximum temperature with 5 °C/min, [19] nor by Zhou *et al.* using a heating rate of 2 °C/min to reach a maximum temperature of 280 °C where the samples were stabilized for 3 h. [20]

In several other papers, it is not possible to assess whether these undesired conglutinations due to fiber melting are established. Ma *et al.*, e.g., tested temperatures between 200 °C and 340 °C with a heating rate of 1 °C/min and concluded that stabilization is finished between 280 °C and 300 °C. They also mention the necessity to fix at least one of the nanofiber mat dimensions by applying a weight or another mechanism during stabilization to avoid shrinkage. [21] Lee *et al.* stabilized in a 6-area furnace from 150 °C to 300°C without mentioning the heating rate or a possible melting of the fibers. [22] Su *et al.* also used a 6-area furnace applying temperatures between 150 °C and 300 °C without defining the

heating rate; they found strong bead formation which is unusual for spinning from DMF. [23] Wu and Qin used a heating rate of 4 °C/min and found stabilization after isothermal treatment for 1 h at 250°C and higher temperatures to be almost complete. [24] After stabilizing for 2 h at a temperature of 280 °C, Wu *et al.* regarded the dehydrogenation as almost complete due to FTIR, XPS and color measurements. [8] Li and Adanur also used a temperature of 280 °C with a heating rate of 1 °C/min, [25] while Zhang *et al.* found a transition temperature of approx. 300 °C, as revealed by differential scanning calorimetry (DSC), thermogravimetric analysis (TGA), and FTIR. [26] Cipriani *et al.* used a TGA with a significantly higher heating rate of 10 °C/min to reach a maximum temperature of 250 °C, [27] similar to Esrafilzadeh *et al.* who used a DSC with a heating rate of 5 °C /min to reach temperatures between 170 °C and 250 °C. According to their results, stabilization is not completed at this temperature. [28]

Only few papers are based on different electrospinning techniques or different solvents. Besides the aforementioned paper by Mólnar *et al.* about electrospinning with a rotating electrode, [12] Kaur *et al.* also used drum-electrospun fibers which they stabilized at 310 °C for 1 h; the heating rate is not mentioned. [29]

Duan *et al.* [30] as well as Qin [31] used DMAc as solvent instead of DMF; while the first suggested that 1 h at 260 °C results in complete stabilization, the latter found 250 °C to be sufficient for complete cyclization and 5 °C/min to be the optimal heating rate, although SEM images show the undesired connections due to melting of the fibers. Finally, Jin *et al.* used hydrolization in NaOH to pre-stabilize electrospun PAN nanofibers which resulted in decreased cyclization temperatures. [32]

It should be emphasized that, to the best of our knowledge, stabilization properties of PAN nanofibers were neither investigated for nanofibers electrospun with the wire-based technology nor for fibers electrospun from DMSO before. All aforementioned studies have been performed on nanofiber mats electrospun from different solvents, most of them by a needle-based technology. Additionally, the problem of undesired conglutinations emerging during stabilization, impeding formation of separated CNFs after carbonization, is often either neglected or not investigated in recent scientific literature. Finally, our study also aims to investigate the beads occurring at relatively low solid contents in the solution and which are often undesired, but can be

very helpful to avoid fiber slippage in a resin matrix and should thus also keep their shapes during stabilization.

This is why in our paper we focus on wire-based electrospinning of PAN nanofibers from DMSO and used SEM images to evaluate possible undesired fiber interconnections.


## 5.3 Materials and Methods

Electrospinning was performed using the wire-based nanospinning machine "Nanospider Lab" (Elmarco, Czech Republic), applying a high voltage of 80 kV, a nozzle diameter of 0.9 mm and a carriage speed of 150 mm/s during a spinning time of 30 min. The distance between the electrode wires was set as 240 mm (the maximally possible value), the relative humidity in the spinning chamber was 32 % , air flow 120 m$^3$/hour and the temperature during spinning was 22 °C.

The PAN solution for spinning has been prepared with 14 % polymer content in DMSO (dimethyl sulfoxide min. 99.9 %, purchased from S3 Chemicals, Germany) by stirring for two hours at room temperature. This concentration was found ideal in previous tests to avoid clogging of the nozzle as well as electrospraying instead of electrospinning.

For stabilization, a muffle furnace B150 by Nabertherm was used, applying heating rates between 0.5 °C/min and 8 °C/min. Additionally, samples were put into the already heated oven, resulting in a sudden decrease of the oven temperature by approx. 40 °C and a new increase to the desired temperature during around 2.5-3 min; the values thus obtained are referred to as 16 °C/min in order to be able to represent them in the heating-rate-dependent diagrams.

PAN nanofiber samples were cut from the electrospun mat in dimensions of 50 mm x 50 mm; a frame of 40 mm x 40 mm was marked and used for dimensional measurements, while the "border" was used to fix some of the samples during stabilization by placing a metal frame of sufficient weight on it with sufficient to maintain the sample dimensions.

For the analysis of the sample dimensions before and after stabilization with different parameters, the program ImageJ 1.51j8 (from National Institutes of Health, Bethesda, MD, USA) was applied using 50 fibers per sample.

Masses of the samples were taken using an analytical balance (VWR). Scanning electron microscopy (SEM) images were taken by a Zeiss 1450VPSE with a resolution of 5 nm, using a nominal magnification of 5000 x. Fourier-transform infrared spectroscopy (FTIR) measurements were performed with an Excalibur 3100 from Varian, Inc., while a sph900 by Color-Lite was used for color measurements. For the differential scanning calorimetry (DSC) measurements, a DSC Q100 (TA Instruments) was used.

## 5.4 Results and Discussion

In a first test series, different maximum temperatures between 120 °C and 300 °C were approached with a heating rate of 2 °C/min. Afterwards isothermal treatment was performed for 1 h.

Fig. 5.1 depicts the normalized masses and areas of the samples. It is clearly visible that both values significantly decrease with increasing stabilization temperature. For the masses, large error bars can be recognized for temperatures of 240 °C and above. This is most likely due to separated parts of the samples which could not be properly added during weighing since electrostatic interactions with gloves and scales etc. increased more and more for higher stabilization temperatures, resulting in the loss of small sample parts. Although they have been removed from the oven with no visible residues, small broken parts along the edges tend to adhere at the pliers used to put them onto the scale, increasing the risk of losing those parts. In addition, the electrostatic forces between the sample on the sample holder and the surrounding shield of the special accuracy balance can also slightly affect the measurement result. Nevertheless, Fig. 5.1(a) shows a clear trend of the expected increase in mass loss for increasing stabilization temperatures.

The problem of splitting samples into different parts is even more evident in the normalized areas, where measurements are differentiated between fixed (as described above) and unfixed samples. At all stabilization temperatures, the unfixed samples

shrink more than the fixed ones. For the highest temperatures of 280 °C or 300 °C, however, the distance between both lines decreases again. This can be explained by the fact that for these temperatures, all of the fixed samples broke partially along the metal mounting frame, resulting in several separated sample parts. We assume that this effect occurred in the early stages of stabilization, so that the parts of the samples which were no longer fixed shrank more and thus the normalized areas approached each other.

It should also be mentioned that for the freely shrinking samples, there may be a minimum area reached above 300 °C. This was not examined in detail since at 300 °C the samples were increasingly unstable and thus difficult to handle.



(a)                                         (b)
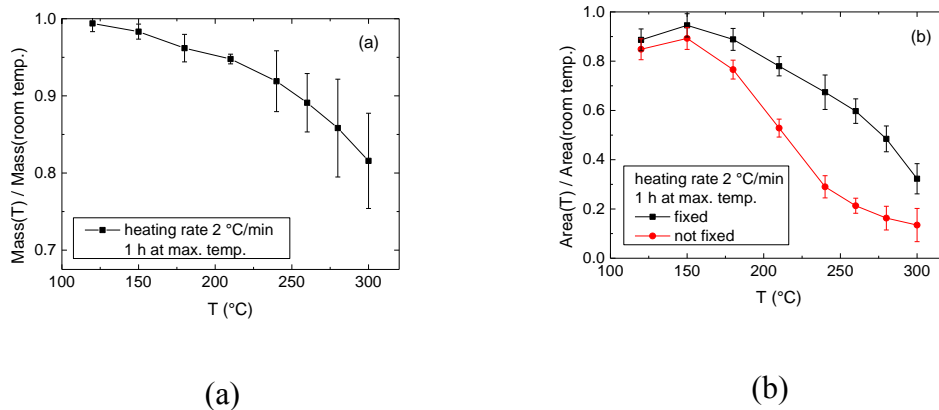
Fig. 5.1 Normalized masses (a) and areas (b) of samples stabilized at different end temperatures with identical heating rates of 2 °C/min and staying for 1 h at the maximum temperature.

The influence of different maximum temperatures has also been investigated by SEM imaging. Table 5.1 shows the results for the three temperatures which, according to the literature, are most likely sufficient for complete stabilization, in comparison to the original nanofiber mat.

The beads visible here are typical for PAN nanofibers mats electrospun from solutions with relatively low solid content, as it is typical for PAN dissolved in DMSO. Since these beads are not described extensively in the literature, temperature treatment may be one way to better understand their formation and to find out whether they should be avoided in future experiments. This could be done by increasing the PAN concentration but would be associated with a significant reduction in the possible material output per time due to the greatly increased viscosity.

In addition, for the typical application of integrating carbonized nanofibers into composite materials to increase their mechanical properties, these beads can be supportive since they will help avoiding slippage of the fibers inside the resin matrix. The ideal stabilization parameters would thus not only result in single, not conglutinated nanofibers, but also preserve these beads as possible ―anchors‖ for future integration in a resin matrix.

Table 5.1 SEM images of the original PAN nanofiber mat and samples stabilized at different temperatures with and without fixing them. All scales depict a length of 2 μm, the nominal magnification is 5000 x in all SEM images shown in this article.
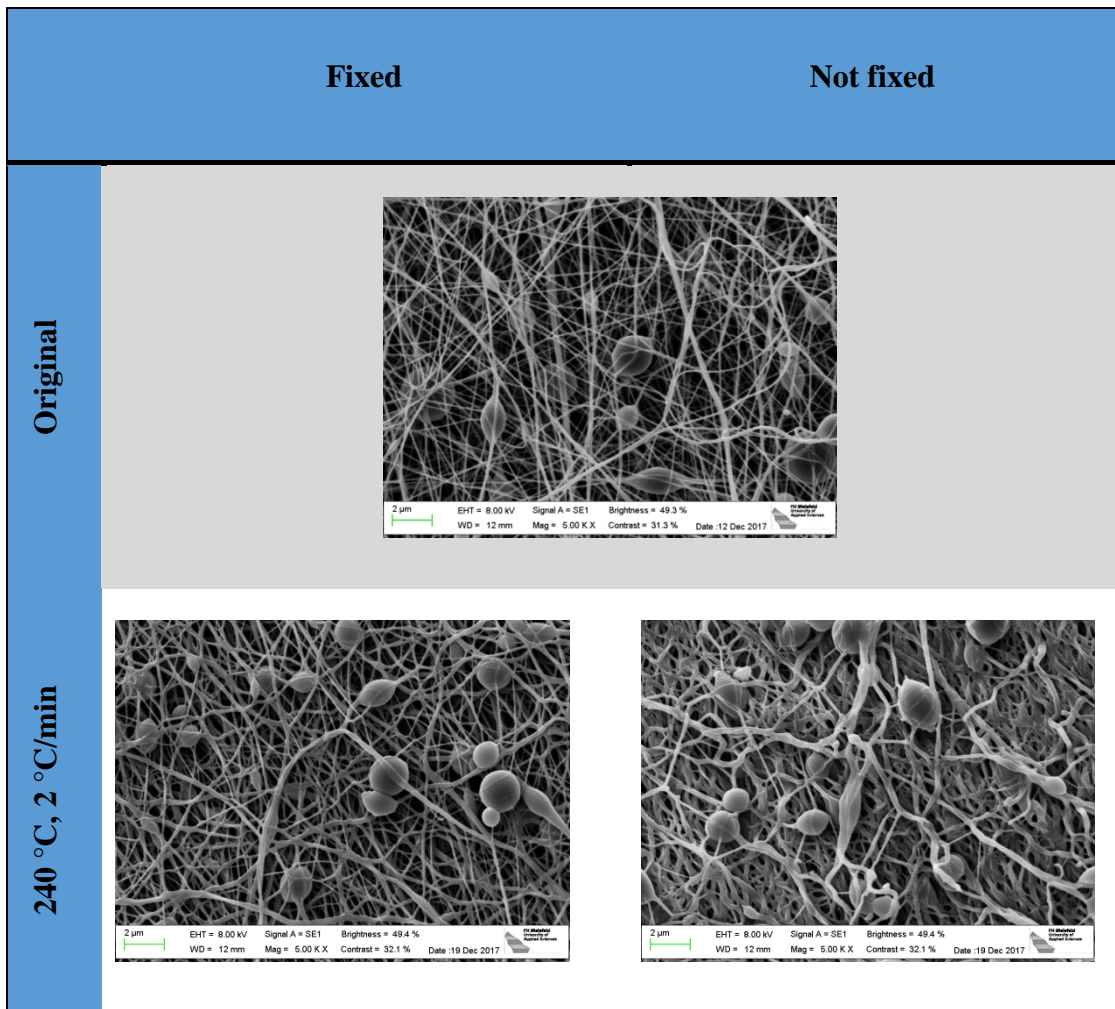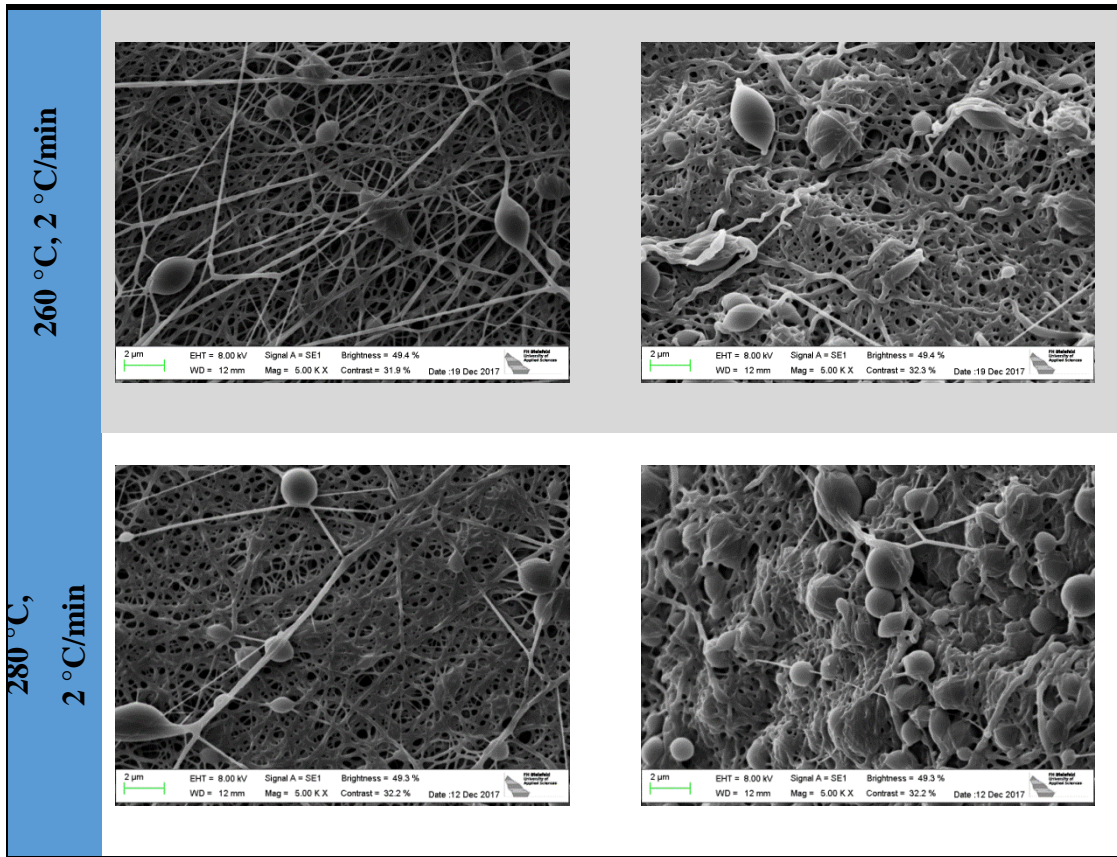
Comparing the images in Table 5.1, there is obviously a significant difference in the samples stabilized at identical temperatures with and without fixing. This has not been described in the literature before. While for a final temperature of 280 °C strong conglutinations are visible in both cases, these undesired connections are reduced for samples fixed at lower temperatures.

Nevertheless, it should be noted that even for fixed stabilization at 240 °C, which is below the lowest temperature indicated in literature, several small conglutinated areas are visible. These results indicate that not only FTIR and other chemical examination methods are essential for the investigation of stabilized or carbonized nanofibers, but SEM or similar methods must also be applied to avoid unexpected and undesired changes in the fiber mat morphology.

In further test series, a maximum temperature of 280 °C has been approached by different heating rates to investigate whether the conglutinations can be avoided in this way. The results are depicted in Fig. 5.2.



(a)                                                              (b)
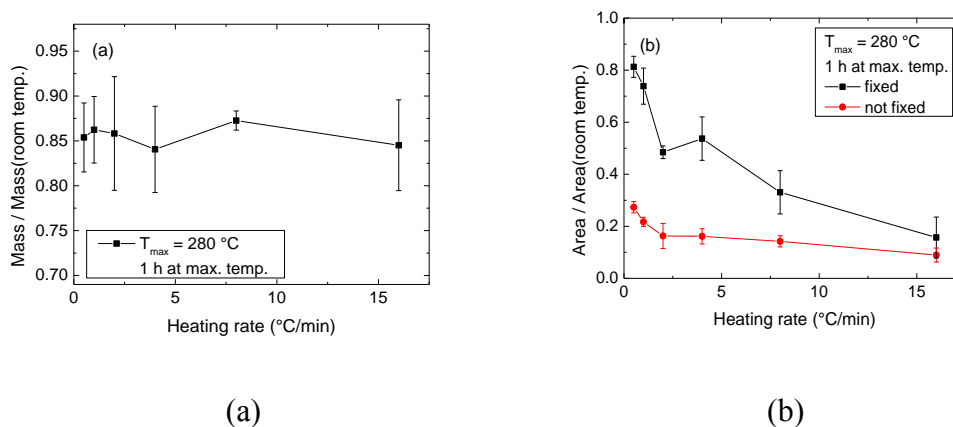
Fig. 5.2 Normalized masses (a) and areas (b) of samples stabilized at 280 °C with different heating rates and isothermal treatment for 1 h at the maximum temperature.

While the mass does not show a dependence on the heating rate, the areas are apparently influenced by this parameter. This can be attributed to higher forces working on the samples for higher heating rates and thus breaking the fixed samples at an earlier stage, leaving more time to relax.

Interestingly, both values for the highest heating rate (marked as 16 °C/min, which means immediate introduction of the samples into the hot muffle furnace, as described above) are nearly identical, which can be explained by the observation that in this case, the fixed sample nearly completely broke along the mounting frame, allowing it to relax almost freely during the stabilization process.

Table 5.2 SEM images of the original PAN nanofiber mat and samples stabilized at 280 °C approached with different heating rates, with and without fixing them.

| | Fixed | Not fixed |
|---|---|---|
| 280 °C, 0.5 °C/min | | |
| 280 °C, 1 °C/min | | |
| 280 °C, 2 °C/min | | |
| 280 °C, instant. | | |
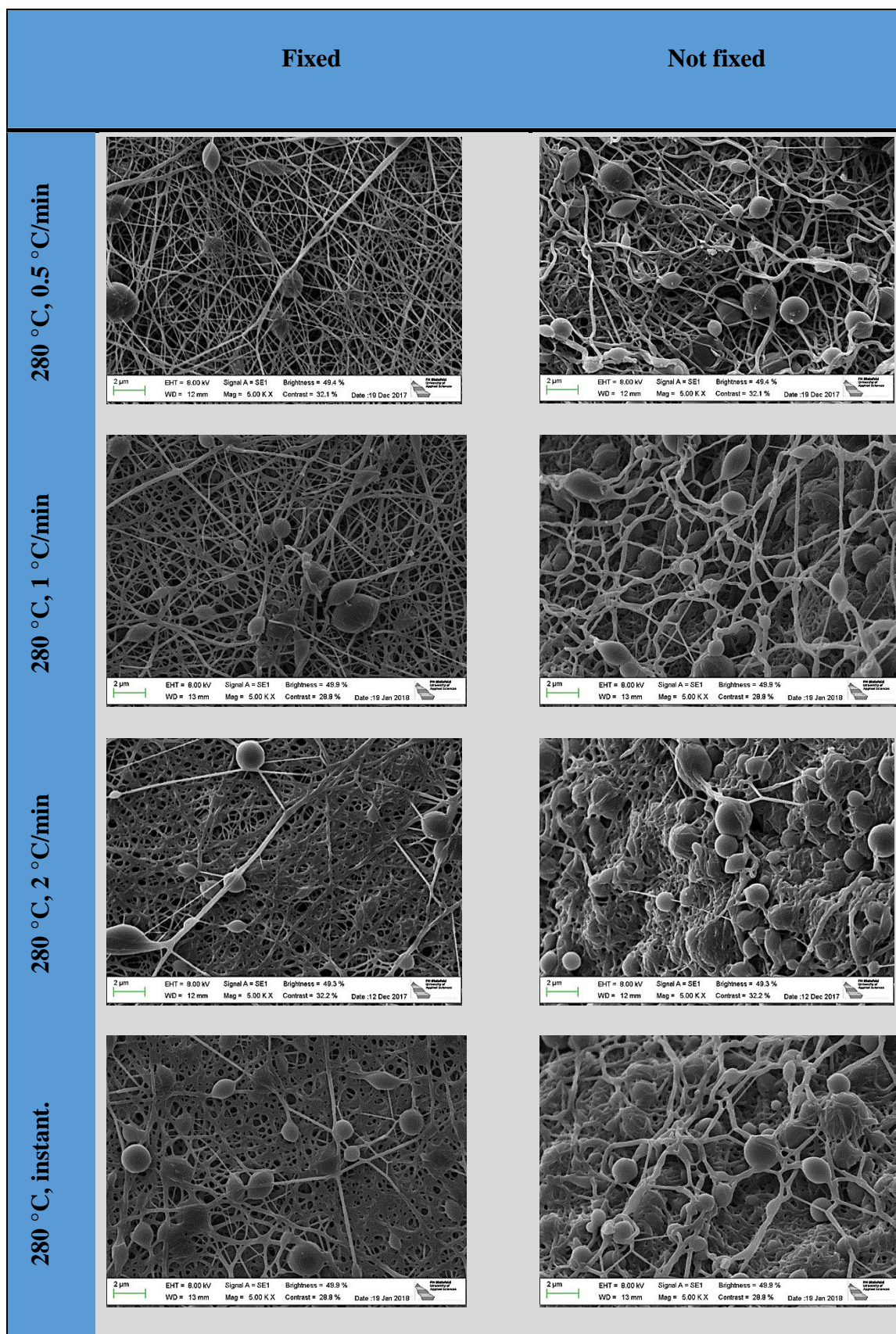
Again, SEM images were taken to compare the different heating rates. Table 5.2 shows the results of some heating rates. The strong influence of fixing the samples is visible for all heating rates, even the highest ones for which the measured areas were already approaching a common value (Fig. 5.2). Especially for the slowest heating rates of 0.5 ℃/min and 1 ℃/min, significant differences between the fixed and the freely relaxed samples are visible, again indicating the importance of fixing the samples during stabilization to avoid shrinkage of the nanofibers, while at the same time their diameters increased visibly. It should be noted, however, that even at a heating rate of 1 ℃/min, molten fibers and resulting undesirable connections can be observed. From the SEM images, it can be concluded that the final stabilization temperature should be approached with a heating rate of only 0.5 °C/min. Nevertheless, higher heating rates may be applicable for lower maximum temperatures. Tests with a stabilization temperature of 260 °C, however, have revealed the same qualitative behavior (not shown here) – again, only with a heating rate of 0.5 °C/min it was possible to avoid conglutinations completely. This finding underlines the importance of SEM images for the investigation of the fiber morphology after stabilization in addition to the chemical test methods usually reported in the literature.

In the next step, the samples were analyzed with FTIR to determine the temperatures at which stabilization processes are completed and whether the heating rates influence these findings.



(a)          (b)
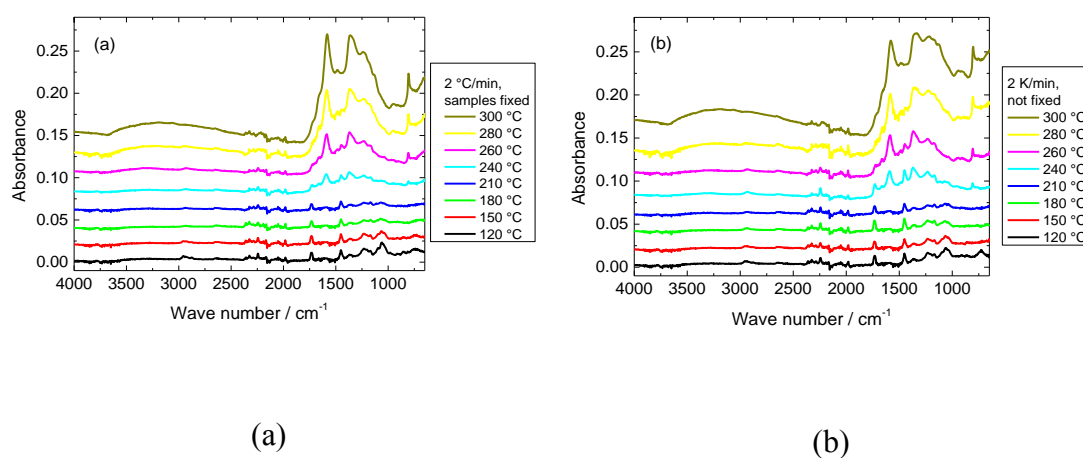
Fig. 5.3 FTIR absorbance measurements on fixed (a) and unfixed samples (b), stabilized at different temperatures approached with a heating rate of 2 °C/min. The lines are offset vertically for clarity.

Fig. 5.3 depicts FTIR measurements on samples stabilized at different temperatures with a heating rate of 2 °C/min. The first small changes are already visible at a temperature of 180 °C, while the most significant changes begin between 240 °C and 260 °C. The different peaks can be attributed to the following chemical groups:

The stretching vibration of the C≡N nitrile functional group at 2240 cm$^{-1}$ occurring at low temperatures [12] is still visible at 260 °C, nearly vanished at 280 °C and is completely gone at 300 °C. For high temperatures, this bond is converted to the large peak of C=N stretching vibrations at 1582 cm$^{-1}$ or C=C stretching vibration at 1660 cm$^{-1}$, [12] both of which become visible at 240 °C and above. The second large high-temperature peak around 1360 cm$^{-1}$ can be attributed to C-H bending and C-H$_2$ wagging. [27] The carbonyl (C=O) stretching peak at 1732 cm$^{-1}$ vanishes around 260 °C-280 °C, indicating that stabilization may be completed in this temperature range. [12] According to Mólnar *et al.*, [12] the peaks in the ranges of 1230-1250 cm$^{-1}$ and 1050-1090 cm$^{-1}$ can be attributed to ester (C–O and C–O–C) vibrations of the co-monomers like itaconic acid or methyl acrylate which are often applied in industrial production of PAN. Since they vanish around 210 °C, they seem to be unproblematic for the resulting stabilized or even carbonized fibers. The peaks at 2938 cm$^{-1}$ and 1452 cm$^{-1}$, both vanishing only at 300 °C, and 1380 cm$^{-1}$, being superposed by a new peak, are correlated with bending and stretching vibrations of CH$_2$. [12] The peak around 800 cm$^{-1}$, beginning to occur at 240 °C and above, was attributed to aromatic C−H vibrations which originated in the presence of oxygen from oxidative dehydrogenation aromatization, by this removing hydrogen in the form of H$_2$O. [15]

Comparing Fig. 5.3 (a) and (b), it should be mentioned that the results of fixed and unfixed samples are qualitatively the same, while quantitative differences occur in some parts of the spectra, especially related to the CH and CH$_2$ peak around 1360 cm$^{-1}$. Nevertheless, in both cases the FTIR spectra indicate that stabilization starts around 240 °C and seems to be completed between 280 °C and 300 °C.

(a)                                                              (b)
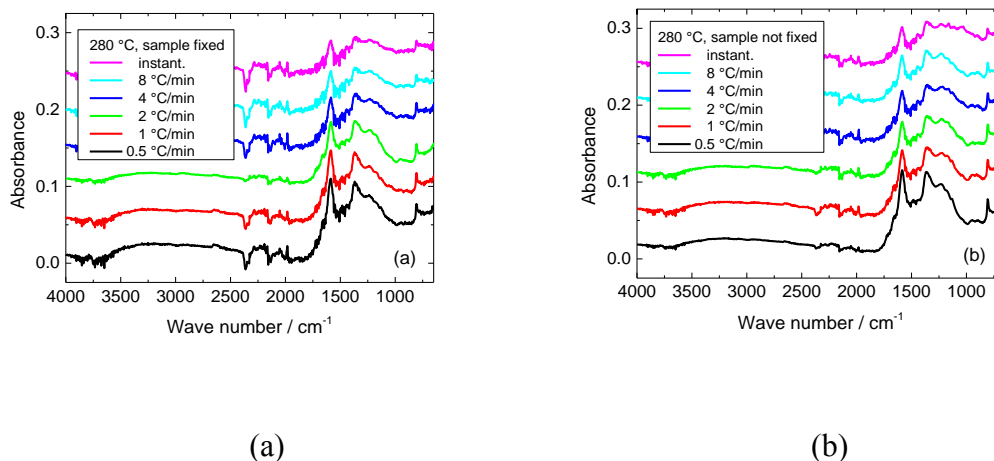
Fig. 5.4 FTIR absorbance measurements on fixed (a) and not fixed samples (b), stabilized at 280 °C approached with different heating rates. The lines are vertically offset for clarity.

In the next test series, FTIR measurements of samples stabilized at 280 °C for one hour were taken, the results of which are depicted in Fig.5.4. Qualitatively, the results of all measurements are very similar, while the unfixed samples show higher absorbance which can be attributed to the samples being thicker after stabilization due to the stronger decrease in lateral dimensions. This may also be the reason why the freely relaxed samples show less noise.

Additionally, in both cases the CH and $CH_2$ peaks around 1360 cm$^{-1}$ are qualitatively different for different heating rates, i.e. much more pronounced for smaller heating rates. This finding supports the idea of using lower heating rates to increase the stabilization process.
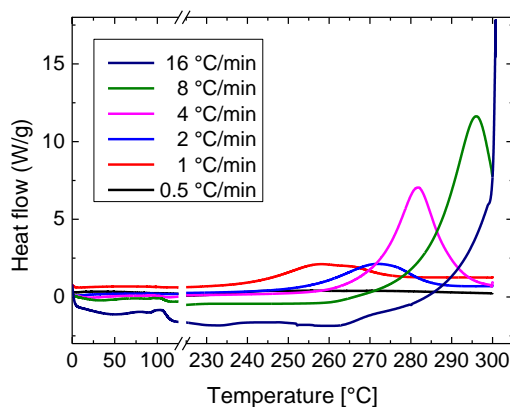


Fig. 5.5 DSC measurements of untreated PAN nanofiber mats with different heating rates in the DSC.

78

The influence of the heating rate was also examined by DSC measurements, as shown in Fig. 5.5. The expected cyclization reaction is an exothermic reaction, which is shown here by positive values. Since the test series was performed with unstabilized PAN nanofiber mats before cyclization, the areas under the exothermic peaks could be expected to be identical for equal heating rates, i.e. should be doubled for doubled heating rates. [24] According to Fig. 5.5, both predictions are fulfilled.

Interestingly, the position of the maximum is shifted to higher temperatures with an increasing heat rate. Further tests are necessary to evaluate whether this finding indicates that different heating rates necessitate indeed different final temperatures or whether the isothermal heating process at the maximum temperature compensates these effects. Since the maximum of the curve measured with a heating rate of 0.5 °C/min is barely noticeable, the next heating rate of 1 °C/min is used to estimate the temperature range of the cyclization process which seems to be completed around 280 °C. It should be noted, however, that no isothermal step is added here, so that it cannot be excluded from the DSC measurements that stabilization at 260 °C for 1 h is also sufficient to finish cyclization.
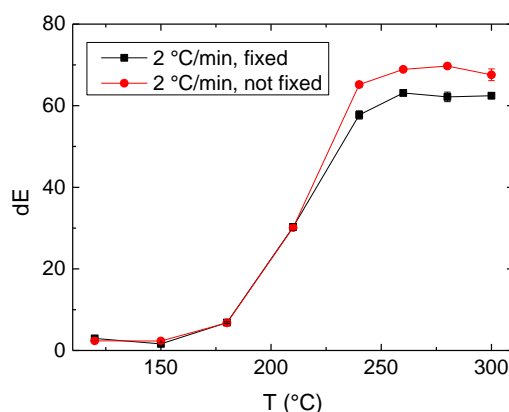


Fig. 5.6 Color differences dE of samples stabilized at different end temperatures with identical heating rates of 2 °C/min and isothermal treatment at the maximum temperature for 1 h.

In the next step, the colors of the samples were investigated. Fig. 5.6 depicts the results of samples stabilized at different temperatures, approached with a heating rate of 2 °C/min. Up to a temperature of 210 °C the colors of the fixed and the freely relaxed samples are identical, indicating again that stabilization starts around 240 °C. Afterwards, the unfixed samples show darker colors, most probably due to greater

shrinkage. The color measurements suggest that stabilization is already completed around 260 °C.

Fig. 5.7 shows the results of color measurements on samples stabilized at 280 °C and 260 °C, respectively, in fixed and unfixed state, approached with different heating rates. Similar to Fig. 5.2 (b), the results approach a constant value for heating rates of 4 °C/min or higher. No significant difference is visible between the colors reached at temperatures of 260 °C or 280 °C, while the difference between fixed and unfixed samples, which was also visible in Fig. 5.6, is underlined here.

At first glance, these results may indicate that a heating rate of min. 4 °C/min is necessary to approach a constant value of the color differences. On the other hand, a comparison between Fig. 5.7 and the areas depicted in Fig. 5.2 (b) suggests that the brighter colors for smaller heating rates have to be attributed to the larger areas of the respective samples.
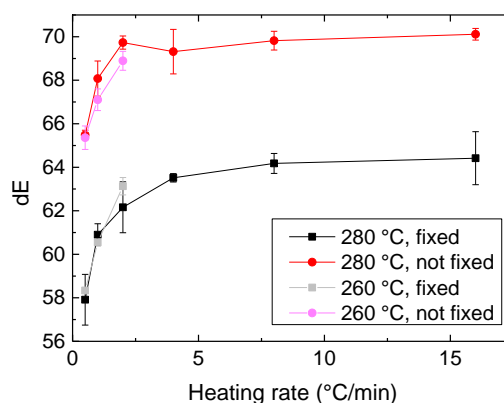


Fig. 5.7 Color differences dE of samples stabilized at 260 °C or 280 °C approached with different heating rates and isothermal treatment at the maximum temperature for 1 h.

Finally, a simple experiment was performed to test the degree of stabilization of the PAN nanofiber mats by evaluating their resistance against DMSO, the solvent from which the nanofiber mats were previously electrospun. The results are depicted in Fig. 8 for samples with different stabilization temperatures.
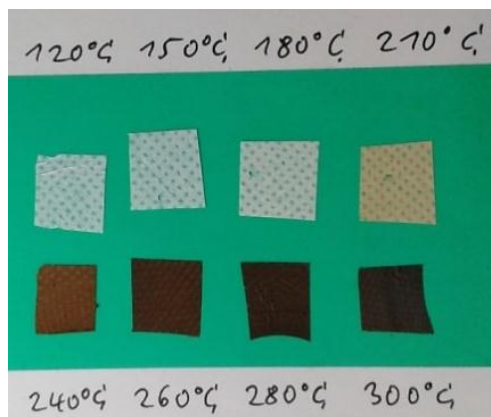
(a)
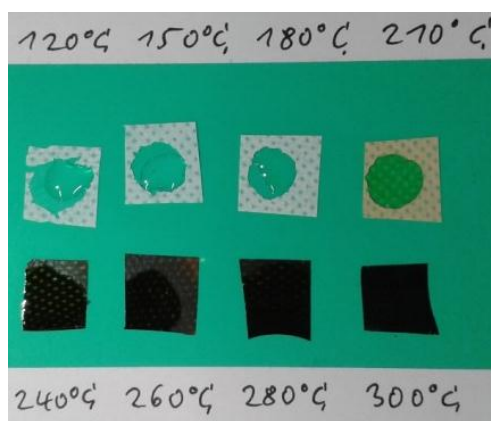


(b)
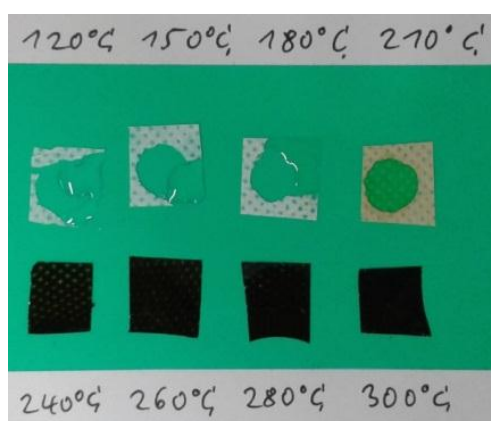


(c)

Fig. 5.8 PAN nanofiber mat samples, stabilized at different temperatures as denoted in the images, in the dry state (a), 10 s after placing DMSO drops on the samples (b) and 2 h after this (c).

It is clearly visible that the sample is immediately dissolved by the DMSO drop for the first three temperatures. For a stabilization temperature of 210 °C, corresponding to the first significant color change (cf. Fig. 5.6), a weak stabilization process has already occurred; the respective sample is partly dissolved due to the DMSO but not completely destroyed. Starting from 240 °C, no influence of the DMSO can be recognized; the darker color can be attributed to the influence of the liquid in the samples.

## 5.5 Conclusions

In a recent project we have examined the influence of stabilization temperature and heating rate on PAN nanofiber mats, electrospun using a wire-based technology from a solution in DMSO. Investigations by different means showed slightly different optima for the stabilization temperature and the heating rate: While the simple DMSO test used to dissolve the stabilized mats indicated that a temperature of 240 °C is sufficient for stabilization, color measurements show a necessary temperature of 260 °C to approach a constant value in color change. DSC measurements suggest optimal temperatures between 260 °C and 280 °C, while in FTIR measurements, depending on the peaks under examination, the stabilization seems to be completed between 280 °C and 300 °C.

This finding explains the broad variety of values which can be found in the literature. Since stabilization is a combination of diverse chemical processes, i.e. cyclization, dehydrogenation, oxidation, aromatization, and crosslinking, [8] different examinations probe different processes which apparently are not finished at same temperatures. It turns out that more detailed investigations are necessary to identify which of these processes is essential for the subsequent carbonization process and thus to enable tailoring the stabilization process to the needs of the final carbon nanofibers.

Additionally, the importance of a slow heating rate, and in particular of mechanical fixation of the samples during stabilization, was underlined in order to avoid undesired conglutinations and an increase in fiber diameter. While the beads embedded here to increase the fiber-matrix adhesion by avoiding fiber slippage survived stabilization even at high heating rates and without fixation, the fiber morphology can only be maintained at low heating rates and in fixed samples.

## 5.6 References

1. Sabantina L, Mirasol J R, Cordero T, Finsterbusch K and Ehrmann A. Investigation of Needleless Electrospun PAN Nanofiber Mats. *AIP Conf Proc* 2018; 1952: 020085.

2. Greiner A, Wendorff J H. Electrospinning: a fascinating method for the preparation of ultrathin fibers. *Angew Chem Int Ed* 2007; 46: 5670-5703.

3. Rahaman M, Ismail A F, Mustafa A. A review of heat treatment on polyacrylonitrile fiber. *Polym Degrad Stab* 2007; 92: 1421-1432.

4. Manoharan M P, Sharma A, Desai A V, Haque M A, Bakis C E, Wang K W. The interfacial strength of carbon nanofiber epoxy composite using single fiber pullout experiments. *Nanotechnology* 2009; 20: 5.

5. Ji L W, Yao Y F, Toprakci O, Lin Z, Liang Y Z, Shi Q, Medfort A J, Millns C R, Zhang X W. Fabrication of carbon nanofiber-driven electrodes from electrospun polyacrylonitrile/polypyrrole bicomponents for high-performance rechargeable lithium-ion batteries. *J Power Sourc* 2010; 195: 2050-2056.

6. Jung H R, Lee W J. Preparation and characterization of Ni-Sn/carbon nanofibers composite anode for lithium ion battery. *J Electrochem Soc* 2011; 158: A644-652.

7. Liu J W, Essner J, Li J. Hybrid supercapacitor based on coaxially coated manganese oxide on vertically aligned carbon nanofiber arrays. *Chem Mater* 2010; 22: 5022-5030.

8. Wu M, Wang, Q Y, Li K, Wu Y Q, Liu H Q. Optimization of stabilization conditions for electrospun polyacrylonitrile nanofibers. *Polymer Degradation and Stability* 2012; 97: 1511-1519.

9. Fitzer E, Frohs W, Heine M. Optimization of stabilization and carbonization treatment of PAN fibres and structural characterization of the resulting carbon fibres. *Carbon* 1986; 24: 387-395.

10. Mathur R, Bahl O, Mittal J. A new approach to thermal stabilization of PAN fibres. *Carbon* 1992; 30: 657-663.

11. Moon S C, Farris R J. Strong electrospun nanometer-diameter polyacrylonitrile carbon fiber yarns. *Carbon* 2009; 47: 2829-2839.

12. Mólnar K, Szolnoki B, Toldy A, Vas L M. Thermochemical stabilization and analysis of continuously electrospun nanofibers. *J Therm Anal Calorim* 2014; 117: 1123-1135.

13. Gu H, Li Y W, Li N. Electrical Conductive and Structural Characterization of Electrospun Aligned Carbon Nanofibers Membrane. *Fibers and Polymers* 2015; 16: 2601-2608.

14. Rafiei S, Noroozi B, Arbab Sh, and Haghi A K. Characteristic Assessment of Stabilized Polyacrylonitrile Nanowebs for the Production of Activated Carbon Nano-Sorbents. *Chinese Journal of Polymer Science* 2014; 32: 449-457.

15. Gergin I, Ismar E, and Sarac A S. Oxidative stabilization of polyacrylonitrile nanofibers and carbon nanofibers containing graphene oxide (GO): a spectroscopic and electrochemical study. *Beilstein J. Nanotechnol.* 2017; 8: 1616-1628.

16. Alarifi I M, Alharbi A, Khan W S, Swindle A, and Asmatulu R. Thermal, Electrical and Surface Hydrophobic Properties of Electrospun Polyacrylonitrile Nanofibers for Structural Health Monitoring. *Materials* 2015; 8: 7017-7031.

17. Arbab S, Teimoury A, Mirbaha H, Adolphe D C, Noroozi B, Nourpanah P. Optimum stabilization processing parameters for polyacrylonitrile-based carbon nanofibers and their difference with carbon (micro) fibers. *Polymer Degradation and Stability* 2017; 142: 198-208.

18. Dhakate S R, Gupta A, Chaudhari A, Tawale J, Mathur R B. Morphology and thermal properties of PAN copolymer based electrospun nanofibers. *Synthetic Metals* 2011; 161: 411-419.

19. Arshad S N, Naraghi M, Chasiotis I. Strong carbon nanofibers from electrospun polyacrylonitrile. *Carbon* 2011; 49: 1710-1719.

20. Zhou Z, Lai C, Zhang L, Qian Y, Hou H, Reneker D H, Fong H. Development of carbon nanofibers from aligned electrospun polyacrylonitrile nanofiber bundles and characterization of their microstructural, electrical, and mechanical properties. *Polymer* 2009; 50: 2999-3006.

21. Ma S, Liu J, Liu Q, Liang J Y, Zhao Y, Fong H. Investigation of structural conversion and size effect from stretched bundle of electrospun polyacrylonitrile copolymer nanofibers during oxidative stabilization. *Materials and Design* 2016; 95: 387-397.

22. Lee J-Y, Hsu C-H, Su C-I, Murakami R-I, Lin C-W, and Lu C-H. Study on Activated Carbon Nanofibrous Adsorbents Prepared by Technology for Electrospun Composite Yarn. *Fibers and Polymers* 2015; 16: 2437-2444.

23. Su C-I, Lu C-H, Wong J-W, and Liu Y-S. The Optimal Continuous Manufacturing Conditions for Oxidized PAN Nanofiber Nonwovens. *Fibers and Polymers* 2014; 15: 1822-1827.

24. Wu S-H, Qin X-H. Effects of the stabilization temperature on the structure and properties of polyacrylonitrile-based stabilized electrospun nanofiber microyarns. *J Therm Anal Calorim* 2014; 116: 303-308.

25. Li W and Adanur S. Properties of Electrospun Polyacrylonitrile Membranes and Chemically-activated Carbon Nanofibers. *Text Res J* 2010; 80: 124-134.

26. Zhang W-X, Wang Y-Z, Sun C-F. Characterization on oxidative stabilization of polyacrylonitrile nanofibers prepared by electrospinning. *J Polym Res* 2007; 14: 467-474.

27. Cipriani E, Zanetti M, Bracco P, Brunella V, Luda M P, Costa L. Crosslinking and carbonization processes in PAN films and nanofibers. *Polymer Degradation and Stability* 2016; 123: 178-188.

28. Esrafilzadeh D, Morshed M, Tavanai H. An investigation on the stabilization of special polyacrylonitrile nanofibers as carbon or activated carbon nanofiber precursor. *Synthetic Metals* 2009; 159: 267-272.

29. Kaur N, Kumar V, and Dhakate S R. Synthesis and characterization of multiwalled CNT–PAN based composite carbon nanofibers via electrospinning. *SpringerPlus* 2016; 5: 483.

30. Duan Q-J, Wang B, and W H-P. Effects of Stabilization Temperature on Structures and Properties of Polyacrylonitrile (PAN)-Based Stabilized Electrospun Nanofiber Mats. *Journal of Macromolecular Science B* 2012; 51: 2428-2437.

31. Qin X-H. Structure and Property of Electrospun PAN Nanofibers by Different Pre-oxidated Heating Rates. *Journal of Industrial Textiles* 2011; 41: 57-69.

32. Jin S Y, Kim M H, Jeong Y G, Yoon Y I, Park W H. Effect of alkaline hydrolysis on cyclization reaction of PAN nanofibers. *Materials and Design* 2017; 124: 69-77.

CHAPTER 6


DEVELOPMENT OF CARBON NANOFIBERS FOR
INTERGRATION IN 3D PRINTING FILAMENTS

# 6. DEVELOPMENT OF CARBON NANOFIBERS FOR INTEGRATION IN 3D PRINTING FILAMENTS

## 6.1 Abstract

Nanotechnologies as well as additive manufacturing technologies are gaining increasing economic importance worldwide and have a great application potential in many industrial sectors such as automotive industry. New polymeric composites, so-called nanofiber-reinforced composites, combine the advantages of different materials. In this way, highly complex structures can be produced that are extremely light and stable at the same time. Furthermore, the use of bio-based plastics in nanofiber reinforced sandwich composites provides the opportunity to reduce negative environmental impacts.

The aims of this project are development and evaluation of polyacrylonitrile (PAN) based nanofiber mats for the production of carbon nanofibers. After electrospinning the PAN with different solution and spinning parameters, the gained nanofiber mats are carbonized using a horizontal furnace in a nitrogen ($N_2$) atmosphere at a controlled temperature. The resulting carbon nanofibers are evaluated by scanning electron microscopy (SEM).

The article will give an overview of the properties of these carbon nanofibers and an outlook to embedding them in poly (lactide acid) (PLA) or other 3D printing polymers.

## 6.2 Introduction

Carbon nanofibers can be produced by carbonizing nanofibers of different precursors, e.g. lignin [1-3], polyacrylonitrile (PAN) [4-6], or PAN blended with biochar [7] or cellulose acetate [8].

The production of such submicron- or nano-fibers is usually done by electrospinning. PAN nanofibers are often prepared for the possible use as electrode materials [9-11], but also for biotechnological and other applications [12]. Their morphology and diameter – which are essential for the morphology and diameter of the carbon nanofibers gained from them – are influenced by diverse spinning and solution parameters, such as capillary diameter, collector-capillary distance, solution feed rate

and voltage in needle-based electrospinning [13] or additionally the carriage speed and other parameters in diverse techniques of needleless electrospinning [14-17].

Another crucial factor for successful carbonization of PAN nanofibers is the previous stabilization process to avoid the degradation of the fibers [18]. For this, thermal treatment under slow heating up to 280 °C and following isothermal treatment at 280 °C for 2 h was found to be suitable [19], while temperatures higher than 300 °C caused combustion of the fibers and were thus not suggested [20]. Another group found a reaction temperature of 201°C [18].

Due to the expected deviations of the ideal stabilizing processes, depending on the PAN fiber morphology and fiber diameters, and the limited literature especially about carbonizing PAN nanofibers created by needleless electrospinning [18], this article gives an overview of carbonizing PAN nanofibers from a needleless electrospinning process after stabilization at relatively low temperatures.


## 6.3 Materials and Methods

PAN nanofiber mats were electrospun using the needleless electrospinning machine "Nanospider Lab" (Elmarco, Czech Republic). The spinning parameters were as follows: voltage 80 kV, nozzle diameter 0.9 mm, carriage speed 150 mm, substrate speed 20 mm/min, ground-substrate distance 50 mm, electrode-electrode distance 240 mm, temperature in the spinning chamber 23 °C, air flow 120 m$^3$/hour and relative humidity in the spinning chamber 32 %. A PAN solution was prepared using 14 % PAN in DMSO by stirring for 2 hours at room temperature.

Stabilizing was performed in a drying and sterilizing oven "Digitheat" (J. P. Selecta, Barcelona/Spain). Temperature was swept from 60 °C to 200 °C with a sweep rate of 20 °C /h. Afterwards, isothermal treatment at 200 °C was performed for 9 h.

To investigate the influence of multiple layers during this process, PAN nanofiber mats were introduced into the oven with different numbers of layers (Fig. 6.1).



Fig. 6.1 Multi-layer nanofiber mat (left boat) and single-layer nanofiber mats (middle and right boat) in the stabilizing oven.

For carbonizing, the furnace CTF 12 / TZF 12 (Carbolite Gero Ltd., UK) was used. The stabilized samples as well as one original nanofiber mat were introduced before the furnace was evacuated and purged with $N_2$. The furnace was heated to 800 °C with a heat rate of 10 °C/min in a nitrogen flow of 150 ml/min. Carbonizing happened for 2 hours at 800 °C.

These processes resulted in the following samples: 1S / 1SC (single layer, stabilized / also carbonized), MS / MSC (multi-layer, stabilized / also carbonized), 1C (single layer, not stabilized, but carbonized), and 1O (single layer, original state after electrospinning) as a reference. The nanofibers are evaluated by scanning electron microscopy (SEM) JSM-6490 LV, Jeol Ltd., Japan.

## 6.4 Results and Discussions

Fig. 6.2 depicts sample 1O, i.e. the original PAN nanofiber after electrospinning. Fiber diameters are in the range between 100 nm and 400 nm. The large droplets are typical for electrospinning PAN.
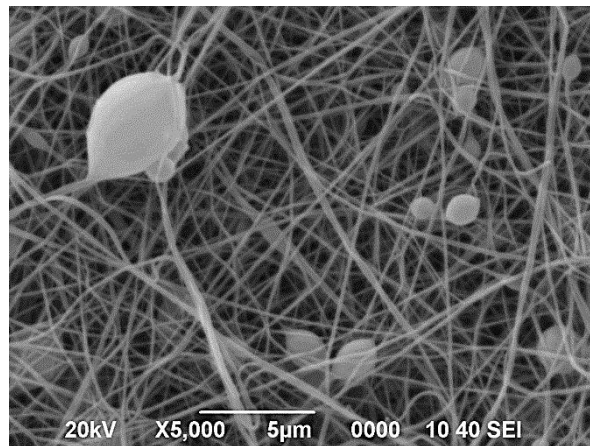


Fig. 6.2 PAN nanofibers after electrospinning with the above defined parameters (sample 1O).

After stabilizing the PAN nanofiber mats, the fibers have changed their morphology (Fig. 6.3). The original smooth, even fibers now seem to be more crinkled, an effect which has been described in the literature before [18]. Differences between the multi-layer and the single-layer samples, however, were not detected; the single layers of the multi-layer sample could easily be separated again after the stabilizing step.
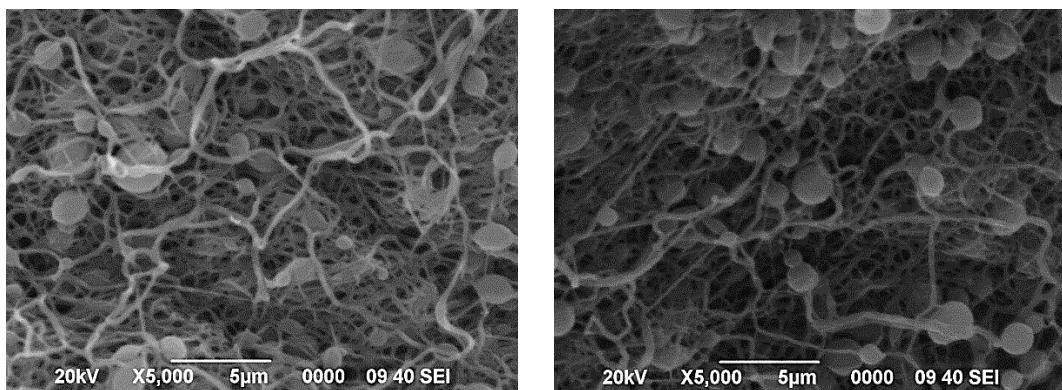


(a)                                                        (b)

Fig. 6.3 Samples MS (a) and 1S (b).

After the carbonization step, fiber morphology has changed again (Fig. 6.4). Whether stabilized before (sample MSC) or not (sample 1C), the crinkled structure gained by the stabilizing step is visible again. The nanofibers look similar in both images, too.

Nevertheless, it must be mentioned that the sample without previous stabilization step was nearly completely vanished after carbonizing, although it could not be burnt in the inert gas atmosphere. Although the morphology of the residual fibers does differ significantly, this effect clearly shows the necessity of the stabilizing step.



(a)                                   (b)
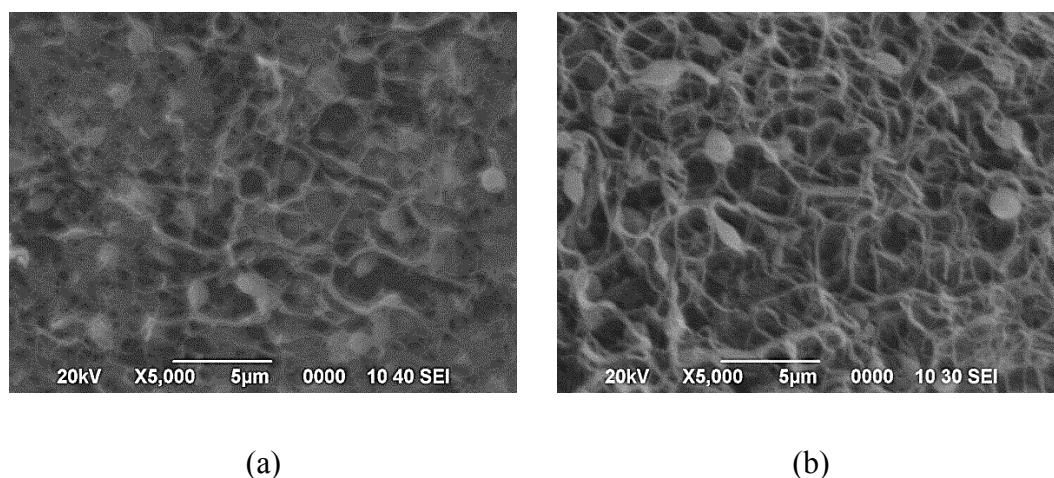
Fig. 6.4 Samples MSC (a) and 1C (b).

## 6.5 Conclusion

In a recent project, PAN nanofiber mats were created by needleless electrospinning and used as precursors for carbon nanofiber production. Both the stabilizing step and the carbonizing process are known to influence the morphology of the resulting carbon nanofibers significantly. Especially in needleless nanospinning which often lacks the possibility to create oriented fiber mats, fiber crinkling during heat treatment is hard to avoid by the mechanical means described in the literature [18].

After first experiments have in principle revealed the possibility to create carbon nanofibers by wire-based needleless electrospinning, opposite to the experimental setups mostly used in the literature, future tests will concentrate on final temperature and heating rate dependence of the carbon nanofiber morphology during the stabilizing and the carbonization step.

## 6.6 References

1. Garcia-Mateos F. J., Cordero-Lanzac T., Berenguer R., Morallon E., Cazorla-Amoros D., Rodriguez-Mirasol J., Cordero T., Lignin-derived Pt supported carbon (submicron)fiber electrocatalysts for alcohol electro-oxidation; Applied Catalysis B – Environmental 211, 18-30 (2017).

2. Berenguer R., Garcia-Mateos F.-J., Ruiz-Rosas R., Cazorla-Amoros D., Morallon E., Rodriguez-Mirasol J, Cordero T., Biomass-derived binderless fibrous carbon electrodes for ultrafast energy storage; Green Chemistry 18, 1506-1515 (2016).

3. Ruiz-Rosas R., Bedia J., Lallave M., Loscertales I. G., Barrero A., Rodriguez-Mirasol J., Cordero T., The production of submicron diameter carbon fibers by the electrospinning of lignin; Carbon 48, 696-705 (2010).

4. Kim D. W., Jung D. W., Adelodun A. A., Jo Y. M., Evaluation of $CO_2$ adsorption capacity of electrospun carbon fibers with thermal and chemical activation; Journal of Applied Polymer Science 134, 45534 (2017).

5. de Oliveira M. S., Rodrigues B. V. M., Marcuzzo J. S., Guerrini L. M., Baldan M. R., Rezende M. C., A statistical approach to evaluate the oxidative process of electrospun polyacrylonitrile ultrathin fibers; Journal of Applied Polymer Science 134, 45458 (2017).

6. Cipriani E., Zanetti M., Bracco P., Brunella V., Luda M. P., Costa L., Crosslinking and carbonization processes in PAN films and nanofibers; Polymer Degradation and Stability 123, 178-188 (2016).

7. Nan W., Zhao Y., Ding Y. C., Shende A. R., Fong H., Shende R. V., Mechanically flexible electrospun carbon nanofiber mats derived from biochar and polyacrylonitrile; Materials Letters 205, 206-210 (2017).

8. Ju Y.-W., Oh G.-Y., Behavior of toluene adsorption on activated carbon nanofibers prepared by electrospinning of a polyacrylonitrile-cellulose acetate blending solution; Korean Journal of Chemical Engineering 34, 2731-2737 (2017).

9. Samuel E., Joshi B., Jo H. S., Kim Y. I, An S., Swihart M. T., Yun J. M., Kim K. H., Yoon S. S., Carbon nanofibers decorated with $FeO_x$ nanoparticles as a flexible electrode material for symmetric supercapacitors; Chemical Engineering Journal 328, 776-784 (2017).

10. Liu Y. W., Peng X. X., Cao Q., Jing B., Wang X. Y., Deng, Y. Y., Gel Polymer Electrolyte Based on Poly(vinylidene fluoride)/Thermoplastic Polyurethane/Polyacrylonitrile by the Electrospinning Technique; Journal of Physical Chemistry C 121, 19140-19146 (2017).

11. Noh S., Nguyen D. N., Park C. S., Kim Y., Kong H. J., Kim S., Kim S., Hur S. M., Yoon H., Development of Effective Porosity in Carbon Nanofibers Based on Phase Behavior of Ternary Polymer Blend Precursors: Toward High Performance Electrode Materials; Journal of Physical Chemistry C 121, 18480-18489 (2017).

12. Großerhode C., Wehlage D., Grothe T., Grimmelsmann N., Fuchs S., Hartmann J., Mazur P., Reschke V., Siemens H., Rattenholl A., Homburg S. V., Ehrmann A., Investigation of microalgae growth on electrospun nanofiber mats; AIMS Bioengineering 4, 376-385 (2017).

13. da Silva Vaz B., Vieira Costa J. A., de Morais M. G., Production of polymeric nanofibers with different conditions of the electrospinning process; Materia-Rio de Janeiro 22, E-11847 (2017).

14. Zhang J. N., Song M. Y., Li D. W., Yang Z. P., Cao J. H., Chen Y., Xu Y., Wei Q. F., Preparation of self-clustering highly oriented nanofibers by needleless electrospinning methods; Fibers and Polymers 17, 1414-1420 (2016).

15. Lomos S. V., Molnar K., Compressibility of carbon fabrics with needleless electrospun PAN nanofibrous interleaves; Express Polymer Letters 10, 25-35 (2016).

16. Niu H. T., Wang X. G., Lin T., Upward needleless electrospinning of nanofibers; Journal of Engineered Fibers and Fabrics 7, 17-22 (2012).

17. Sabantina L., Mirasol J. R., Cordero T., Finsterbusch K., Ehrmann A., Investigation of Needleless Electrospun PAN Nanofiber Mats; AIP Conference Series, 1952, 020085 (2018)

18. Molnár K., Szolnoki B., Toldy A., Mihály Vas L., Thermochemical stabilization and analysis of continuously electrospun nanofibers; Journal of Thermal Analysis and Calorimetry 117, 1123-1135 (2014).

19. Wu M. Y., Wang Q. Y., Li K. N., Wu Y. Q., Liu H. Q., Optimization of stabilization conditions for electrospun polyacrylonitrile nanofibers; Polymer Degradation and Stability 97, 1511-1159 (2012).

20. Arshad S. N., Naraghi M., Chasiotis I., Strong carbon nanofibers from electrospun polyacrylonitrile; Carbon 49, 1710–1719 (2011).

# CHAPTER 7

# STABILIZATION OF ELECTROSPUN PAN/GELATIN NANOFIBER MATS FOR CARBONIZATION

# 7. STABILIZATION OF ELECTROSPUN PAN/GELATIN NANOFIBER MATS FOR CARBONIZATION

## 7.1 Abstract

Due to their electrical and mechanical properties, carbon nanofibers are of large interest for diverse applications, from batteries to solar cells to filters. They can be produced by electrospinning polyacrylonitrile (PAN), stabilizing the gained nanofiber mats and afterwards carbonizing them in inert gas. The electrospun base material as well as the stabilization process are crucial for the results of the carbonization process, defining the whole fiber morphology. While blending PAN with gelatin to gain highly-porous nanofibers has been reported a few times in the literature, no attempts have been made yet to stabilize and carbonize these fibers. This paper reports on the first tests of stabilizing PAN/gelatin nanofibers, depicting the impact of different stabilization temperatures and heating rates on the chemical properties as well as the morphologies of the resulting nanofiber mats. Similar to stabilization of pure PAN, a stabilization temperature of 280 °C seems suitable, while the heating rate does not significantly influence the chemical properties. Compared to stabilization of pure PAN nanofiber mats, approximately doubled heating rates can be used for PAN/gelatin blends without creating undesired conglutinations, making this base material more suitable for industrial processes.

## 7.2 Introduction

Functional nanofibers are used in a broad variety of applications, from nanofibrous membranes for filters [1] to substrates in tissue engineering [2,3] to electrocatalysis [4], capacitors [5] and other applications based on the conductivity of the nanofibers [6]. Especially for batteries and other energy applications, often carbon nanofibers are used [7-11].

Such carbon nanofibers are often prepared via the electrospinning route, followed by stabilization and afterwards carbonization. Both steps influence the morphologies, the mechanical and electrical properties of the final carbon nanofibers significantly. While carbon nanofibers can be produced from a broad variety of materials [12-14], one of the most common materials for this purpose is polyacrylonitrile (PAN). PAN changes fiber diameters and mat morphologies significantly for varying spinning and

solution parameters [15,16], while the fibers themselves keep their flat, even surfaces.

In most applications, however, it is advantageous to further increase the surface: volume ratio of the nanofibers. This can be done by blending PAN with other polymers or inorganic material, a method which may also alter other physical properties, such as the conductivity. Increased crystallinity and conductivity were found, e.g., when PAN/pitch nanofibers were carbonized [17]. Blending PAN with cellulose acetate resulted in increased adsorption properties of the carbonized nanofibers [18]. Combined with diverse water-soluble polymers, only gelatin showed a significant influence on the PAN fiber diameters [19]. PAN/gelatin blends have also shown to create highly-porous fibers by electrospinning [20]. Nevertheless, to the best of our knowledge, no investigations on the stabilization of such electrospun PAN/gelatin nanofiber mats were performed yet.

In this paper, the influence of the stabilization temperatures and heating rates on the chemical properties and morphologies of the resulting nanofiber mats will be reported.


## 7.3 Materials and Methods

Electrospinning was performed with a "Nanospider Lab" (Elmarco, Czech Republic), a needleless electrospinning machine based on the wire technology, using a polypropylene fiber mat as the substrate. The spinning parameters were: high voltage 70 kV, nozzle diameter 1.5 mm, carriage speed 100 mm/s, ground-substrate distance 240 mm, electrode-substrate distance 50 mm, temperature in chamber 22 °C, relative humidity in chamber 33 % and air flow 120 $m^3$/hour.

The spinning solution contained 16 % PAN in DMSO (min 99.9 %, purchased from S3 chemicals, Germany) and 9 % gelatin (Abtei, Germany).

Samples of 50 mm x 50 mm of the electrospun nanofiber mats were stabilized in a muffle furnace B150 (Nabertherm), approaching stabilization temperatures between 240 °C and 300 °C at heating rates between 0.5 °C/min and 4 °C/min, and then 1 h of isothermal treatment at the final temperature. For each combination of heating rate and temperature, samples were stabilized with their borders fixed by placing a metal frame with sufficient weight on them as well as freely, without any fixation.

Carbonization was performed in a furnace CTF 12/TZF 12 (Carbolite Gero Ltd., Hope, UK) was used, approaching a temperature of 800 °C with a heating rate of 10 °C/min in a nitrogen flow of 150 mL/min (STP), followed by isothermal treatment for 1 h.

Masses of the samples were taken before and after stabilization using an analytical balance (VWR). Samples dimensions were analyzed by the program ImageJ 1.51j8.

For Fourier-transform infrared (FTIR) spectroscopy, an Excalibur 3100 (Varian, Inc.) was used. Color measurements were performed with a sph900 spectrometer (Color-Lite). Scanning electron microscopy (SEM) images were taken by a Zeiss 1450VPSE with a resolution of 5 nm or a JSM-840 microscope, respectively, using a nominal magnification of 5000 x. Optical images of the nanofiber mats were taken using a confocal laser scanning microscope (CLSM) VK-100 with a nominal magnification of 2000×.

## 7.4 Results and Discussion

Fig. 7.1 depicts the relative mass changes for different stabilization temperatures (Fig. 7.1a) and different heating rates (Fig. 7.1b), respectively. The trend of smaller normalized masses, i.e. larger losses, for higher stabilization temperatures is clearly visible. Compared to a previous study on pure PAN nanofiber mats [21], the normalized masses here are generally smaller, and the mass loss is stronger increased for higher temperatures. This indicates clearly the influence of the gelatin in the fibers – since gelatin denaturalizes around 40-90 °C, depending on the water content [22], it can be expected to be released from the nanofibers as long as it is not completely embedded in the fiber.

Opposite to mass measurements on stabilized PAN nanofibers, showing an approximately constant value of ~ 85 % of the original mass [21], here a clear heating rate dependence is visible for the lower heating rates. This suggests that here the duration of the heating time plays an important role, i.e. the lower the heating rate is, the higher is the polymer decomposition obtained due to pyrolysis and recombination reactions.

(a)                  (b)
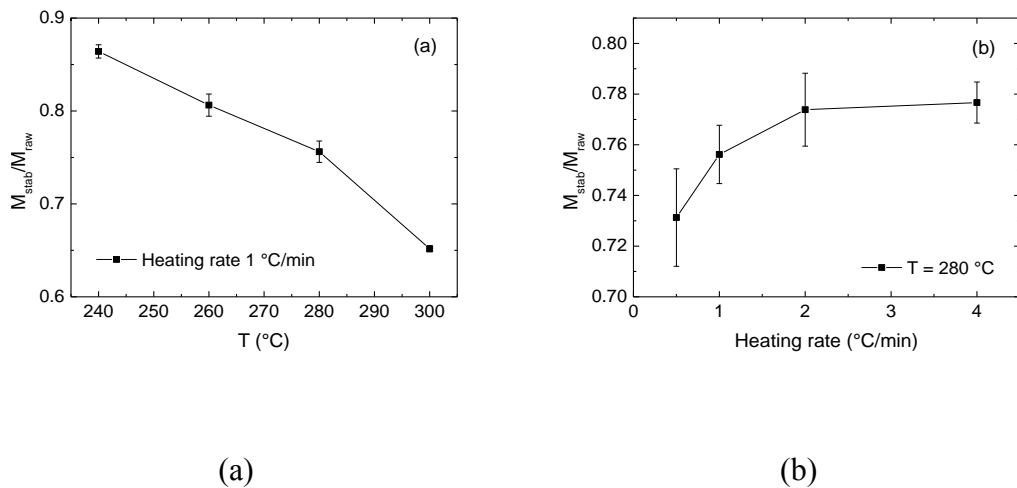
Fig. 7.1 Normalized masses after stabilization at different temperatures (a) and using different heating rates (b).

Besides the masses, the areas of the stabilized samples in fixed and unfixed states were measured. The results are depicted in Fig.7.2, depending on the temperature (a) and the heating rate (b), respectively. The ratio of the areas of the unfixed and the fixed samples decreases with increasing temperature as well as with increasing heating rate, showing that high temperatures and large heating rates cause more stress in the unfixed samples and lets them crumple stronger than under less extreme conditions. This finding underlines the importance of fixing the samples during stabilization.



(a)                  (b)
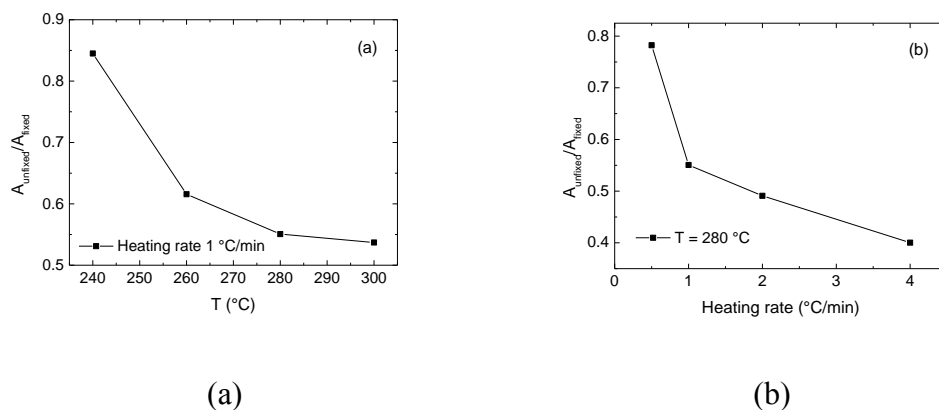
Fig. 7.2 Normalized areas after stabilization at different temperatures (a) and using different heating rates (b).

FTIR measurements were performed on the PAN/gelatin nanofiber mat before stabilization. Fig.7.3 shows the result together with pure PAN and pure gelatin

nanofiber mats. Comparing the spectra shows that the PAN/gelatin line is composed of the typical PAN peaks in the range between 950 cm$^{-1}$ and 1700 cm$^{-1}$, at 2240 cm$^{-1}$ and 2938 cm$^{-1}$ [23,24] as well as gelatin peaks. The latter can be differentiated into the region around 2700-3600 cm$^{-1}$ which is attributed to the amides A and B, the region around 900-1900 cm$^{-1}$ showing the amides I, II, and III, and finally the region below 900 cm$^{-1}$ depicting amide IV [25]. It should be mentioned that several peaks are hard to distinguish between both pure PAN and pure gelatin. The most prominent peaks which are not existent in pure PAN are the peak around 3400 cm$^{-1}$, corresponding with amide A, and the peak near 700 cm$^{-1}$, corresponding to amide IV. In the original state after electrospinning, there are also clear differences between PAN and gelatin around 1640 cm$^{-1}$ (amide I) and 1540 cm$^{-1}$ (amide II); however, it is well-known that in this region significant changes will occur during the stabilization process, making these peaks possibly less suitable for the examination whether gelatin stays in the fabric during stabilization.
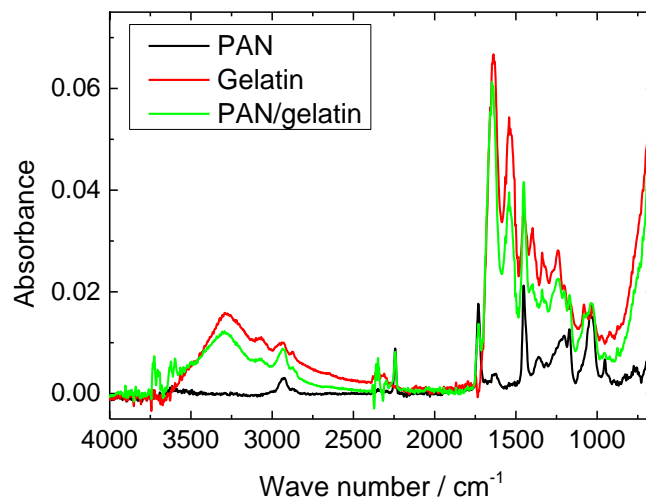


Fig. 7.3 FTIR measurements on PAN, gelatin and PAN/gelatin nanofiber mats.
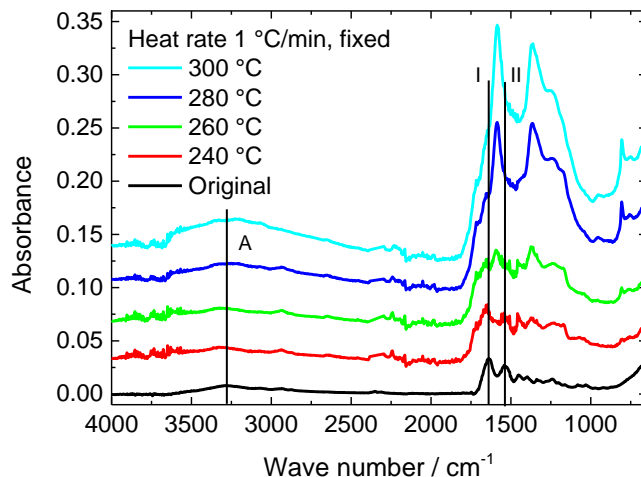
Fig. 7.4 FTIR absorbance measurements on fixed samples, stabilized at different temperatures approached with 1 °C/min. The lines are offset vertically for clarity.

A comparison of the FTIR measurements on PAN/gelatin samples, heated at 1 °C/min to different stabilization temperatures, is given in Fig. 7.4. At first glance, the results look very similar to those gained by stabilizing pure PAN nanofiber mats [21,24,25]. Following the most prominent peaks of the original PAN/gelatin peaks shows that during stabilization (amides A, I and II, as marked in Fig. 7.4) shows that there is no evidence for residual gelatin in the stabilized fiber mat. The same results are visible for the not fixed samples.

Optical examination of the samples after taking them out of the muffle oven revealed dark, nearly black areas on the back in the areas which had touched the underground during stabilization. Since the gelatin is no longer visible in the FTIR measurements taken on the upper surface of the samples, it can be assumed that gelatin – which decomposes above approx. 100 °C, but needs more than approx. 500 °C for complete combustion – has precipitated here after melting. Fig. 7.5 thus depicts FTIR scans of these dark areas.
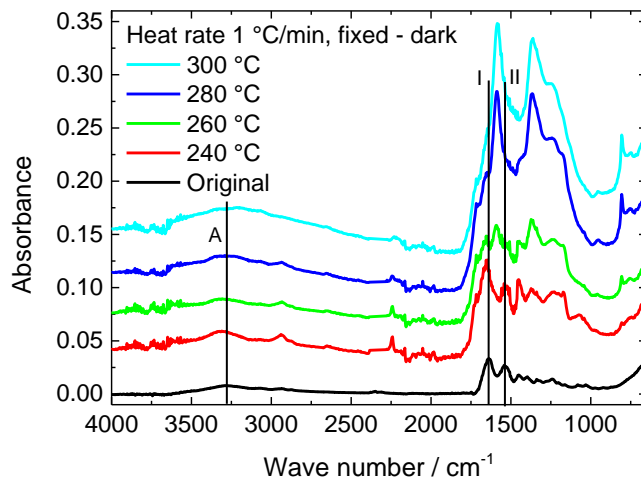
Fig. 7.5 FTIR absorbance measurements on the dark areas on the back of fixed samples, stabilized at different temperatures approached with 1 °C/min. The lines are offset vertically for clarity.

While for a stabilization temperature of 240 °C the peaks for amides A and I are still clearly visible, they are superposed by the growing PAN stabilization peaks for higher temperatures. Thus, the FTIR results can in this case not clearly state which material causes the black areas on the back.
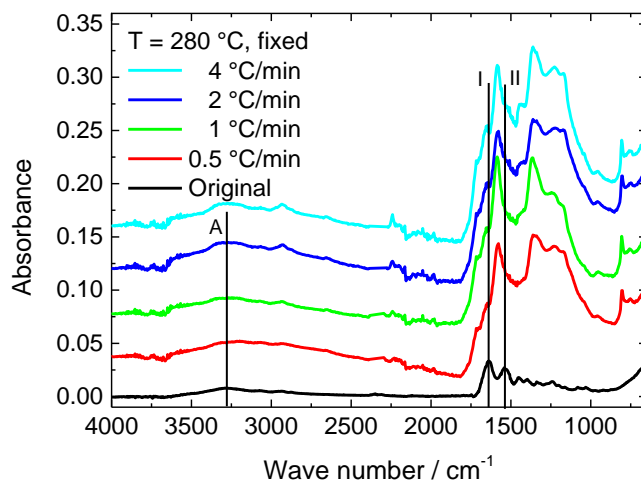


Fig. 7.6 FTIR absorbance measurements on the dark areas on the back of fixed samples, stabilized at 280 °C, approached with different heating rates. The lines are offset vertically for clarity.

Fig. 7.6 shows the heating rate dependence of PAN/gelatin nanofiber mats, stabilized at 280 °C. While stabilizing pure PAN revealed significant differences in the FTIR measurements for different heating rates [28], here all curves are very similar. A closer look, however, shows that for higher heating rates, the peaks for the amides A, I and II stay visible, although strongly superposed by the large peaks of the stabilized

PAN in these areas. This indicates that faster heating allows the gelatin to stay in the nanofiber mat to a certain amount. Similar results were found on the dark back of these samples (not shown here). Optical investigations were performed, using a CLSM. Fig. 7.7 depicts a comparison of an original PAN/gelatin nanofiber mat (a) and a sample stabilized in fixed position at 280 °C, approached at 1°C/min (b).



<p style="text-align:center">(a)          (b)</p>
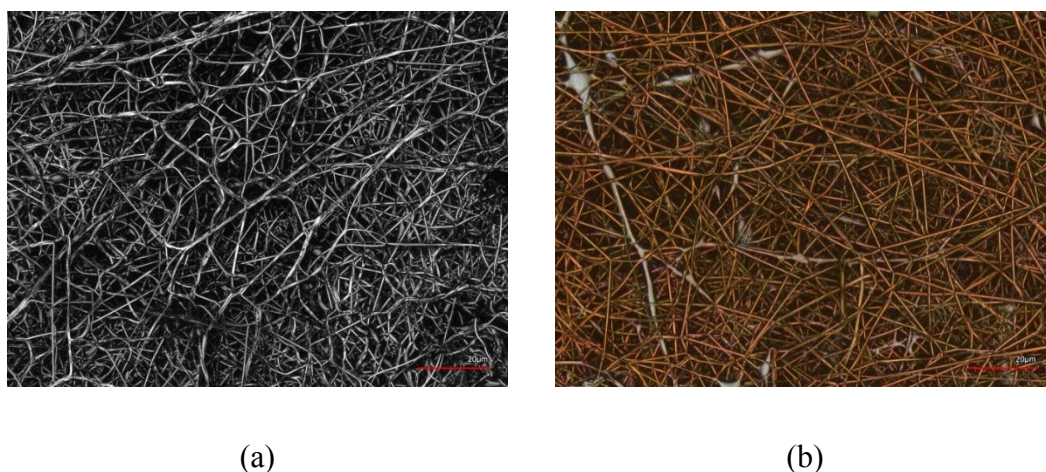
Fig. 7.7 CLSM images of an untreated PAN/gelatin nanofiber mat (a) and a sample stabilized at 280 °C, approached at 1 °C/min (b). The scale bars indicate 20 μm.

Firstly, both images show the typical relatively thick and straight fibers which are typical for gelatin or PAN/gelatin [19]. After stabilization, the usual brown color of the stabilized PAN is visible. Here, however, some silvery fibers can be recognized, clearly indicating gelatin. It should be mentioned that – opposite to stabilization of pure PAN [21] – the stabilization process here seems to straighten the fibers. Another important remark is that no undesired conglutinations are visible in the stabilized sample, as opposed to the stabilization process of pure PAN under identical conditions [21]. Table 7.1 compares the samples stabilized at different temperatures, approached with 1 °C/min, in fixed and unfixed state. Firstly, most images show some areas in which silvery regions or fibers are visible which can clearly be attributed to gelatin since stabilized PAN shows a strong color change. Second, the typical crumpling of pure PAN fibers during stabilization is invisible for the fixed samples and severely reduced for the unfixed samples. This finding is independent from the stabilization temperature, thus possibly allowing using higher stabilization temperatures without a problematic influence on the nanofiber dimensions. This observation shows clearly that blending PAN with gelatin can help to gain straight, long carbon nanofibers, as desired for most technical applications.

Table 7.1 CLSM images of PAN/gelatin nanofiber mat, stabilized in fixed (left panels) and unfixed state (right panels) at different temperatures, approached with 1 °C/min. For a better overview, the scale bars here indicate 50 µm.
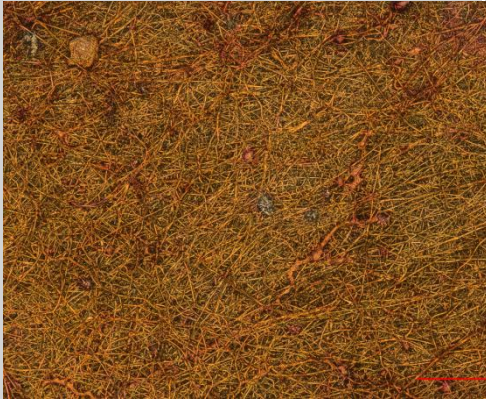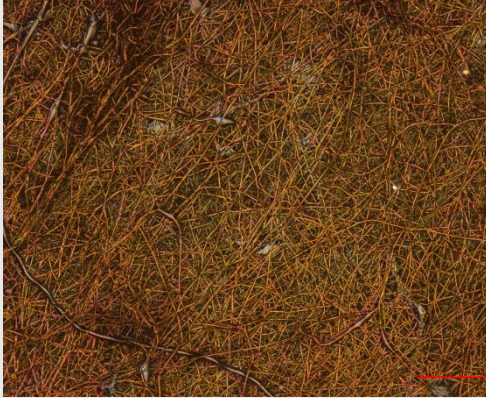
| | fixed | unfixed |
|---|---|---|
| 240 °C |  |  |
| 260 °C |  |  |
| 280 °C |  |  |

Table 7.2 CLSM images of PAN/gelatin nanofiber mat, stabilized in fixed (left panels) and unfixed state (right panels) at 280 °C, approached with different heating rates. The scale bars indicate 50 µm.
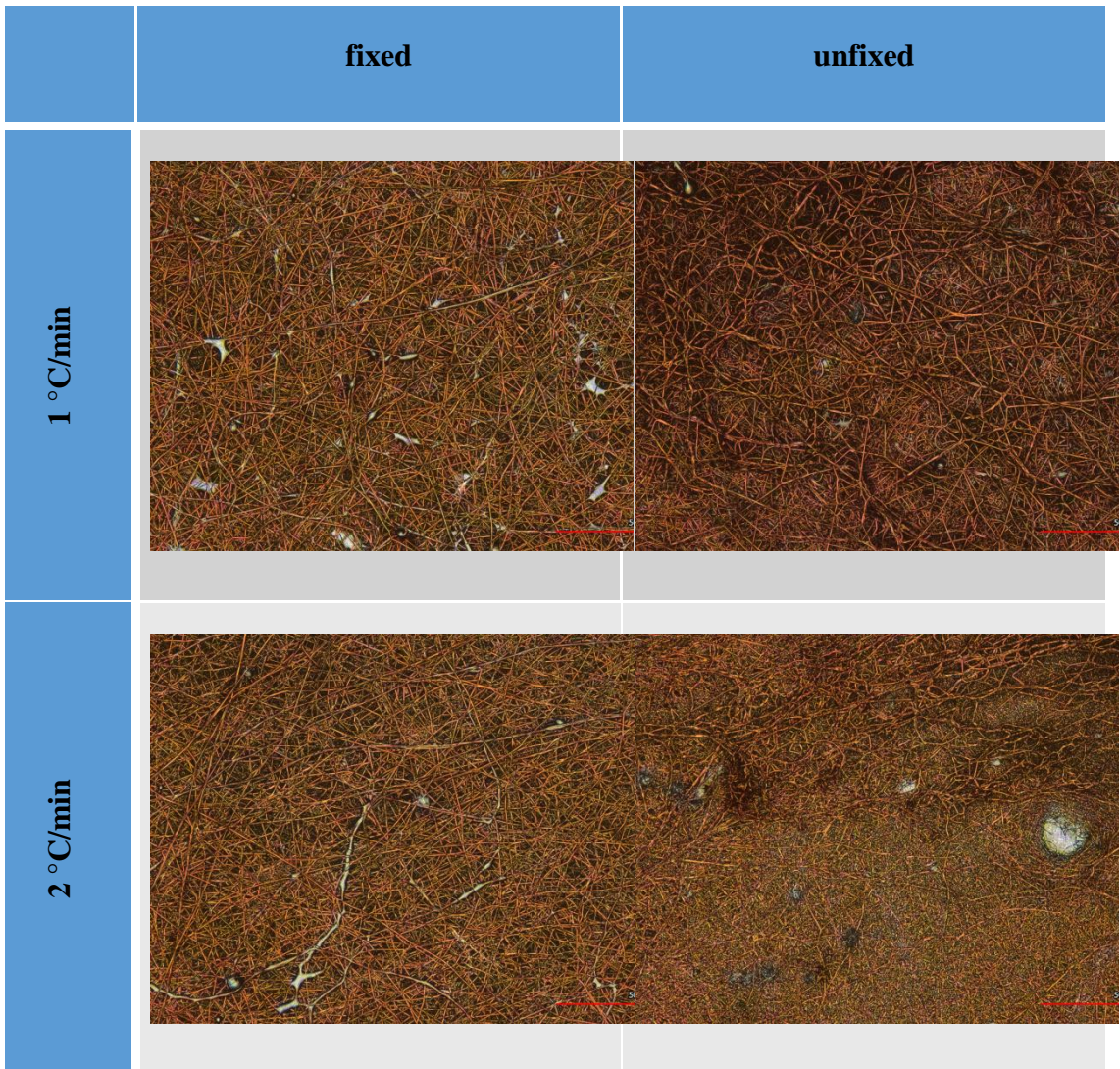
**4 °C/min**
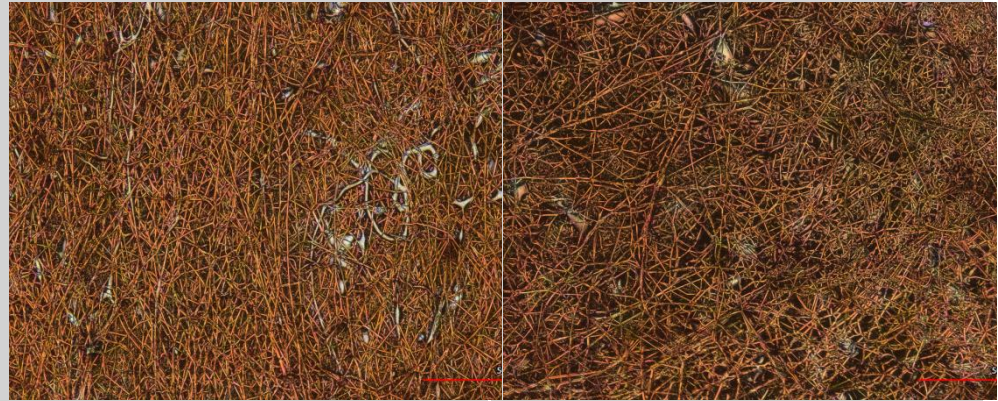
Table 7.2 depicts the dependence of the nanofiber mat morphology after stabilization at 280 °C, approached with different heating rates. For the higher heating rates, the more chaotic fiber distribution for the unfixed samples is visible; however, still no undesired conglutinations seem to appear. The assumption due to Fig. 7.6 that faster heating leads to more remaining gelatin cannot be verified or falsified from these images, especially since gelatin inside PAN fibers or blended fibers cannot be distinguished from pure PAN fibers.

All samples were also investigated from the back, where residual gelatin was expected due to the dark color and the slight differences in the FTIR spectra. Some results of fixed samples are depicted in Fig. 7.8.
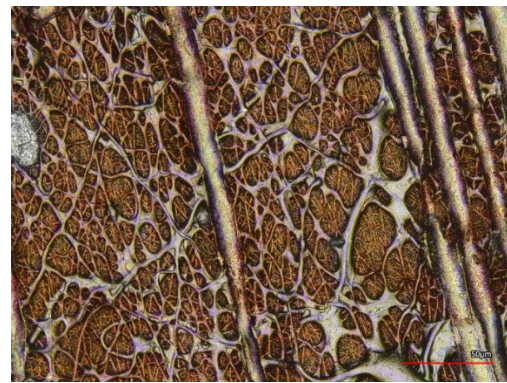


T = 240 °C, 1 °C/min          T = 260 °C, 1 °C/min
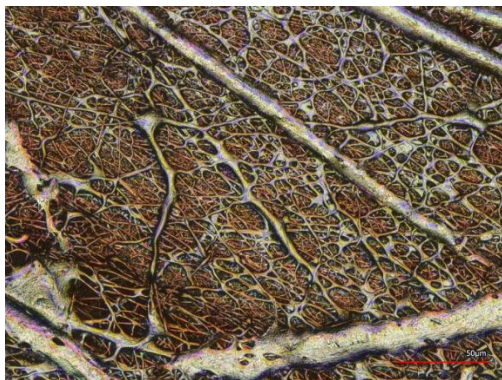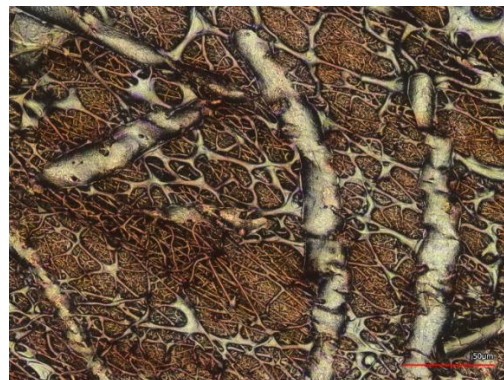
| T = 280 °C, 0.5 °C/min | T = 280 °C, 4 °C/min |

Fig. 7.8 CLSM images of the back of different samples (see insets), stabilized under fixed conditions. The scale bars indicate 50 μm.

Firstly, a significant color change from 240 °C to 260 °C can be recognized. This fits well to the starting point of the main thermal degradation zone of gelatin reported in the literature [26,27]. Thermal degradation between 250 °C and 600 °C includes breakage of protein chains and rupture of peptide bonds, involving the evolution of volatile compounds and formation of new C-C and C-N bonds in the solid matrix.

Independent from this finding, in all cases (including the images not shown here), a mixture of broad gelatin bands and fine gelatin membranes connecting PAN fibers can be identified. No clear influence of the heating rate or the temperature (as long as it is higher than 240 °C) is visible.

These images show that a stabilization process using hanging samples, without contact to the underground, may be favorable to reduce these large gelatin agglomerations. On the other hand, it should be mentioned that the next step, carbonization of the samples, is usually performed at temperatures higher than 600 °C so that gelatin will most probably completely be degraded after the carbonization process. Nevertheless, the influence of such gelatin agglomerations on the morphology of carbonized nanofiber mats should be investigated in the future.

Next, the morphology of the fibers themselves was investigated using SEM. The results for different temperatures are depicted in Table 7.3, while Table 7.4 shows the influence of different heating rates.

Table 7.3 SEM images of PAN/gelatin nanofiber mat, stabilized in fixed (left panels) and unfixed state (right panels) at different temperatures, approached with 1 °C/min. All images were taken using a nominal magnification of 5000 x.

| | fixed | unfixed |
|---|---|---|
| 240 °C |  |  |
| 260 °C |  |  |
| 280 °C |  |  |

300 °C
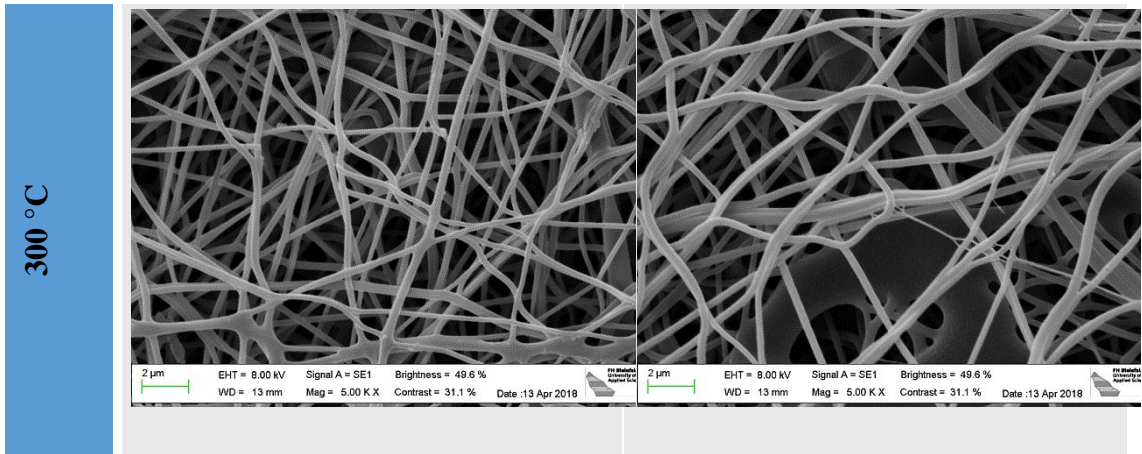
Table 7.4 SEM images of PAN/gelatin nanofiber mat, stabilized in fixed (left panels) and unfixed state (right panels) at 280 °C, approached with different heating rates. All images were taken using a nominal magnification of 5000 x.

| | fixed | unfixed |
|---|---|---|
| 0.5 °C/min | | |
| 1 °C/min | | |
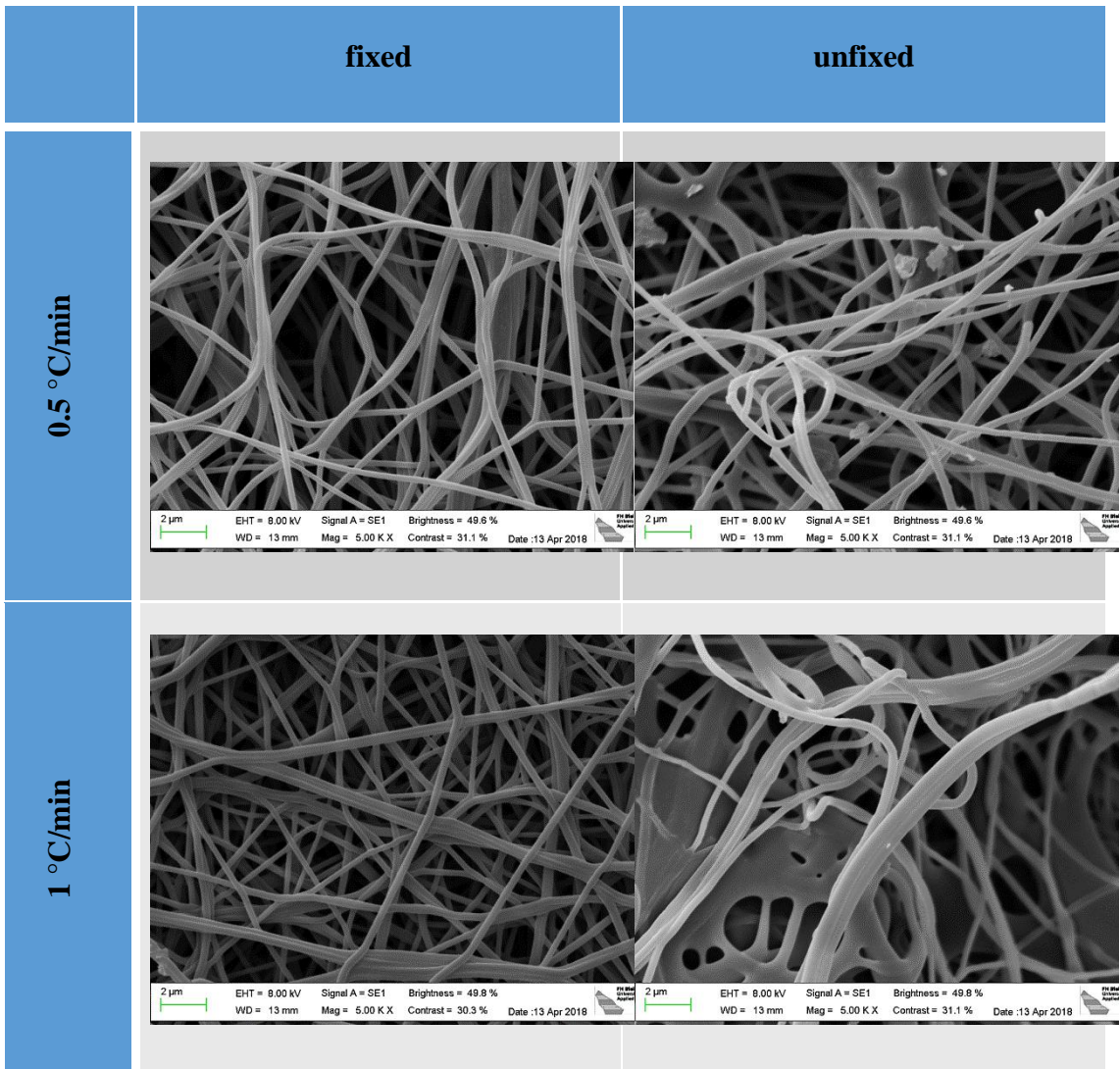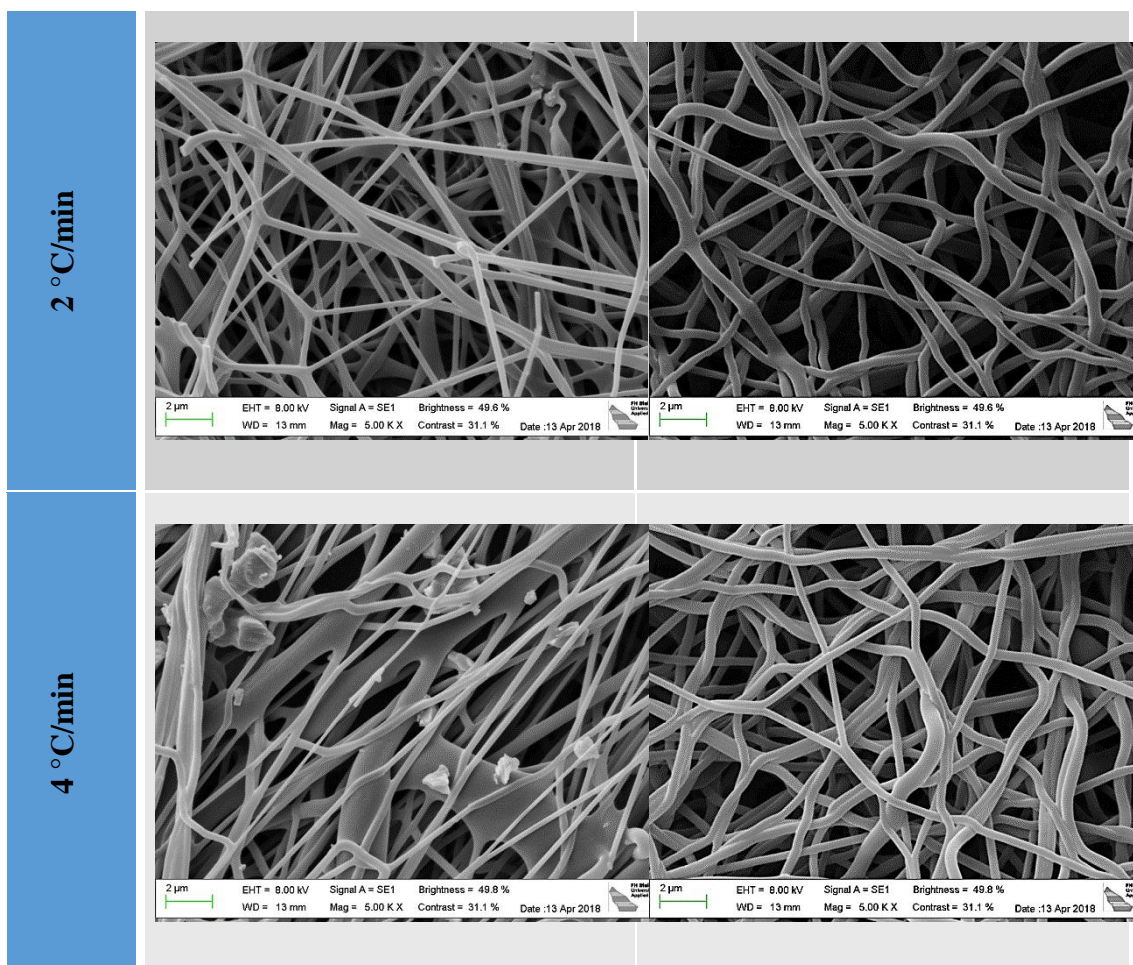
In all cases the unfixed samples show stronger meandering of the fibers, an effect which is supported by high temperatures and high heating rates. Stabilization of fixed nanofiber mats results in most cases in straight, even fibers. Similar to the CLSM images, some gelatin fibers are still visible between the thinner PAN fibers. For the highest temperature and the highest heating rates, the fixed PAN fibers seem to be more irregular; 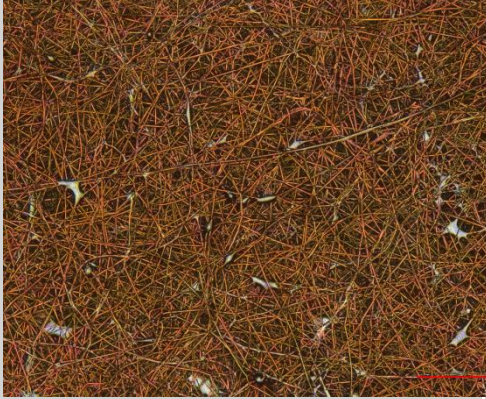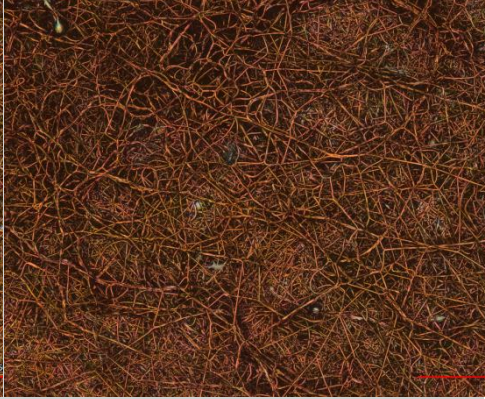thus the SEM images suggest stabilization at 280 °C (which is sufficient for stabilization, based on the FTIR results) and 1 °C/min which is twice as high as the best stabilization temperature for pure PAN nanofiber mats of 0.5 °C/min. It must be mentioned that the original aim of this study, creation and stabilization of PAN/gelatin nanofibers with porous surfaces, was not reached here, while the investigation gives a new approach to create smoother, more even fibers which can be stabilized with a higher heating rate than pure PAN nanofibers.

Finally, spectroscopic examinations of the stabilized nanofiber mats were performed. The color differences for the brighter front and the darker back compared to the original white nanofiber mat are depicted in Fig. 7.9.
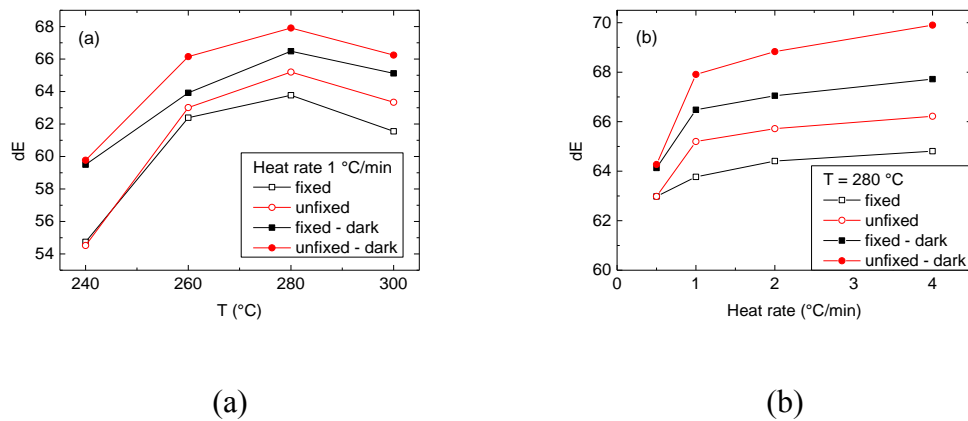
Fig. 7.9 Color differences dE of samples stabilized at different end temperatures (a) and different heating rates (b) and isothermal treatment at the maximum temperature for 1 h.

The difference between the dark and the ―normal" areas is also visible in these measurements for all temperatures and heating rates. Interestingly, the maximum color difference is achieved at 280 °C and decreases again at 300 °C. This may be attributed to structural effects due to the degradation of gelatin. This explanation corresponds to the slightly increasing color differences with increased heating rates, for which larger amounts of residual gelatin were found in the FTIR measurements (Fig. 7.6).

It should be mentioned that for the smallest heating rate of 0.5 °C/min as well as for the lowest temperature of 240 °C (i.e. below the start of the gelatin degradation), there are no differences between fixed and unfixed samples visible. This may indicate that under these stabilization conditions the fixation of the samples is not necessary to gain straight fibers without undesired meandering.

Finally, some of the optimally stabilized samples (all fixed during stabilization) were carbonized at a temperature of 800 °C. Fig. 7.10 depicts the SEM images taken after carbonization.
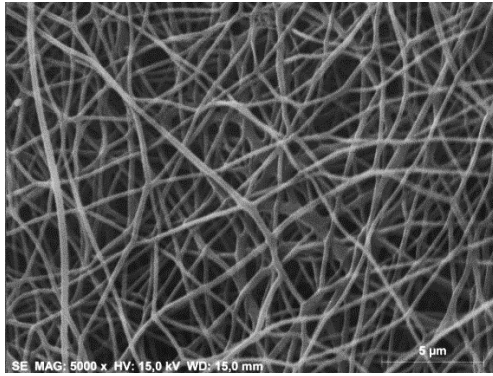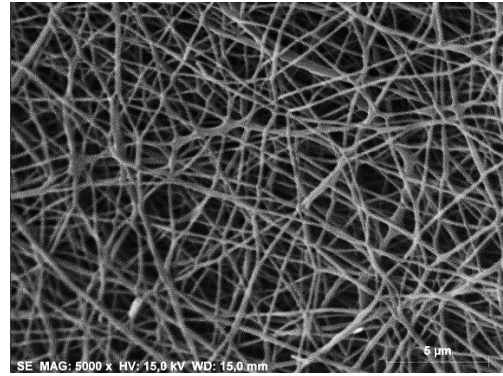
<center>$T_{stab} = 260\ °C,\ 1\ °C/min$          $T_{stab} = 280\ °C,\ 1\ °C/min$</center>
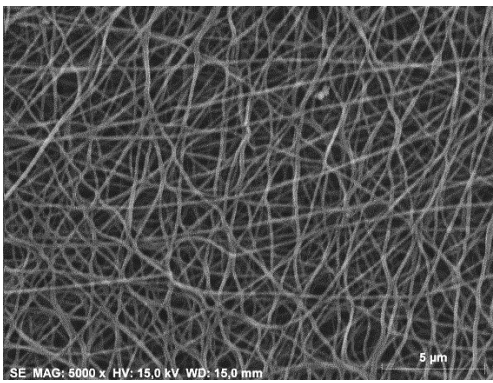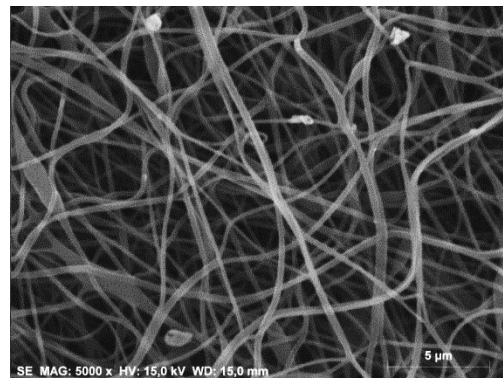


<center>$T_{stab} = 300\ °C,\ 1\ °C/min$          $T_{stab} = 280\ °C,\ 0.5\ °C/min$</center>

Fig. 7.10 SEM images of some samples carbonized at 800 °C.

Comparing these images, it is clearly visible that thicker fibers are achieved by smaller stabilization temperatures (260 °C) and lower heating rates (0.5 °C/min). This corresponds to the results of the stabilization process, as depicted in Tables 7.3 and 7.4, and suggests future tests combining relatively low stabilization temperatures and heating rates to support this property. This result clearly shows that by carefully choosing the stabilization conditions, the intended increase of the fiber diameter can survive the stabilization process, while the blending material responsible for this diameter increase melts at much lower temperatures.

On the other hand, these properties must be balanced against the carbonization yields. Here we found the values given in Table 7.5.

Table 7.5 Stabilization and carbonization yields as well as overall yield after the whole process for the samples depicted in Fig. 4.5-10.

| | Stabilization yield | Carbonization yield | Overall yield |
|---|---|---|---|
| $T_{stab}$ = 260 °C, 1 °C/min | 79.8 % | 14.3 % | 11.3 % |
| $T_{stab}$ = 280 °C, 1 °C/min | 74.8 % | 36.4 % | 27.2 % |
| $T_{stab}$ = 300 °C, 1 °C/min | 64.9 % | 25.0 % | 16.2 % |
| $T_{stab}$ = 280 °C, 0.5 °C/min | 71.8 % | 28.6 % | 20.5 % |

According to these numbers, a stabilization temperature of 280 °C in combination with a stabilization heating rate of 1 °C/min should be preferred. The temperature of 260 °C results in a small carbonization yield, while the highest temperature of 300 °C leads to a reduced stabilization yield. Comparing both alternatives resulting in relatively thick fibers, a small heating rate of 0.5 °C/min in combination with the typical stabilization temperature of 280 °C is preferable since the overall yield is nearly twice as high as in case of the lower stabilization temperature.

Fig. 7.11 shows the results of FTIR measurements on the samples depicted in Fig. 7.10. After stabilization, the peaks visible after stabilization are nearly vanished. Only very few functional groups are left after this process, corresponding to the high absorbance of carbon, as it is well-known from the carbonization process of PAN and other carbon precursors [29,30]. It should be mentioned that the small peaks visible here are neither identical with those stemming from PAN nor stabilized PAN nor gelatin, showing that the samples are carbonized to a high degree.
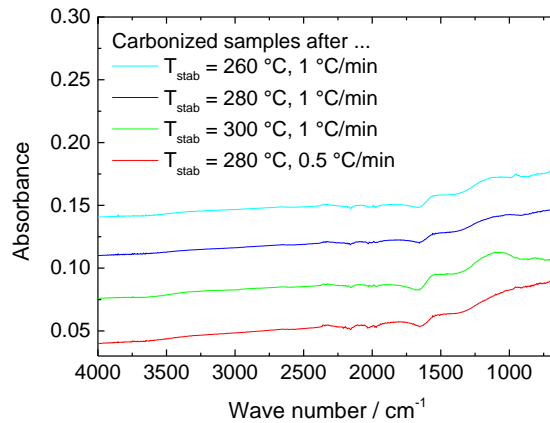
Fig. 7.11 FTIR results of the samples carbonized at 800 °C. The lines are offset vertically for clarity.

## 7.5 Conclusion

In this study, we have investigated electrospun PAN/gelatin nanofiber mats in terms of stabilization parameters and their influences on the resulting stabilized nanofibers. In all cases, the amount of gelatin was significantly reduced, especially above the onset of gelatin degradation at 250 °C, as revealed by FTIR, CLSM and SEM measurements. While adding gelatin did not result in creating porous PAN nanofibers after stabilization, we showed that using PAN/gelatin blends as precursors for carbon nanofibers offers a new possibility to create long, straight fibers without many undesired conglutinations. Future tests will concentrate on investigating the influence of the PAN:gelatin ratio on stabilization and subsequent carbonization processes.

## 7.6 References

1. J. J. He, W. Wang, R. S. Shi, W. J. Zhang, X. Yang, W. X. Shi, F. Y. Cui, Chemical Engineering Journal 337, 428-435 (2018).

2. E. M. Cagil, F. Oczan, S. Ertul, Journal of Nanoscience and Nanotechnology 18, 5292-5298 (2018).

3. G. Potewyd, S. Moxon, T. Wang, M. Domingos, N. M. Hooper, Trends in Biotechnology 36, 457-472 (2018).

4. H. J. Tang, W. Chen, J. Y. Wang, T. Dugger, L. Cruz, D. Kisailus, Small 14, 1703459 (2018).

5. Y. L. Li, Y. Y. Zheng, Journal of Applied Polymer Science 135, 46103 (2018).

6. Y. C. Li, J. Y. Ji, Y. Wang, R. F. Li,, W. H. Zhong, Journal of Materials Science 53, 8653-8665 (2018).

7. H. Wang, Y. Jiang, A. Manthiram, Advanced Energy Materials 8, 1701953 (2018).

8. S. S. Yao, J. Cui, J. Q. Huang, J. Q. Huang, W. G. chong, L. Qin, Y. W. Mai, J. K. Kim, Advanced Energy Materials 8, 1702267 (2018).

9. K. S. Wu, Y. Hu, Z. Shen, R. Z. Chen, X. He, Z. L. Chen, P. Pan, Journal of Materials Chemistry A 6, 2693-2699 (2018).

10. X. Song, S. Q. Wang, G. P. Chen, T. Gao, Y. Bao, L. X. Ding, H. H. Wang, Chemical Engineering Journal 333, 564-571 (2018).

11. L. Zhu, L. J. You, P. H. Zhu, X. Q. Shen, L. Z. Yang, K. S. Xiao, ACS Sustainable Chemistry & Engineering 6, 248-257 (2018).

12. Y. Zhao, Y. Liu, C. C. Tong, J. Ru, B. y. Geng, Z. Q. Ma, H. Z. Liu, L. K. Wang, Journal of Materials Science 53, 7637-7647 (2018).

13. F. J. Garcia-Mateos, R. Berenguer, M. J. Velero-Romero, J. Rodriguez-Mirasol, T. Cordero, Journal of Materials Chemistry A 6, 1219-1233 (2018).

14. W. Fang, S. Yang, T. Q. Yuan, A. Charlton, R. C. Sun, Industrial & Engineering Chemistry Research 56, 9551-9559 (2017).

15. T. Grothe, D. Wehlage, T. Böhm, A. Remche, A. Ehrmann, Tekstilec 60, 290-295 (2017).

16. L. Sabantina, J. R. Mirasol, T. Cordero, K. Finsterbusch and A. Ehrmann, AIP Conference Series 1952, 020085 (2018).

17. C. Liu, K. Lafdi, Journal of Applied Polymer Science 134, 45388 (2017).

18. Y. W. Ju, G. Y. Oh, Korean Journal of Chemical Engineering 34, 2731-2737 (2017).

19. D. Wehlage, R. Böttjer, T. Grothe, A. Ehrmann, AIMS Materials Science 5, 190-200 (2018).

20. L. W. Yu, L. X. Gu, European Polymer Journal 45, 1706-1715 (2006).

21. L. Sabantina, M. Klöcker, M. Wortmann, J. R. Mirasol, T. Cordero, E. Moritzer, K. Finsterbusch, A. Ehrmann, Optimizing stabilization parameters for needleless-electrospun PAN nanofiber mats, submitted.

22. A.Bigi, G. Cojazzi, S. Panzavolta, K. Rubini, N. Roveri, Biomaterials 22, 763-768 (2001).

23. E. Cipriani, M. Zanetti, P. Bracco, V. Brunella, M. P. Luda, L. Costa, Polymer Degradation and Stability 123, 178-188 (2016).

24. K. Mólnar, B. Szolnoki, A. Toldy, L. M. Vas, Journal of Thermal Analysis and Calorimetry 117, 1123-1135 (2014).

25. G. S. Al-Saidi, A. Al-Alawi, M. S. Rahman, and N. Guizani, International Food Research Journal 19, 1167-1173 (2012).

26. C. Peña, K. d. l. Caba, A. Eceiza, R. Ruseckaite, I. Mondragon, Bioresour. Technol. 101, 6836-6842 (2010).

27. S. Gautam, A. K. Dinda, N. C. Mishra, Materials Science and Engineering C 33, 1228-1235 (2013).

28. L. Sabantina, M. Ángel Rodríguez-Cano, M. Klöcker, F. J. García-Mateos, J. J. Ternero-Hidalgo, A. Mamun, F. Beermann, M. Schwakenberg, A.-L. Voigt, J. Rodríguez Mirasol, T. Cordero, A. Ehrmann, Polymers 10, 735 (2018).

29. S. N. Arshad, M. Naraghi, and I. Chasiotis, Carbon 49, 1710 (2011).

30. C.-W. Park, W.-J. Youe, S.-Y. Han, Y. S. Kim, S.-H. Lee, Holzforschung 71, 743-750 (2017).

CHAPTER 8


FIXING PAN NANOFIBER MATS DURING STABILIZATION FOR
CARBONIZATION AND CREATING NOVEL METAL/CARBON
COMPOSITES

## 8. FIXING PAN NANOFIBER MATS DURING STABILIZATION FOR CARBONIZATION AND CREATING NOVEL METAL/CARBON COMPOSITES

### 8.1 Abstract

Polyacrylonitrile (PAN) is one of the materials most often used for carbonization. PAN nanofiber mats, created by electrospinning, are an especially interesting source to gain carbon nanofibers. A well-known problem in this process is fixing the PAN nanofiber mats during the stabilization process which is necessary to avoid contraction of the fibers, correlated with an undesired increase in the diameter and undesired bending. Fixing this issue typically results in breaks in the nanofiber mats if the tension is too high, or it is not strong enough to keep the fibers as straight as in the original state. This article suggests a novel method to overcome this problem by electrospinning on an aluminum substrate on which the nanofiber mat adheres rigidly, stabilizing the composite and carbonizing afterwards either with or without the aluminum substrate to gain either a pure carbon nanofiber mat or a metal/carbon composite.

### 8.2 Introduction

Electrospinning can be used to create nanofiber, e.g., from polyacrylonitrile (PAN) which is a typical precursor of carbon nanofibers [1–3]. Such carbon nanofibers can be applied, e.g., to improve the mechanical properties of plastic materials by forming a composite with a polymer or a resin, the electrical properties of batteries and super-capacitors, etc. [4–7].

To gain carbon nanofibers, the first step is a stabilization process which is typically performed in air, resulting in cyclization and thermally stable aromatic ladder polymer formation [8] which increases the chemical and mechanical stability of the nanofiber mat and is essential before the carbonization step. The whole stabilization process also includes dehydrogenation, aromatization, oxidation, and crosslinking [9–11].

In previous articles discussing the stabilization and subsequent carbonization of PAN nanofiber mats, stabilization temperatures, and heating rates are strongly discussed. Fitzer et al., e.g., investigated different stabilization temperatures between 260 °C

and 290 °C and heating rates up to 5 °C /min, showing that for the PAN they used a heating rate of 1 °C/min and a final temperature of 270 °C resulted in maximum tensile strength of the final carbon fibers carbonized at 1350 °C [12]. On the contrary, Mathur et al. found that temperatures up to 300 °C were not sufficient for thermal stabilization, but temperatures between 350 and 400 °C were needed to reach low hydrogen contents and correspondingly only little tar formation during carbonization [13]. A completely different thermal treatment was found ideal by Moon and Ferris. They suggested performing a first stabilization step with a high heating rate of 5 °C/min up to 150 °C, followed by a first isothermal treatment for 2 h to completely remove water and solvent. Afterwards, stabilization was carried further to 200 °C where a second isothermal step followed for 2 h. Carbonization was even split in four steps with decreasing heating rates up to a temperature of 1350 °C. In this way, the best ultimate strengths of the carbon yarns were reached [14]. Mólnar et al. found different conversion temperatures for the completed stabilization process, depending on the measurement method they applied. The color examination revealed the lowest conversion temperature of approx. 195 °C, followed by the temperature based on FTIR of 207 °C, while the DSSC indicated a conversion temperature of 244 °C. In all cases, the standard deviations were found to be 34–56 °C; thus these conversion temperatures are not exact values [15]. Gu et al. examined the conductivity of carbon nanofibers, stabilized at different temperatures, and found that while the morphology of the carbon nanofibers was desirable for a stabilization temperature of 250 °C, a stabilization temperature of 270 °C resulted in fiber conglutinations which were supportive for an increased conductivity [16]. Rafiei et al. found stabilization temperatures of 150–270 °C in combination with a heating rate below 2 °C/min ideal according to the stabilization index and the aromatization index [17].

A problem which is less often mentioned, however, is the dimensional change of the nanofibers during the stabilization process. On the one hand, conglutinations are formed which are sometimes helpful [16] but in most cases undesired. Some publications show such conglutinations in the SEM images without discussing them further [18,19] or describing how to overcome this problem by changing solution and stabilization parameters [20]. On the other hand, shrinkage and bending of fibers may occur if they are not fixed during the temperature treatment. Ma et al. stretched a bundle of PAN nanofibers by knotting them together with a carbon fiber cord, tying

them with a metal hook, and tying the other cord with a displacement device to apply a programmed tension, in this way stretching them by approximately a factor of 3 and afterwards stabilizing them at fixed length by stretching them over a metal frame [21]. Wu et al. used hot-stretching during stabilization to gain an elongation by a factor of 1.7, fixing one side of the sample on a frame and putting a defined weight at the opposite side [22]. Xie et al. stretched the fibers in an oven by applying a weight at a middle temperature of 140 °C up to different pre-defined drawing ratios, followed by stabilization at 250 °C for 4 h under a constant load. Comparison between raw and drawn yarn showed an increase in yarn and fiber uniformity after drawing as well as better fiber alignment, polymer chain orientation, and corresponding tensile strength [23]. Ma et al. found that even the tension during carbonization influenced the tensile strength and Young's modulus, suggesting a moderate carbonization tension of 20 cN per nanofiber bundle [24]. These experiments are usually applied to nanofiber bundles and cannot be transferred to nanofiber mats produced with needleless electrospinning. Such samples are either stabilized freely or fixed during this process to avoid conglutinations and undesired morphological changes of the fibers. Fixing the samples, however, is not easy. If only two opposite sides are fixed by a weight, e.g., the other sides will shrink [25,26]. If all sides are fixed, the samples can break even at low heating rates since the forces working on the nanofiber mat are not well distributed [27,28].

This article thus aims at suggesting a simple new approach to overcome this problem which at the same time offers the possibility to create a novel metal–carbon composite. It should be mentioned that the mechanical properties of the single nanofibers, as well as the nanofiber mats, were not investigated. The first is technologically quite demanding; the latter does not correspond to the planned application of single carbon nanofibers in composites. Instead, the focus of the recent study is the development of an increased stabilization method as well as a new method to create metal/carbon composites.

## 8.3 Materials and Methods

The electrospinning machine—Nanospider Lab (Elmarco, Liberec, Czech Republic), a needleless electrospinning machine based on the wire technology—was used to create nanofiber mats. Spinning parameters were as follows: high voltage 60 kV,

current approx. 0.04 mA, electrode–substrate distance 240 mm, nozzle diameter 0.8 mm, carriage speed 50 mm/s, substrate speed 50 mm/min, relative humidity 33%, and temperature 22.0 °C, air flow 120 m$^3$/hour.

T.he spinning solution contained 15% PAN dissolved in DMSO (min 99.9%, purchased from S3 chemicals, Bad Oeynhausen, Germany). As a substrate, household aluminum foil (from Rewe, Bielefeld, Germany) was used. For comparison, samples electrospun on the usual polypropylene (PP) substrate (from Elmarco) under identical conditions are used. Samples of the electrospun nanofiber mats were stabilized in a muffle furnace B150 (Nabertherm, Lilienthal, Germany), approaching a typical stabilization temperature of 280 °C at a heating rate of 1 °C/min, followed by isothermal treatment at this maximum temperature for 1 h. The samples electrospun on PP were separated from the substrates before stabilization (since PP melts below stabilization temperature), while the samples electrospun on aluminum were not separated from their substrates. For carbonization, a furnace CTF 12/TZF 12 (Carbolite Gero Ltd., Hope, UK) was used, approaching temperatures of 500 °C or 800 °C, respectively, with a heating rate of 10 °C/min in a nitrogen flow of 150 mL/min (STP), followed by isothermal treatment for 1 h.

Scanning electron microscopy (SEM) images were taken by a Zeiss 1450VPSE (Oberkochen, Germany) with a resolution of 5 nm, using a nominal magnification of 5000×. Additionally, a confocal laser scanning microscope (CLSM) VK-9700 by Keyence (Neu-Isenburg, Germany) was applied. For Fourier-transform infrared (FTIR) spectroscopy, an Excalibur 3100 (Varian, Inc., Palo Alto, CA, USA) was used. The software ImageJ 1.51j8 (from National Institutes of Health, Bethesda, MD, USA) was applied to determine the nanofiber diameters from 50 fibers per sample

## 8.4 Results and discussions

Fig. 8.1 depicts PAN nanofiber mats, prepared during the same electrospinning process, on PP and aluminum foil as substrates, respectively. On the aluminum foil, the nanofibers show a slightly larger diameter, connected with fewer undesired beads. The latter are typically for PAN nanofiber mats spun from DMSO with relatively low solid contents. Apparently, spinning on aluminum foil can on the one hand reduce the beads, probably due to shaping the electric field in the spinning chamber differently; on the other hand, the slightly thicker nanofibers may be

unwanted. This shows that spinning and solution parameters must be carefully adjusted to gain the desired morphology if the substrate is changed. This parameter study will be performed in the near future.

Fig. 8.2 shows the effect of stabilization on PAN nanofiber mats on both substrates. The nanofiber mat produced on the usual PP substrate and stabilized purely (without the substrate) without fixing it has strong conglutinations between the single fibers, the latter are clearly thicker than in the original state. It should be mentioned that fixing the sample by weights significantly reduces the effect, but cannot completely eliminate it [27,28]. The samples stabilized via adhering on the aluminum foil, however, have not changed their morphology (Fig. 8.2b). Apparently, this simple method can help increasing the formation of long, straight stabilized PAN fibers.
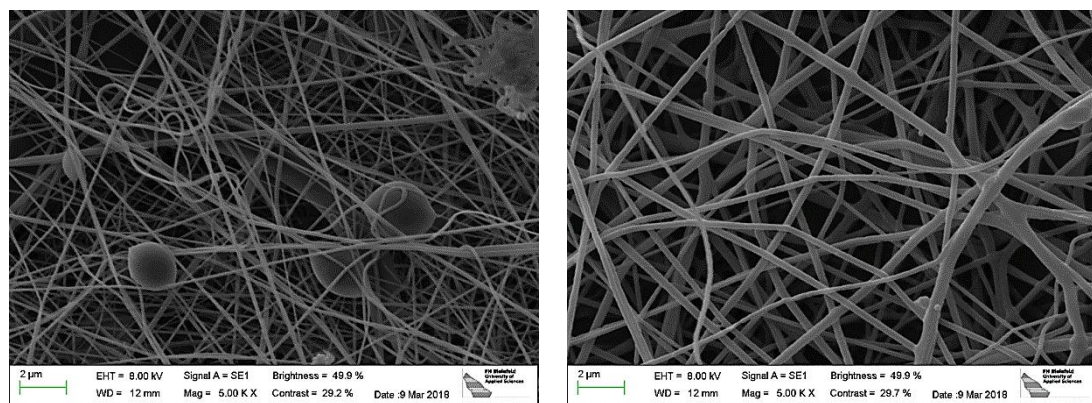


(a)                                                        (b)

Fig. 8.1 Electrospun PAN nanofiber mats: (a) PP as substrate; (b) aluminum foil as substrate.
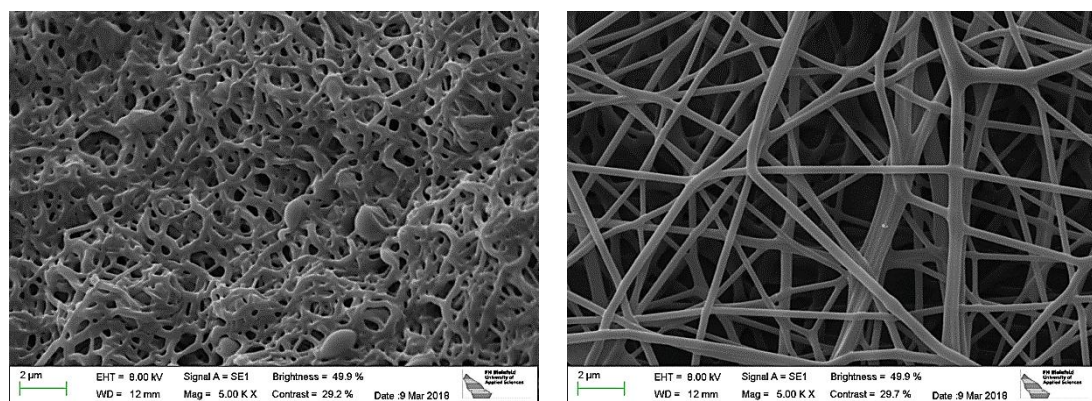


(a)                                                        (b)

Fig. 8.2 PAN nanofiber mats after stabilization: (a) electrospun on PP (substrate separated before stabilization); (b) electrospun on aluminum foil (substrate not removed before stabilization).

121

The same result can also be found on a macroscopic scale. As shown in Fig. 8.3, the nanofiber mats electrospun on the usual PP substrate and on aluminum foil look very similar in their original state (Fig. 8.3a). After stabilization at 280 °C for 1 h (Fig. 8.3b), the PAN nanofiber mat on aluminum has the same dimensions as before. The unfixed pure PAN nanofiber mat has reduced its widths and lengths by approximately a factor of 2 each. The fixed pure PAN nanofiber mat was broken during stabilization; only the upper right corner remained under the weights, while the residual area shrank stronger. This significant dimensional change can also be recognized by the colors of the samples after stabilization—the brown color is much brighter for the PAN stabilized on aluminum, corresponding to less PAN per area due to the dimensional stability.



(a)                                        (b)
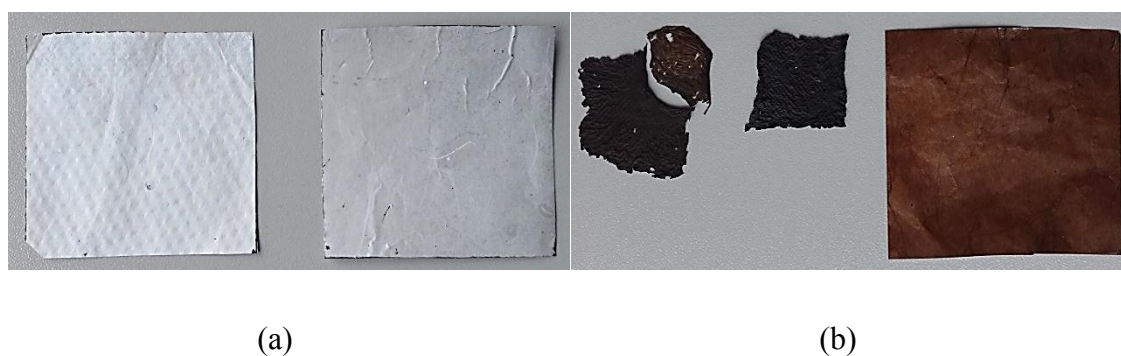
Fig. 8.3 PAN nanofiber mats electrospun on different substrates: (a) after spinning; (b) after stabilization (and separating from the substrate in case of the PP substrates) at 280 °C for 1 h.

Such a strong adhesion between aluminum and polyacrylonitrile is usually not reported in the scientific literature. Aluminum oxide membranes, for example, can be used as a template to create PAN nanofibers by extrusion into this template and polymerizing in its nano-pores. In this case, the template can be recycled by washing, suggesting that the adhesion is not very strong [29,30]. Similarly, coating polyacrylonitrile and other polymers with aluminum resulted in condensation on the polymer substrate, forming a uniform metal layer there, while metals like copper and nickel migrated into the substrate [31]. Only by plasma polymerization of acrylonitrile gas is the adhesion of PAN layers on aluminum reported in the literature [32].

On the other hand, the solvent DMSO cannot contribute to the adhesion between the nanofiber mat and the aluminum substrate, either. Aluminum oxide (which forms a thin film on the surface of the uncleaned aluminum foil) is known to be stable in organic solvents, including DMSO [33–36].

Finally, one process which is sometimes mentioned in the literature may be responsible for the adhesion between both materials: for chemical vapor deposition coating of PAN with aluminum, the formation of aluminum carbide was observed [37], a reaction which is more typical for carbon/aluminum surfaces [38]. Another possible reaction—also typically only observed at high temperatures—is the formation of aluminum nitride [39]. In order to investigate whether any of these chemical reactions has occurred during electrospinning PAN on aluminum foil, FTIR investigations were performed. Exemplary results are depicted in Fig. 8.4. The graphs show the typical peaks of pure and stabilized PAN in both cases, with an additionally increased absorbance for the smaller wavenumbers, as it can be expected from the aluminum oxide underground.

As described in detail by Mólnar et al. [15] and Sabantina et al. [27], PAN shows several characteristic peaks before stabilization, some of them from PAN and other from the different copolymers used to improve the properties of the fibers such as methyl acrylate. At 2938 $cm^{-1}$ and 1452 $cm^{-1}$ as well as 1380 $cm^{-1}$, peaks correlated with bending and stretching vibrations of $CH_2$ are visible. The peak at 2240 $cm^{-1}$ is attributed to the stretching of nitrile functional group C≡N. The carbonyl (C=O) stretching peak can be recognized at 1732 $cm^{-1}$. In the ranges of 1230–1250 $cm^{-1}$ and 1050–1090 $cm^{-1}$ peaks occur due to ester (C–O and C–O–C) vibrations of the co-monomers like itaconic acid or methyl acrylate.

After stabilization, these peaks attributed to nitrile and carbonyl functional groups are mostly vanished. Instead, C=N stretching vibrations at 1582 $cm^{-1}$ and C=C stretching vibrations at 1660 $cm^{-1}$ appear as a consequence of the cyclization–aromatization of the polymers. Additionally, the peak at 1360 $cm^{-1}$ can be attributed to C–H bending and C–$H_2$ wagging. Finally, the peak around 800 $cm^{-1}$ is related to aromatic C–H vibrations due to oxidative dehydrogenation aromatization. As a consequence of the stabilization in oxidative atmosphere (air), oxygen cross-linking is formed between polymer chains and an increase in the absorbance can be observed in Fig. 8.4 in the ranges of 1230–1250 $cm^{-1}$ and 1050–1090 $cm^{-1}$ attributed to C–O

and C–O–C vibrations, in the case of the spectra of the stabilized fibers with respect to the electrospun ones.
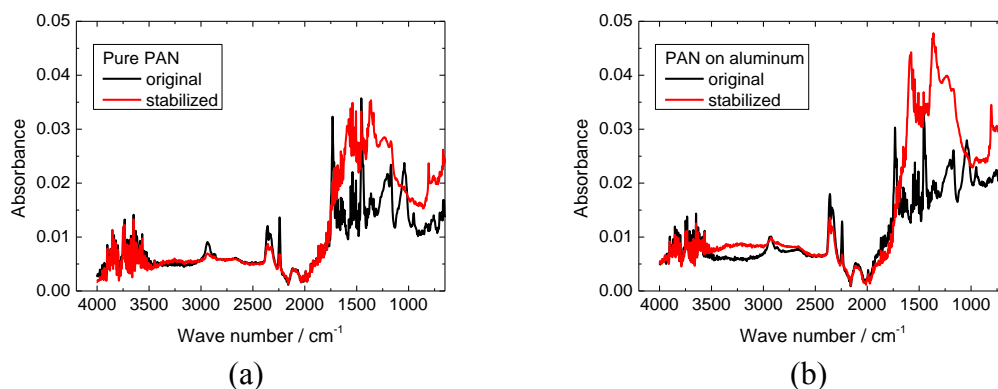


Fig. 8.4 FTIR investigation of PAN nanofiber mats before and after stabilization: (a) pure PAN; (b) PAN on aluminium substrate.

Comparing PAN electrospun on aluminum with the pure PAN nanofiber mat electrospun on PP, no additional peaks are visible. Aluminum carbide should show peaks related to C–C and C=C in the range between 1350 and 1700 $cm^{-1}$ which are not visible here [40]. This, however, is not sufficient to exclude the possibility that a thin layer of AlC is created along the interfacial surface. Aluminum nitride only shows a peak around 550 $cm^{-1}$ and would thus not be visible in our FTIR instrument. The FTIR analysis cannot help in understanding the good adhesion between both materials in this test series.

Carefully separating the PAN nanofiber mat from the aluminum substrate shows that the adhesion between both materials is mostly of electrostatic nature, i.e., introduced by the electrospinning process itself. Nevertheless, the fibers at the interface are chemically bonded to the aluminum foil and cannot be separated without destroying the metal surface, as Fig. 8.5 reveals. Apparently the adhesion between both materials can be attributed to a strong electrostatic interaction in combination with a chemical bonding of yet unknown nature.
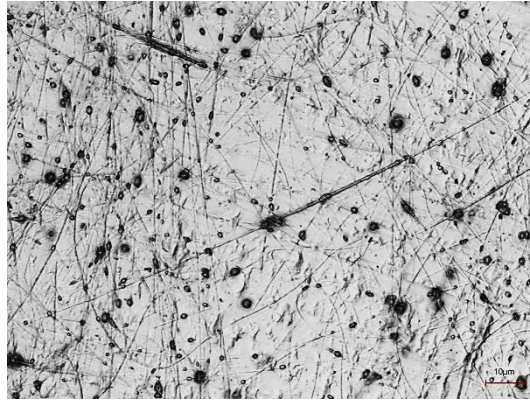
Fig. 8.5 Aluminum surface after separating the PAN nanofiber mat electrospun on it. The scale bar indicates 10 μm.

Subsequent, the stabilized samples were carbonized at 500 °C (Fig. 8.6). In both cases, the carbonized samples show morphologies very similar to those obtained after stabilization. Afterwards, it is possible to separate the nanofiber mat and aluminum foil with any scraping tool, if desired.



(a)                                                              (b)
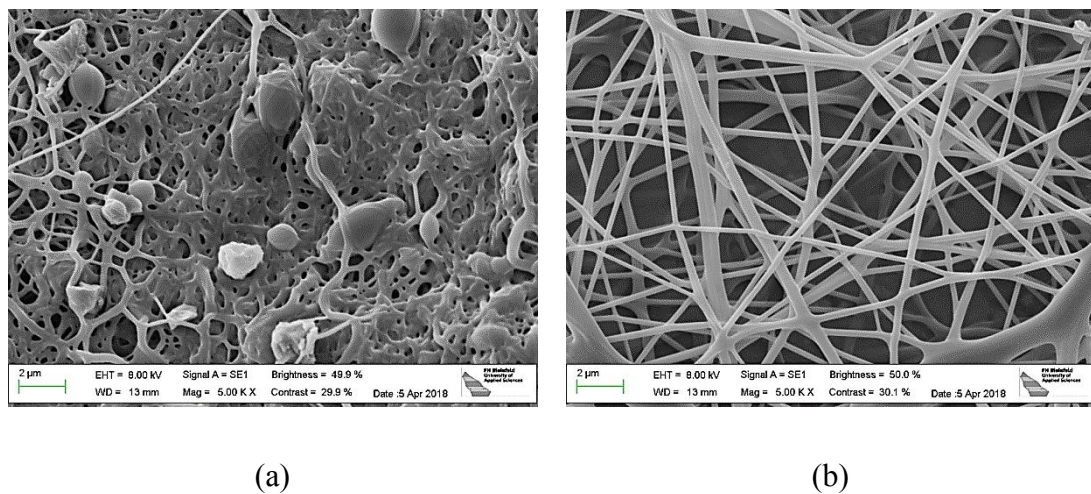
Fig. 8.6 PAN nanofiber mats after carbonization at 500 °C: (a) electrospun on PP (substrate separated before stabilization); (b) electrospun on aluminum foil (substrate not removed before stabilization or carbonization).

Finally, the stabilized PAN nanofiber mats were carbonized at 800 °C (Fig. 8.7). Since this temperature is higher than the melting temperature of aluminum of approx. 660 °C, now both materials start intermixing and forming a composite, as can be recognized in Fig. 8.7b. This technological approach of composite production is, to the best of our knowledge, not yet found in the scientific literature.

(a)                                                    (b)
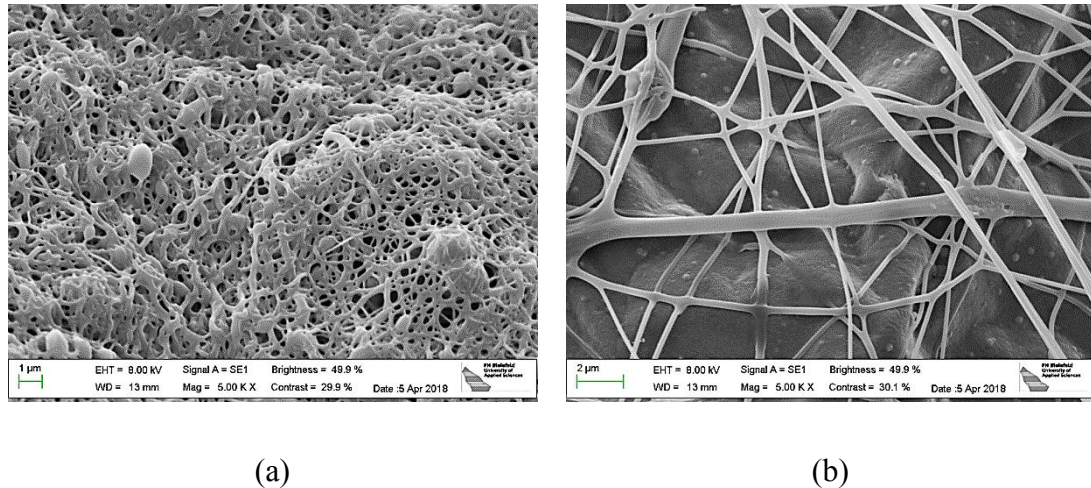
Fig. 8.7 PAN nanofiber mats after carbonization at 800 °C: (a) electrospun on PP (substrate separated before stabilization); (b) electrospun on aluminum foil (substrate not removed before stabilization).

A strong adhesion between aluminum and PAN has also been reported for other technologies in which both these materials were coated on each other in different ways. Carbon fibers were, e.g., coated with aluminum to create carbon/aluminum composites. Fibers along a fracture surface were not found to be pulled out of the aluminum composite, indicating a good adhesion [41]. When mixing short carbon fibers into liquid aluminum, their wettability was found poor [42]; thus, this new attempt may give rise to an interesting method to produce carbon/aluminum composites.

To summarize the morphological changes during stabilization and carbonization, Fig. 8.8 depicts a quantitative comparison of all nanofiber diameters, measured in the SEM images on 50 fibers per sample.

As already visible from the SEM images themselves, the diameters of the electrospun PAN nanofibers on aluminum were significantly larger than those of the fibers spun on the PP nonwoven (Fig. 8.8 a, b). The stabilization of PAN fibers (prepared on PP substrate) produces an increase in the fiber diameter while the average nanofiber diameter on the aluminum foil stays constant (the undesired conglutinations, as visible from the SEM images, were not taken into account for calculation of this value, only clearly visible fibers) (Fig. 8.8 c, d). Carbonization at 500 °C (Fig. 8.8 e, f) or 800 °C (Fig. 8.8 g,h) does not change the average diameters anymore, neither for the nanofiber mats spun on PP nor for those stabilized and carbonized on aluminum. It should be mentioned that the standard deviation—i.e., the distribution

126

of the nanofiber diameters—is slightly larger for the nanofibers prepared on the nonwoven PP after stabilization and carbonization.
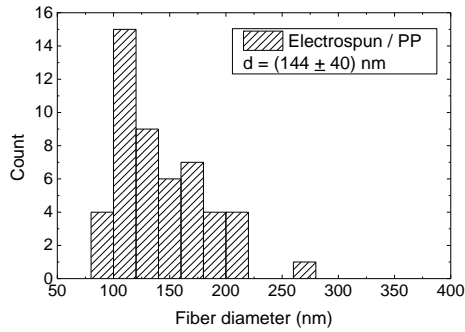


(a)
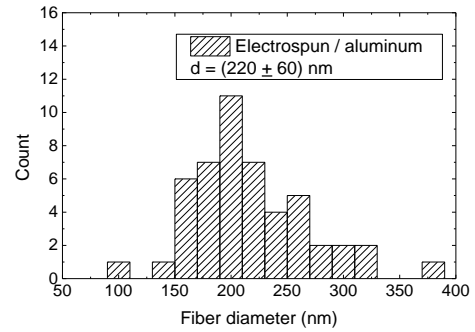
(b)
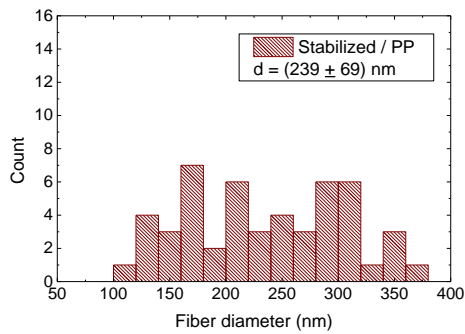
(c)
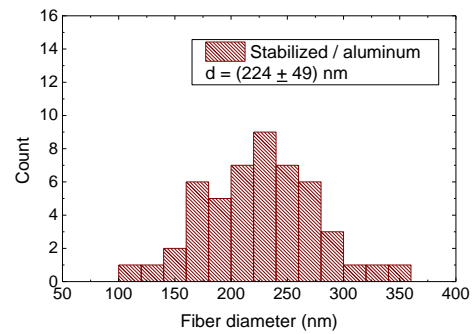
(d)
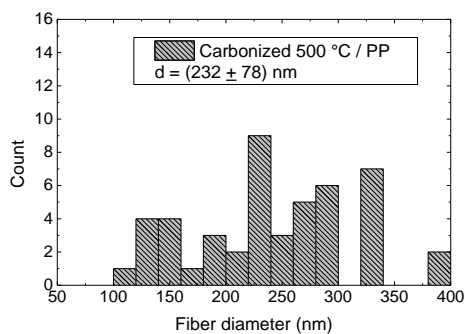
(e)
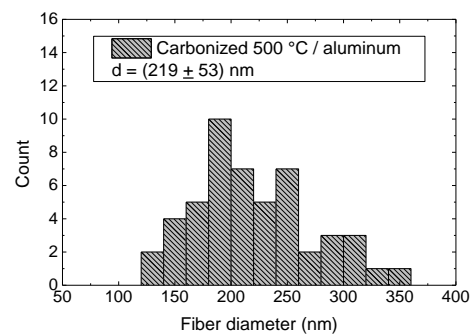
(f)
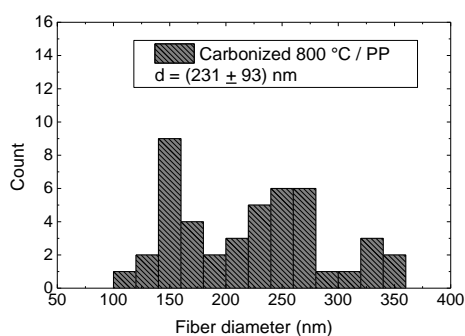
<center>(g)</center>
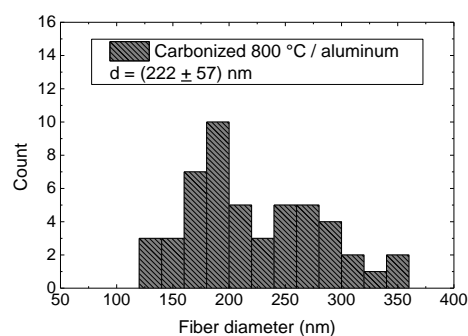


<center>(h)</center>

Fig. 8.8 Diameters of PAN nanofiber mats electrospun on PP (a) or aluminum substrates (b), measured directly after spinning, after stabilization (c, d, respectively), and after carbonization at 500 °C (e, f) and 800 °C (g, h), respectively. Average diameters and their standard deviations are given in the insets.

## 8.5 Conclusion

Electrospinning PAN nanofiber mats on aluminum substrates was shown to offer a simple possibility to overcome the problem of how to fix the nanofiber mats during the stabilization process, which is indispensable for keeping unconglutinated, straight nanofibers. Additionally, at higher carbonization temperatures, aluminum–carbon composites can be formed.

It should be mentioned that in the study reported here, this composite formation was neither forced (e.g., by placing a weight on top during carbonization) nor investigated further since the main aim was finding a solution for the problem of undesired fiber shrinkage and bending during stabilization. Nevertheless, this effect results in many possible applications in the area of composites and will be investigated further in the near future, especially with respect to composite formation during carbonization and the mechanical properties of the resulting composites.

## 8.6 References

1.  Greiner, A.; Wendorff, J.H. Electrospinning: A fascinating method for the preparation of ultrathin fibers. Angew. Chem. Int. Ed. 2007, 46, 5670–5703.

2.  Rahaman, M.S.A.; Ismail, A.F.; Mustafa, A. A review of heat treatment on polyacrylonitrile fiber. Polym. Degrad. Stab. 2007, 92, 1421–1432.

3.  Sabantina, L.; Mirasol, J.R.; Cordero, T.; Finsterbusch, K.; Ehrmann, A. Investigation of Needleless Electrospun PAN Nanofiber Mats. AIP Conf. Proc. 2018, 1952, 020085, doi:10.1063/1.5032047.

4.  Manoharan, M.P.; Sharma, A.; Desai, A.V.; Haque, M.A.; Bakis, C.E.; Wang, K.W. The interfacial strength of carbon nanofiber epoxy composite using single fiber pullout experiments. Nanotechnology 2009, 20, 5.

5.  Ji, L.W.; Yao, Y.F.; Toprakci, O.; Lin, Z.; Liang, Y.Z.; Shi, Q.; Medfort, A.J.; Millns, C.R.; Zhang, X.W. Fabrication of carbon nanofiber-driven electrodes from electrospun polyacrylonitrile/polypyrrole bicomponents for high-performance rechargeable lithium-ion batteries. J. Power Sources 2010, 195, 2050–2056.

6.  Jung, H.R.; Lee, W.J. Preparation and characterization of Ni-Sn/carbon nanofibers composite anode for lithium ion battery. J. Electrochem. Soc. 2011, 158, A644–A652.

7.  Liu, J.W.; Essner, J.; Li, J. Hybrid supercapacitor based on coaxially coated manganese oxide on vertically aligned carbon nanofiber arrays. Chem. Mater. 2010, 22, 5022–5030.

8.  Chen, J.; Harrison, I. Modification of polyacrylonitrile (PAN) carbon fiber precursor via postspinning plasticization and stretching in dimethyl formamide (DMF). Carbon 2002, 40, 25–45, doi:10.1016/S0008-6223(01)00050-1.

9.  Bashir, Z. A critical review of the stabilisation of polyacrylonitrile. Carbon 1991, 29, 1081–1090, doi:10.1016/0008-6223(91)90024-D.

10. Dalton, S.; Heatley, F.; Budd, P.M. Thermal stabilization of polyacrylonitrile fibres. Polymer 1999, 40, 5531–5543, doi:10.1016/S0032-3861(98)00778-2.

11. Ismar, E.; Sezai Sarac, A. Oxidation of polyacrylonitrile nanofiber webs as a precursor for carbon nanofiber: Aligned and non-aligned nanofibers. Polym. Bull. 2017, 75, 485–499, doi:10.1007/s00289-017-2043-x.

12. Fitzer, E.; Frohs, W.; Heine, M. Optimization of stabilization and carbonization treatment of PAN fibres and structural characterization of the resulting carbon fibres. Carbon 1986, 24, 387–395.

13. Mathur, R.; Bahl, O.; Mittal, J. A new approach to thermal stabilization of PAN fibres. Carbon 1992, 30, 657–663.

14. Moon, S.C.; Farris, R.J. Strong electrospun nanometer-diameter polyacrylonitrile carbon fiber yarns. Carbon 2009, 47, 2829–2839.

15. Mólnar, K.; Szolnoki, B.; Toldy, A.; Vas, L.M. Thermochemical stabilization and analysis of continuously electrospun nanofibers. J. Therm. Anal. Calorim. 2014, 117, 1123–1135.

16. Gu, H.; Li, Y.W.; Li, N. Electrical Conductive and Structural Characterization of Electrospun Aligned Carbon Nanofibers Membrane. Fibers Polym. 2015, 16, 2601–2608.

17. Rafiei, S.; Noroozi, B.; Arbab, S.; Haghi, A.K. Characteristic Assessment of Stabilized Polyacrylonitrile Nanowebs for the Production of Activated Carbon Nano-Sorbents. Chin. J. Polym. Sci. 2014, 32, 449–457.

18. Alarifi, I.M.; Alharbi, A.; Khan, W.S.; Swindle, A.; Asmatulu, R. Thermal, Electrical and Surface Hydrophobic Properties of Electrospun Polyacrylonitrile Nanofibers for Structural Health Monitoring. Materials 2015, 8, 7017–7031.

19. Arbab, S.; Teimoury, A.; Mirbaha, H.; Adolphe, D.C.; Noroozi, B.; Nourpanah, P. Optimum stabilization processing parameters for polyacrylonitrile-based carbon nanofibers and their difference with carbon (micro) fibers. Polym. Degrad. Stab. 2017, 142, 198–208.

20. Dhakate, S.R.; Gupta, A.; Chaudhari, A.; Tawale, J.; Mathur, R.B. Morphology and thermal properties of PAN copolymer based electrospun nanofibers. Synth. Met. 2011, 161, 411–419.

21. Ma, S.; Liu, J.; Liu, Q.; Liang, J.Y.; Zhao, Y.; Fong, H. Investigation of structural conversion and size effect from stretched bundle of electrospun polyacrylonitrile copolymer nanofibers during oxidative stabilization. Mater. Des. 2016, 95, 387–397.

22. Wu, S.; Zhang, F.; Yu, Y.H.; Li, P.; Yang, X.P.; Lu, J.G.; Rye, S.K. Preparation of PAN-based carbon nanofibers by hot-stretching. Compos. Interfaces 2008, 15, 671–677, doi:10.1163/156855408786778311.

23. Xie, Z.; Niu, H.; Lin, T. Continuous polyacrylonitrile nanofiber yarns: Preparation and drydrawing treatment for carbon nanofiber production. RSC Adv. 2015, 5, 15147–15153, doi:10.1039/C4RA16247A.

24. Ma, S.; Liu, J.; Qu, M.; Wang, X.; Huang, R.; Liang, J. Effects of carbonization tension on the structural and tensile properties of continuous bundles of highly aligned electrospun carbon nanofibers. Mater. Lett. 2016, 183, 369–373, doi:10.1016/j.matlet.2016.07.144.

25. Santos de Oliveira, M., Jr.; Manzolli Rodrigues, B.V.; Marcuzzo, J.S.; Guerrini, L.M.; Baldan, M.R.; Rezende, M.C. A statistical approach to evaluate the oxidative process of electrospun polyacrylonitrile ultrathin fibers. J. Appl. Polym. Sci. 2017, 134, 45458, doi:10.1002/app.45458.

26. Wu, M.; Wang, Q.Y.; Li, K.; Wu, Y.Q.; Liu, H.Q. Optimization of stabilization conditions for electrospun polyacrylonitrile nanofibers. Polym. Degrad. Stab. 2012, 97, 1511–1519, doi:10.1016/j.polymdegradstab.2012.05.001.

27. Sabantina, L.; Klöcker, M.; Wortmann, M.; Rodrígues Mirasol, J.; Cordero, T.; Moritzer, E.; Finsterbusch, K.; Ehrmann, A. Optimizing stabilization parameters for needleless-electrospun PAN nanofiber mats. Journal of Industrial Textiles 2018, submitted.

28. Sabantina, L.; Wehlage, D.; Klöcker, M.; Mamun, A.; Grothe, T.; Rodrígues Mirasol, J.; Cordero, T.; Finsterbusch, K.; Ehrmann, A. Stabilization of electrospun PAN/gelatin nanofiber mats for carbonization. Journal of Nanomaterials 2018, submitted.

29. Feng, L.; Li, S.H.; Zhai, J.; Song, Y.L.; Jiang, L.; Zhu, D.B. Template based synthesis of aligned polyacrylonitrile nanofibers using a novel extrusion method. Synth. Met. 2003, 135–136, 817–818.

30. Feng, L.; Li, S.H.; Zhai, J.; Song, Y.L.; Jiang, L.; Zhu, D.B. Super-hydrophobic surface of aligned polyacrylonitrile nanofibers. Angew. Chem. Int. Ed. 2002, 41, 1221–1223.

31. Bébin, P.; Prud'homme, R.E. Comparative XPS Study of Copper, Nickel, and Aluminum Coatings on Polymer Surfaces. Chem. Mater. 2003, 15, 965–973, doi:10.1021/cm020599x.

32. Hammermesh, C.L.; Crane, L.W. Adhesion of Plasma Polymer Films to Metal Substrates. J. Appl. Polym. Sci. 1978, 22, 2395–2396, doi:10.1002/app.1978.070220830.

33. Masuda; H.; Fukuda, K. Ordered Metal Nanohole Arrays Made by a Two-Step Replication of Honeycomb Structures of Anodic Alumina. Science 1995, 268, 1466–1468, doi:10.1126/science.268.5216.1466.

34. Li, F.; Zhang, L.; Metzger, R.M. On the growth of highly ordered pores in anodized aluminum oxide. Chem. Mater. 1998, 10, 2470–2480, doi:10.1021/cm980163a.

35. Ossensky, O.; Müller, F.; Gösele, U. Self-organized formation of hexagonal pore arrays in anodic alumina. Appl. Phys. Lett. 1998, 72, 1173–1175, doi:10.1063/1.121004.

36. Yin, A.J.; Li, J.; Jian, W.; Bennett, A.J.; Xu, J.M. Fabrication of highly ordered metallic nanowire arrays by electrodeposition. Appl. Phys. Lett. 2001, 79, 1039–1041.

37. Suzuki, T. The compatibility of pitch-based carbon fibers with aluminum for the improvement of aluminum-matrix composites. Compos. Sci. Technol. 1996, 56, 147–153.

38. Warrier, S.G.; Blue, C.A.; Lin, R.Y. Control of interfaces in Al-C fibre composites. J. Mater. Sci. 1993, 28, 760–768, doi:10.1007/BF01151253.

39. Jain, M.K.; Nadkarni, S.K.; Gesing, A. Process of Producing Aluminum and Titanium Nitrides. Patent US5114695A, 14 April 1987.

40. Yate, L.; Caicedo, J.C.; Hurtado Macias, A.; Espinoza-Beltrán, F.J.; Zambrano, G. Composition and mechanical properties of AlC, AlN and AlCN thin films obtained by r.f. magnetron sputtering. Surf. Coat. Technol. 2009, 203, 1904–1907.

41. Ohsaki, T.; Yoshida, M.; Fukube, Y.; Nakamura, K. The properties of carbon fiber reinforced aluminum composites formed by the ion-plating process and vacuum hot pressing. Thin Solid Films 1977, 45, 563–568.

42. Akbarzadeh, E.; Picas Barrachina, J.A.; Puig, M.B. Thixomixing as Novel Method for Fabrication Aluminum Composite with Carbon and Alumina Fibers. Int. J. Chem. Mol. Nucl. Mater. Metall. Eng. 2015, 9, 822–826.

CHAPTER 9

CONCLUSIONS AND SUGGESTIONS FOR THE FUTURE WORK

## 9. Conclusions and Suggestions for the Future Work

In this dissertation the low-toxic solvent DMSO (dimethyl sulfoxide) was used for needleless electrospinning process to produce PAN nanofibers, PAN/gelatin blends and metal/carbon composites. At the beginning of this work, three main objectives were set and the research results show that these goals have been achieved in the context of this work.

It has been shown that it was possible to tailor the desired fiber/membrane ratio by varying the distance between the electrodes. Investigations have been underlined, that while the areal weights depend significantly on all parameters under investigation, the nanofiber diameters often show only weak trends or no deviations at all. Moreover, the nanofiber mat morphologies change severely with the electrode distance, the carriage speed, the high voltage and the nozzle diameter. It should be mentioned that the electrospinning conditions such as the spinning mechanism, the spinning chamber geometry, air flow through the chamber and especially the relative humidity in the spinning chamber significantly influence the nanofiber mat morphologies. But the membrane area for a typical electrospinning situation is often not exactly zero because small membrane-like areas are often visible in ‒pure" nanofiber mats. This depends on the relative humidity in the spinning chamber and the solid content in the spinning solution. This leads to the conclusion, that it is indispensable to examine the electrospun nanofiber mats by confocal laser scanning microscope (CLSM), scanning electron microscope (SEM) or other techniques which allow for investigating the nanofibers with sufficient resolution. Finally, for each spinning situation the optimal electrospinning conditions should be investigated separately.

The water vapor resistance of PAN nanofiber mats with varying morphologies between pure nanofibers and pure membranes has been examined. This property is essential for many applications, especially for filtration, medical applications such as wound dressing or protective clothing. The water vapor resistance of nanofiber mats it is only scarcely investigated in the literature and investigations of the transition between nanofiber mat and membrane in terms of water vapor permeability cannot be found in the literature. Depending on the spinning parameters, nano-membranes and nanofiber mats were produced as well as a wide range between both morphologies. The distance between the high voltage electrode and the substrate

influences significantly the ratio of membrane to fibrous areas. Furthermore, the water vapor permeability was measured between 0.1 Pa·m²/W and more than 10 Pa·m²/W. Finally, it was possible to create mixtures between fibers and membranes or pure membranes by modifying the electrospinning parameters. It has been shown that creation of finest filters as well as nearly impenetrable thin membranes by varying the electrospinning parameters is realizable. These findings underline an approximately exponential correlation between the absolute evaporation resistance and the membrane ratio.

The influence of stabilization temperature and heating rate on PAN nanofiber mats, electrospun using a wire-based technology from a solution in DMSO, has been evaluated. The optimal balance between not burning the fibers and chemical reaction to proceed sufficiently fast to allow complete stabilization is significant for the carbonization step and the resulting nanofiber mat morphologies. Moreover, investigations of the beads occurring at relatively low solid contents in the solution which are often undesired, but in some cases advantageous to avoid fiber slippage in a resin matrix and should thus also keep their shapes during stabilization, were performed. This is the case for integrating carbonized nanofibers into composite materials to increase their mechanical properties, where these beads can deal as ―anchors‖ in the matrix. In this dissertation nanofiber mats fixed and unfixed during the stabilization process were compared in order to minimize undesired conglutinations and nanofiber dimensional changes, which has not been described in the literature before. It can be underlined that by carefully controlling the maximum stabilization temperature and especially the heating rate, fully stabilized PAN fibers without undesired interconnections can be created as precursors for carbonization. Moreover, at all stabilization temperatures, the unfixed samples shrink more than the fixed ones. By evaluation of stabilized and carbonized nanofiber mats the SEM, CLSM or similar methods must also be applied to avoid unexpected and undesired changes in the fiber mat morphology and not only FTIR and other chemical examination methods are essential. In addition, the importance of a slow heating rate and in particular a mechanical fixation of the samples during the stabilization was underlined in order to avoid unwanted bonding and an increase in the fiber diameter. It has been shown that more detailed investigations are needed to find out which of these processes are essential for the subsequent carbonation process. Thus, stabilization processes can be tailored to the needs of the resulting carbon nanofibers.

It should be mentioned that by blending PAN with gelatin no differences between fixed and unfixed samples after finishing of stabilization process were visible. This may indicate that under these stabilization conditions the fixation of the samples is not necessary to gain straight fibers without undesired bending and conglutinations. This result underlines the assumption that by careful selection of stabilization conditions, the intended increase of the fiber diameter can survive the stabilization process, while the blending material responsible for this diameter increase melts at much lower temperatures. Future tests combining relatively low stabilization temperatures and heating rates to support this property are needed. Using PAN/gelatin blends as precursors for carbon nanofibers can offer a new possibility to create long, straight fibers without many undesired conglutinations. Future tests should concentrate on investigating the influence of the PAN:gelatin ratio on stabilization and subsequent carbonization processes. This investigation shows clearly that blending PAN with gelatin can help to gain straight, long carbon nanofibers, as desired for most technical applications.

Moreover, this dissertation suggests a novel method to overcome the problem of insufficient fixing of the nanofiber mats during the stabilization process by electrospinning on an aluminum substrate. The nanofiber mat adheres rigidly on aluminum and keeps its morphology during stabilization and carbonization processes. After the stabilization process, the nanofiber mat can be separated from the aluminum substrate to form pure carbon nanofibers after carbonization, or it can be carbonized together with the aluminum substrate to form a metal/carbon composite. In this dissertation, a simple new approach to overcome the problem of undesired morphological changes of the nanofibers during stabilization process which at the same time offers the possibility to create a novel metal/carbon composite was developed. The findings should make an important contribution to the field of metal/carbon composites.

It should be noted that the mechanical properties of the single nanofibers, as well as the nanofiber mats, were not investigated in this study, but can be a part of future investigations. Instead, the focus was the development of an increased stabilization method as well as a new method to create metal/carbon composites. It has been shown that the PAN nanofiber mats stabilized via adhering on the aluminum foil have not changed their morphology. Such a strong adhesion between aluminum and

polyacrylonitrile is usually not reported in the scientific literature. Apparently, this simple method can be used to ensure the formation of long, straight stabilized PAN fibers. Apparently such as strong adhesion between polyacrylonitrile and aluminum can be attributed to a strong electrostatic interaction in combination with a chemical bonding of yet unknown nature. Nevertheless, this effect can lead to many other possible applications in the field of composites and should be further investigated in the near future, especially with regard to composite formation during carbonization and the mechanical properties of the resulting composites.

In addition to the applications described above for materials investigated in this dissertation, the following future investigations can be made on the basis of this work: Experiments can be performed, e.g., to cultivate animal, plant and fungal cells on nanofiber mats. Thus new application areas in medicine, transport, air or water purification can be included. Some studies on the growth of animal cells (chinese hamster ovary strain DP12 cells) on nanofiber mats have already been undertaken by the working group of textile technologies of Bielefeld University of Applied Sciences (see Fig. 1.6). Currently further research groups are trying to cultivate fungal mycelium on nanofibers in order to produce new hybrid composites. Plant cells on nanofibers can be used, for example, for a wide range of applications in the greening of house facades or in geotextiles against mountain erosion. The greening of facades and houses in conurbations plays a special role today. In the future, the demand for a harmonious coexistence of humans and nature will be even greater.

Membranes and nanofiber mats can be used in water purification, air purification or protective clothing applications. Several layers of different nanofiber mats with different morphologies, for example with a defined membrane ratio, can be effectively used together to form a hybrid composite with other materials. Depending on the nanofiber diameter and variations of the distances between the nanofibers, effective barriers for bacteria can be created. Due to the very narrow gaps, bacteria can no longer pass through nanofiber mats. This application would be interesting for protective clothing in hospitals or in the military as protection against chemicals and bacterial interventions. It would also be conceivable to use a hybrid composite of defined membranes in the field of water purification, for example to filter out dyes or micro plastic particles. Nowadays, every household produces micro plastics when clothing containing synthetic fibres is washed in a washing machine.

Metal/carbon nanocomposites can be widely used in aerospace, transportation, aircraft components, space systems, sports equipment, building materials or can be used as energy storage. Especially metal/carbon nanocomposites are promising in many applications. The composition of carbon nanofibres and aluminum results in reinforced composites that are thinner and much lighter than conventional materials such as steel or cement. In addition, these composites can be produced much cheaper, have better electrical and thermal conductivity as well as improved properties and performance.

In this dissertation, many different aspects of nanofiber fabrication, optimization of electrospinning parameters, stabilization and carbonization as well composite fabrication were investigated. This dissertation gives new insights and impulses for further research.

## APPENDIX A: RESUMEN EXTENDIDO

Los objetivos generales de esta Tesis Doctoral, que se presenta para optar al grado de doctor por la Universidad de Málaga, en el programa de doctorado de ─Química y Tecnologías Químicas. Materiales y nanotecnología" son los siguientes:

(1) Investigación sobre los parámetros de electrohilado del proceso de electrospinning sin aguja de poliacrilonitrilo (PAN) disuelto en dimetil sulfoxido (DMSO) y de las telas de nanofibras resultantes. Desarrollo de membranas finas casi impermeables mediante la modificación de los parámetros de electrospinning.

(2) Estudio de la influencia de la temperatura de estabilización y de las velocidades de calentamiento sobre las propiedades químicas y las morfologías de las telas no tejidas de nanofibras de mezclas de PAN y PAN/gelatina.

(3) El estudio de los cambios dimensionales de las nanofibras durante el proceso de estabilización y optimización de la tecnología de fijación para evitar la contracción y el doblado indeseable de las telas de nanofibras.

Para alcanzar estos objetivos el trabajo realizado, durante el trascurso de la presente Tesis Doctoral, se ha estructurado en 8 capítulos. En el capítulo 1 se introduce el tema y se repasa el estado actual del arte así como los antecedentes bibliográficos. El capítulo 2 se centra en los procedimientos experimentales y los materiales utilizados para el desarrollo experimental de la Tesis Doctoral. Los capítulos 3 al 8 constituyen el bloque de Resultados y Discusión de la Tesis y en ellos se presentan los resultados obtenidos, en los distintos estudios realizados, de manera ordenada, de acuerdo a como se han enviado a publicar. Dichas publicaciones se han añadido como anexo al final de la memoria. Se concluye la memoria con un apartado de Referencias bibliográficas que recoge toda la bibliografía usada en la memoria y finalmente se adjuntan los trabajos mencionados, algunos ya publicados y otros aceptados o enviados. En lo que sigue se presenta lo más destacado de cada capítulo.

# 1 Introducción

Esta tesis doctoral se centra en el estudio de la preparación de telas no tejidas de nanofibras de poliacrilonitrilo (PAN) mediante la técnica de electrohilado sin aguja usando como disolvente no tóxico el dimetil sulfóxido (DMSO).

La motivación para este trabajo se basa en el hecho de lo poco estudiada que está la preparación de nanofibras de PAN mediante la técnica de electrohilado sin aguja usando disolventes de baja toxicidad como es el caso del DMSO, así mismo no se han encontrado referencias sobre el estudio de la estabilización y carbonización, en condiciones óptimas, de este tipo de fibras. Se estudia también en esta Tesis Doctoral la permeabilidad al agua de membranas obtenidas a partir de telas no tejidas de nanofibras de PAN y que tampoco se ha encontrado, en la literatura científica, muchas citas bibliográficas sobre este tema.

La mezcla de PAN con la gelatina para producir nanofibras de alta porosidad ha sido reportada varias veces en la literatura, pero en ninguna de esos trabajos se ha realizado un estudio de estabilización y carbonización de estas fibras. En esta Tesis Doctoral se presenta en uno de sus capítulos los primeros ensayos realizados sobre la estabilización de telas de nanofibras de PAN/gelatina y la influencia de la temperatura de estabilización y la velocidad de calentamiento sobre las propiedades de las fibras obtenidas. Además, en esta Tesis se presenta un método novedoso para superar el problema de una insuficiente fijación de las telas que derivan en deformaciones cuando se estabilizan las fibras. Se ha visto que electrohilando sobre un sustrato de aluminio es posible que las telas de nanofibras se adhieran fuertemente al soporte, manteniendo su morfología, durante los procesos de estabilización y carbonización. Habiéndose desarrollado, en estos casos, nuevos tipos de materiales compuestos metal/carbón, lo que puede suponer una importante contribución al campo de los materiales compuestos metal/fibra de carbón.

El electrospinning constituye, actualmente, una de las técnicas más rentables para preparar fibras a escalas nano-micrométricas. Se utiliza principalmente por su facilidad de uso, al tiempo que es susceptible de distintas modificaciones. Mediante el electrospinning se pueden producir fibras muy finas en campos eléctricos de alta tensión, principalmente a partir de soluciones de polímeros o de polímeros fundidos [1].

El término "electrospinning", derivado de "spinning electrostático", se remonta a hace más de 60 años. La base del proceso de electrospinning se puede encontrar en 1902 cuando C. F. Cooley y W. J. Morton patentaron el proceso de electrospray [2, 3]. Farmhals patentó el proceso de electrospinning en 1934 y repatentó su trabajo en 1940 [4]. En los años 1960 Taylor estudió la formación y evolución de la gotita de polímero producida en la punta de la aguja cuando se aplica el campo eléctrico. El electrospinning permite la producción continua de nanofibras con el diámetro de fibra y la morfología controlables, lo que las hace muy interesantes para una amplia gama de aplicaciones como nano-catálisis, filtración, sensores ópticos y químicos, almacenamieno de energía, ropa protectora, defensa y seguridad [5-10]. Desde los años 80, y especialmente en los últimos años, el proceso de electrospinning ha vuelto a llamar la atención debido al creciente interés por la nanotecnología y la posibilidad de producir fibras ultrafinas o estructuras fibrosas a medida [11].

El control y estudio de los parámetros, tanto de la disolución como del proceso de electrospinning, son fundamentales para la obtención de fibras con propiedades adecuadas para sus futuras aplicaciones. Entre los parámetros de la disolución, que deben considerarse, se incluyen la viscosidad, la concentración del polímero, el peso molecular del polímero, la conductividad de la solución y la tensión superficial. En relación con el proceso los parámetros que deben considerarse, por jugar un papel clave, son la diferencia de potencial aplicada, la distancia entre la punta y el colector. La humedad y la temperatura pertenecen al grupo de los parámetros ambientales. Por lo tanto, la comprensión de la técnica de electrospinning y la fabricación de nanofibras es esencial para obtener el conocimiento sobre la dependencia que de los parámetros tiene la obtención de nanofibras a medida. En este sentido, numerosos grupos de investigación han estudiado los efectos de los parámetros del electrospinning en la morfología de las nanofibras. La versatilidad de la técnica permite trabajar con muchos polímeros diferentes, tanto de origen sintético como natural, para la preparación de nanofibras electrohiladas. La mayoría de ellos se preparan en disolución [12], pudiendo ser hilados, polímeros naturales y sintéticos, polímeros precerámicos, metales y óxidos [13]. Así mismo a la formulación se pueden añadir otras sustancias como los nanotubos de carbono (CNTs), partículas metálicas, se pueden producir nanoplacas con propiedades prometedoras que son de interés en aplicaciones biotecnológicas y médicas [14-16] etc.

## 2. Materiales y métodos

Para el trabajo presentado en esta tesis, relativo a la preparación de telas de nanofibras de carbón a partir de electrospinning de PAN (poliacrilonitrilo), se han preparado disoluciones de PAN (aprox 16 %) usando como disolvente de baja toxicidad DMSO (dimetil sulfóxido). Las disoluciones se prepararon a temperatura ambiente, agitando vigorosamente durante 2 horas. La concentración fue encontrada optima en pruebas preliminares ya que se evita la obstrución de los inyectores al tiempo que se evita la formación electrospraying, produciéndose un buen comportamiento en el proceso de electrospinning.

A partir del estudio de la influencia de los parámetros de hilado, en el proceso de electrospinning sin aguja, sobre la preparación de telas de nanofibras de PAN, se seleccionaron los siguientes parámetros: alta tensión de 80 kV, diámetro de boquilla de 0,9 mm y velocidad de carro de 150 mm/s durante un tiempo de hilado de 5 minutos. La velocidad del soporte de recogida de las telas fue de 20 mm/min. La distancia entre el electrodo de alta tensión y el centro del soporte varió entre 120 mm y 240 mm (los valores máximos posibles para darle a las fibras un mayor tiempo de vuelo). La información detallada y los resultados de esta serie de experimentos se pueden encontrar en el capítulo 4.

Para el electrospinning de nanofibras de PAN/gelatina se seleccionaron los siguientes parámetros de hilado: voltaje 70 kV, diámetro de inyector 1.5 mm, distancia al soporte 240 mm, temperatura en la cámara 22 °C, la humedad relativa en la cámara el 33 %. Ver el capítulo 7 para información más detallada.

Para la realización de las telas de nanofibras de carbón se utilizaron los siguientes parámetros de hilatura: alta tensión 60 kV, corriente aprox. 0,04 mA, distancia entre electrodos y soporte 240 mm, diámetro de boquilla 0,8 mm, velocidad del soporte 50 mm/min, humedad relativa 33 % y temperatura 22 °C. Se puede encontrar información más detallada sobre esta serie de experimentos en el capítulo 8.

El proceso de estabilización de una serie nanofibras de PAN se realizó en un horno de secado y esterilización "Digitheat" (J. P. Selecta, Barcelona, España). La temperatura de tratamiento se estudió entre 60 °C y 200 °C con una velocidad de calentamiento de 20 °C/h. Posteriormente se realizó un tratamiento isotérmico a 200

°C. Para el carbonizado de las telas no tejidas de nanofibras se utilizó un horno CTF 12 / TZF 12 (Carbolite Gero Ltd., Reino Unido).

Para el proceso de carbonización las muestras estabilizadas o sin estabilizar se introducen en el horno que una vez cerrado se evacua de aire por desplazamiento con nitrógeno (150 mL (STP)/min). El horno se calentó a 800 °C con una velocidad de calentamiento de 10 °C /min manteniendo constante el flujo de nitrógeno. A continuación se realizó un tratamiento isotérmico durante 2 horas a 800 °C.

En otra serie de experimentos de estabilización nanofibras se utilizó un horno tipo mufla B150 (Nabertherm, Lilienthal, Alemania), usándose en este caso velocidades de calentamiento, mayores que en el caso anterior, de 0,5 °C/min, 1 °C/min, 2 °C/min, 4 °C/min, 8 °C/min y 16 °C/min. Además, las muestras se colocaron en el horno ya precalentado.

Las muestras electrohiladas de PAN/gelatina se estabilizaron en un horno tipo mufla B150 (Nabertherm) con temperaturas de estabilización entre 240 °C y 300 °C con velocidades de calentamiento de 0,5 °C/min, 1 °C/min, 2 °C/min y 4 °C/min. Posteriormente se realizó un tratamiento isotérmico a la temperatura final durante 1 hora. Para cada caso se investigó la diferencia entre muestras que se fijaron sobre un soporte para su estabilización y otras no fijadas.

A continuación, la carbonización de las nanofibras de PAN/gelatina estabilizadas se realizó utilizando el horno CTF 12/TZF 12 (Carbolite Gero Ltd., Hope, Reino Unido). Se realizó un tratamiento térmico hasta una temperatura de 800 °C con una velocidad de calentamiento de 10 °C/min en un flujo de nitrógeno de 150 mL(STP)/min, seguido de un tratamiento isotérmico durante 1 hora.

Para la preparación de materiales compuestos denanofibras de carbono-metal las fibras PAN electrohiladas sobre aluminio no fueron separadas del sustrato. El conjunto fibras/sustrato, en cada caso, se estabilizaron en un horno de mufla B150 (Nabertherm, Lilienthal, Alemania), a una temperatura de estabilización típica de 280 °C a velocidad de calentamiento de 1 °C/min. Esta temperatura máxima se mantuvo durante 1 hora.

 A continuación, los materiales compuesto telas estabilizadas/metal se carbonizaron utilizando el horno CTF 12/TZF 12 (Carbolite Gero Ltd., Hope, Reino Unido), a

temperaturas de 500 °C u 800 °C. La velocidad de calentamiento fue de 10 °C/min y el flujo de nitrógeno de 150 mL(STP)/min. La temperatura máxima se mantuvo durante 1 hora.

Se detallan a continuación otros los dispositivos y métodos que se utilizaron en esta tesis.

− Las masas de las muestras se tomaron utilizando una balanza analítica (VWR).

− El software ImageJ 1.51j8 (de National Institutes of Health, Bethesda, MD, USA) fue aplicado para determinar los diámetros de las nanofibras a partir de las imágenes SEM, tomando 50 fibras en cada muestreo.

− Para las mediciones de color en este trabajo se utilizó el instrumento sph900 de Color-Lite.

− En esta tesis se utilizaron las mediciones de calorimetría de barrido diferencial (DSC), realizadas en un equipo DSC Q100 (TA Instruments).

− Para la presente tesis, las mediciones de la espectroscopia infrarroja por transformada de Fourier (FTIR) se realizaron con un equipo Inc. Excalibur 3100 (Varian, Inc., Palo Alto, CA, USA).

− Las telas no tejidas de nanofibras y los materiales compuestos fueron evaluados en este trabajo mediante microscopía electrónica de barrido (SEM) JSM-6490 LV, Jeol Ltd., Japón, así como imágenes de microscopía electrónica de barrido (SEM) tomadas por un Zeiss 1450VPSE (Oberkochen, Alemania) con una resolución de 5 nm o un microscopio JSM-840, respectivamente, usando una magnificación nominal de 5000 x.

− La investigación de las morfologías de las telas de nanofibras se realizó con un microscopio de barrido láser confocal (CLSM) VK-9000 o VK-9700 (ambos de Keyence, Neu-Isenburg, Alemania) con un aumento nominal de 2000 x, utilizando tres áreas por muestra.

− Un PERMETEST (MODELO DE PIEL), construido por Sensora Textile Measuring Instruments and Consulting, República Checa, fue utilizado en esta tesis para medir la resistencia al vapor de agua en tres áreas por muestra.

**3. Investigación del electrohilado sin aguja de telas de nanofibras de PAN**

El PAN es un polímero impermeable que, al contrario que los biopolímeros, no puede hilarse a partir de soluciones acuosas, en cambio puede hilarse a partir de disoluciones en un disolventede baja toxicidad como es el DMSO. Esto hace que el PAN sea un material interesante para el electrohilado de tlasas de nanofibras que pueden utilizarse en diversas aplicaciones biotecnológicas o médicas, como filtros, crecimiento celular, cicatrización de heridas o ingeniería de tejidos.

Por otro lado, el PAN es una materia prima típica para la producción de nanofibras de carbono, sinembargo el electrospinning requiere parámetros de hilado adecuados para la producción de nanofibras sin demasiadas zonas fundidas o aglomeraciones. Así, en este capítulo se estudió la influencia de los parámetros de hilatura sobre el proceso de electrospinning sin aguja de PAN disuelto en DMSO y las sobre las telas de nanofibras resultantes.

Para concluir, se compararon las telas de nanofibras de PAN electrohiladas con diferentes parámetros de operación. Mientras que los pesos especifios (masa/área de tela) dependen significativamente de todos los parámetros investigados, los diámetros de las nanofibras a menudo muestran sólo tendencias débiles o ninguna desviación independientemente de los parámetros. Sin embargo, las morfologías de las telas de nanofibras electrohiladas cambian drásticamente con la distancia del electrodo, el alto voltaje, la velocidad del carro y el diámetro de la boquilla. Por lo tanto, para la producción de nanofibras de alta calidad es indispensable examinar las telas de nanofibras electrohiladas por CLSM (microscopio de barrido láser confocal), SEM (microscopía electrónica de barrido) u otras técnicas que permitan investigar las nanofibras con suficiente resolución.

**4. Permeabilidad de vapor de agua a través de telas de nanofibras de PAN**

Este capítulo se centra en la preparación de membranas impermeables al agua, modificando las condiciones de electrospinning de disoluciones de PAN. La técnica de electrospinning se puede utilizar para preparar telas de nanofibras a partir de diversos polímeros que se pueden utilizar como filtros, etc. Dependiendo de los parámetros de hilado, también se pueden producir nanomembranas, es decir, laminas poliméricas no fibrosas, así como mezclas entre ambas morfologías. La relación entre la membrana y las áreas fibrosas puede ser modificadas por la distancia entre el

electrodo y el soporte. Aquí se muestra el impacto de la morfología de las telas, de nanofibras de PAN, con diferentes áreas similares a membranas sobre la permeabilidad al vapor de agua a través de ellas. De esta manera es posible producir filtros finos, así como membranas finas casi impenetrables con la misma tecnología.

En conclusión, se han preparado nanomateriales de PAN con diferentes proporciones de áreas de nanofibras y zonas similares a membranas. La relación membrana/nanofibra se puede adaptar modificando la distancia entre el electrodo de alto voltaje y el soporte. La medición de la permeabilidad al vapor de agua mostró una correlación aproximadamente exponencial entre la resistencia absoluta a la evaporación y la relación de la membrana. La permeabilidad al vapor de agua puede variar en más de dos órdenes de magnitud, mostrando las posibilidades de adaptar este valor modificando los parámetros del electrospinning.

## 5. Investigación sobre los parámetros de estabilización de las telas de nanofibras de PAN electrohiladas a partir de disoluciones de DMSO

El poliacrilonitrilo (PAN) puede utilizarse como materia prima para la conversión termoquímica en carbono. Especialmente las telas de nanofibras de PAN, producidas por electrospinning, son de gran interés para producir nanofibras de carbono. Sin embargo, los parámetros óptimos para la estabilización y la carbonización dependen en gran medida de las características de las fibras electrohiladas y del proceso de electohilado. Aunque las diferencias entre las nanofibras y las microfibras son bien conocidas, en este capítulo se muestra que, dependiendo del método de electrospinning y del disolvente utilizado, deben tenerse en cuenta las grandes diferencias entre las distintas telas de nanofibras para la optimización de las condiciones de estabilización.

En esta tesis, por primera vez, se han preparado telas no tejidas de nanofibras de PAN preparadas por electrospinning, sin aguja, de disoluciones de dimetilsulfóxido (DMSO) como disolvente de baja toxicidad, en lugar del típico sistema de electrospinning con boquilla de aguja a partir de disoluciones de dimetilformamida tóxica (DMF). Los resultados muestran que controlando cuidadosamente la temperatura máxima de estabilización y especialmente la velocidad de calentamiento, se pueden preparar fibras PAN completamente estabilizadas, sin interconexiones, no deseadas, como precursores para la carbonización. En un

proyecto reciente se examinó la influencia de la temperatura de estabilización y la velocidad de calentamiento sobre las nanofibras PAN electrohiladas utilizando una tecnología sin aguja de una solución en DMSO. Las investigaciones por diferentes técnicas mostraron óptimos ligeramente diferentes para la temperatura de estabilización y la velocidad de calentamiento: Mientras que una simple prueba DMSO utilizada para disolver las telas estabilizadas indicaba que una temperatura de 240 °C es suficiente para la estabilización (no disolución de la tela), las mediciones de color muestran una temperatura necesaria de 260 °C para acercarse a un valor constante en el cambio de color. Las mediciones DSC sugieren temperaturas óptimas entre 260 °C y 280 °C, mientras que en las mediciones FTIR, dependiendo de los picos que se estén examinando, la estabilización parece haberse completado entre 280 °C y 300 °C.

Este hallazgo explica la amplia variedad de valores, de estos parámetros, que se pueden encontrar en la bibliografía. Dado que la estabilización es una combinación de diversos procesos químicos, como ciclación, oxidación, reticulación, etc. Resulta necesario investigaciones más detalladas para identificar cuál de estos parámetros es esencial para el proceso de carbonización posterior y así poder adaptar el proceso de estabilización a las necesidades de las nanofibras de carbono finales. Así, se ha visto en este capítulo la importancia de una velocidad de calentamiento lenta y, en particular, de la fijación mecánica de las muestras durante la estabilización, a fin de evitar conglutinaciones no deseadas y un aumento del diámetro de las fibras. Por otra parte, se ha observado que las perlas incrustadas aquí para aumentar la adhesión de la matriz de fibra evitando el deslizamiento de la fibra sobrevivieron a la estabilización incluso a altas velocidades de calentamiento y sin fijación, en cambio la morfología de la fibra sólo se puede mantener a bajas velocidades de calentamiento y en muestras fijas.

## 6. Desarrollo de nanofibras de carbono para su integración en filamentos de impresión 3D

Los nuevos materiales compuestos poliméricos reforzados con nanofibras combinan las ventajas de diferentes materiales. De esta manera, se pueden producir estructuras más o menos complejas que son muy ligeras y estables al mismo tiempo. Además, el uso de polímeros plásticos de base biológica en compuestos sándwich reforzados con

nanofibras ofrece la oportunidad de reducir los impactos ambientales negativos. En este capítulo se investigan el desarrollo y la evaluación de nanofibras de poliacrilonitrilo (PAN) para la producción de nanofibras de carbono. Las telas no tejidas de nanofibras PAN se prepararon mediante electrospinning sin aguja y fueron utilizadas como precursores para la producción de nanofibras de carbono. Tanto el paso de estabilización como el proceso de carbonización influyen significativamente en la morfología de las nanofibras de carbono resultantes. Especialmente en el caso del hilado a nanoescala, que a menudo carece de la posibilidad de preparar telas de fibras orientadas, es difícil evitar el arrugamiento de las fibras, durante el tratamiento térmico, por los medios mecánicos descritos en la literatura.

## 7. Estabilización de telas de nanofibras de PAN-gelatina para su carbonización

Debido a sus propiedades eléctricas y mecánicas, las nanofibras de carbón son de gran interés para diversas aplicaciones, desde baterías hasta células solares y filtros. Las nanofibras de carbón se pueden producir mediante electrospinning de poliacrilonitrilo (PAN), seguido de sendas etapas de estabilización y carbonización. Tanto el material de base electrohilado como el proceso de estabilización de las fibras son cruciales para los resultados del proceso de carbonización, definiendo en gran medida la morfología de la fibra. Mientras que la mezcla de PAN con gelatina para obtener nanofibras de alta porosidad ha sido reportada varias veces en la literatura, no se han hecho intentos para estabilizar y carbonizar estas fibras. En este capítulo de la tesis se presentan las primeras pruebas de estabilización de nanofibras de PAN/gelatina, describiendo el impacto de las diferentes temperaturas de estabilización y velocidades de calentamiento sobre las propiedades químicas, así como las morfologías de las telas de nanofibras resultantes. Al igual que la estabilización del PAN puro, una temperatura de estabilización de 280 °C parece adecuada, mientras que la velocidad de calentamiento no influye significativamente en las propiedades químicas. En comparación con la estabilización de las nanofibras de PAN puro, para las mezclas de PAN/gelatina se puede utilizar, aproximadamente, una velocidad de calentamiento del doble, sin crear conglutinaciones no deseadas, lo que hace que este material base sea más adecuado para procesos industriales. En este capítulo se han examinado los parámetros de estabilización de las nanofibras PAN/gelatina y se ha estudiado su influencia sobre las nanofibras estabilizadas resultantes. En todos los casos, la cantidad de gelatina se redujo significativamente,

especialmente por encima del inicio de la degradación de la misma a 250 °C, como revelan las mediciones FTIR, CLSM y SEM. Mientras que la adición de gelatina no resultó en la creación de nanofibras porosas de PAN después de la estabilización, aquí se demostró que el uso de mezclas de PAN/gelatina como precursores de las nanofibras de carbono ofrece una nueva posibilidad de crear fibras largas y lineales sin muchas conglutinaciones no deseadas. Los ensayos futuros se concentrarán en investigar la influencia de la relación PAN: gelatina en la estabilización y los procesos de carbonización subsiguientes.

## 8. Fijación de telas de nanofibras de PAN durante el proceso de estabilización para su carbonización posterior y preparación de nuevos materiales compuestos metal/carbón

El PAN es uno de los materiales más utilizados para la producción de fibras de carbono vía hilado y carbonización. Las telas no tejidas de nanofibras de PAN, prepadas por electrospinning, son una fuente especialmente interesante para obtener nanofibras de carbono. Un problema bien conocido en este proceso son las deformaciones observadas en las fibras durante la estabilización, que están relacionadas con una contracción de las fibras produciéndose, generalmente, un aumento indeseado del diámetro de las fibras que a veces va acompañado de una flexión de las mismas. Solucionar este problema típicamente resulta en roturas en las nanofibras, si la tensión es demasiado alta. En este capítulo de la tesis se propone un método novedoso para superar este problema mediante el electrospinning sobre un sustrato de aluminio sobre el que la tela de nanofibras se adhiere fuertemente. La estabilización y posterior carbonización de las fibras con o sin el sustrato de aluminio para obtener permite producir un material compuesto de aluminio/carbono o una tela de nanofibras de carbono puro. Se ha demostrado que las nanofibras PAN electrohiladas sobre sustratos de aluminio ofrecen una posibilidad sencilla de superar el problema de cómo fijar las telas de nanofibras durante el proceso de estabilización, que es indispensable para mantener las nanofibras rectas y sin aglutinar. Además, los materiales compuestos de aluminio-carbono pueden formarse a temperaturas de carbonización más altas. Cabe señalar que la formación de estos materiales compuestos no fue forzada (por ejemplo, colocando un peso sobre la muestra durante la carbonización) ni investigada más a fondo ya que el objetivo principal, de este capítulo, era encontrar una solución para el problema de la contracción y flexión indeseada de la fibra durante la estabilización. Sin embargo, este efecto resulta de

interés en muchas aplicaciones posibles, en el área de los materiales compuestos y será investigado más a fondo en un futuro cercano.

**Conclusiones y sugerencias para trabajos futuros**

En los últimos años, el electrospinning ha adquirido una importancia cada vez mayor para muchas aplicaciones debido a la gran variedad de polímeros diferentes que pueden ser procesados mediante esta técnica. En esta tesis doctoral se utilizó DMSO (dimetil sulfóxido) como disolvente de baja toxicidad para el proceso de electrospinning sin aguja para producir nanofibras PAN, mezclas PAN/gelatina y compuestos de metal/carbono. Al principio de este trabajo se fijaron tres objetivos principales y los resultados de la investigación muestran que estos objetivos se han alcanzado en el contexto de esta tesis.

Se ha demostrado que es posible adaptar la relación fibra/membrana variando la distancia entre los electrodos. Se ha subrayado que, si bien las relaciones fibra/membrana obtenida dependen en gran medida de todos los parámetros investigados, los diámetros de las nanofibras muestran sólo pequeñas desviaciones, en algún caso, al cambiar los valores de los parámetros de operación. Además, las morfologías de las telas de nanofibras se ven afectadas por los parámetros operacionales como la distancia del electrodo, la velocidad del carro, el voltaje y el diámetro de la boquilla. Cabe mencionar que las condiciones de electrospinning como el mecanismo de hilado, la geometría de la cámara de hilado, el flujo de aire a través de la cámara y especialmente la humedad relativa en la cámara de hilado influyen significativamente en las morfologías de las telas de nanofibras. Por último, para cada situación de hilatura, las condiciones óptimas de electrospinning deben investigarse por separado. Se ha examinado la resistencia al vapor de agua de las alfombras de nanofibras PAN con morfologías variables entre nanofibras puras y membranas puras. La resistencia al vapor de agua de las telas de nanofibras está poco investigada en la literatura y no existen, hasta donde sabemos, investigaciones sobre la transición entre morfología tipo tela de nanofibras y membrana en términos de permeabilidad al vapor de agua.

Dependiendo de los parámetros de electrospinning, se produjeron nanomembranas y telas de nanofibras, así como una amplia gama morfologías entre ambas. Finalmente, fue posible crear mezclas entre fibras y membranas o membranas puras modificando los parámetros de electrospinning. Se ha demostrado que la creación de filtros más finos, así como de membranas finas casi impenetrables mediante la variación de los parámetros de electrospinning, es realizable. Estos resultados subrayan una

correlación aproximadamente exponencial entre la resistencia absoluta a la evaporación y la relación de la estructura de membrana en el material finalmente preparado.

Se ha evaluado la influencia de la temperatura y de la velocidad de calentamiento sobre el proceso de estabilización de las telas no tejidas de nanofibras de PAN electrohiladas a partir de una disolución en DMSO utilizando una tecnología de electrospinning sin aguja. El equilibrio óptimo entre ambos parámetros es fundamental para el proceso de carbonización posterior y la morfología de las nanofibras resultantes. Además, se realizaron investigaciones de las microesferas, que incluso con contenidos relativamente bajos de sólidos en la solución, a menudo se forman y que la mayoría de las veces no son deseadas, pero en algunos casos presentan ciertas ventajas, como por ejemplo cuando se preparan materiales compuestos estas nanoesferas pueden evitar el deslizamiento de las fibras dentro de una matriz de resina y, por lo tanto, sería importante mantener las formas durante la estabilización y carbonización.

Se concluye que controlando cuidadosamente la temperatura máxima de estabilización y especialmente la velocidad de calentamiento, se pueden preparar fibras PAN completamente estabilizadas sin interconexiones, no deseadas, como precursoras de la carbonización. Además, a todas las temperaturas de estabilización, las muestras no fijadas se encogen más que las fijas. Se compararon para minimizar conglutinaciones no deseadas y cambios dimensionales de nanofibras, lo que no se había descrito antes en la literatura.

Además, se subrayó la importancia de una velocidad de calentamiento lenta y, en particular, de una fijación mecánica de las muestras durante la estabilización, a fin de evitar un encogimiento no deseado y un aumento del diámetro de la fibra. Se ha demostrado que los procesos de estabilización pueden adaptarse a las necesidades requeridas para las nanofibras de carbono resultantes. Debe mencionarse que al mezclar PAN con gelatina no se observaron diferencias entre las muestras fijas y no fijas después de terminar el proceso de estabilización. Esto puede indicar que bajo estas condiciones de estabilización la fijación de las muestras no es necesaria para obtener fibras rectas sin dobleces y conglutinaciones no deseadas. Este resultado subraya la suposición de que mediante una cuidadosa selección de las condiciones de estabilización, el aumento previsto del diámetro de la fibra puede permanecer tras el

proceso de estabilización, mientras que el material de mezcla responsable de este aumento de diámetro se funde a temperaturas mucho más bajas. Se necesitan pruebas futuras que combinen temperaturas de estabilización relativamente bajas y velocidades de calentamiento para respaldar esto.

El uso de mezclas de PAN/gelatina como precursores de nanofibras de carbono puede ofrecer una nueva posibilidad de crear fibras largas y rectas sin muchos conglomerados no deseados. Las pruebas futuras deberían concentrarse en investigar la influencia de la relación PAN: gelatina en la estabilización y los procesos de carbonización subsiguientes. Esta investigación muestra claramente que mezclar PAN con gelatina puede ayudar a obtener nanofibras de carbono largas y rectas, como se desea para la mayoría de las aplicaciones técnicas.

Además, esta tesis doctoral sugiere un método novedoso para superar el problema de la fijación insuficiente de las telas no tejidas de nanofibras durante el proceso de estabilización mediante electrospinning sobre un sustrato de aluminio. La telilla de nanofibras se adhiere fuertemente al aluminio y mantiene su morfología durante los procesos de estabilización y carbonización. Después del proceso de estabilización, la tela de nanofibras puede separarse del sustrato de aluminio para formar nanofibras de carbono puro después de la carbonización, o puede carbonizarse junto con el sustrato de aluminio para formar un compuesto de metal/carbono. En esta tesis, se desarrolló un nuevo y sencillo enfoque para superar el problema de los cambios morfológicos no deseados de las nanofibras durante el proceso de estabilización, que al mismo tiempo ofrece la posibilidad de preparar nuevos compuestos metal/carbono. Lo que podría ser una importante contribución al campo de los compuestos de metal/carbono.

Cabe señalar que las propiedades mecánicas de las nanofibras individuales, así como de las telas de nanofibras, no fueron investigadas en este estudio, pero pueden formar parte de futuras investigaciones. En lugar de ello, el enfoque se centró en el desarrollo de un método de estabilización incrementado, así como de un nuevo método para preparar compuestos de metal/carbono. Sin embargo, este efecto puede conducir a muchas otras posibles aplicaciones en el campo de los materiales compuestos y debería ser investigado más a fondo en un futuro próximo, especialmente con respecto a la formación de materiales compuestos durante la carbonización y las propiedades mecánicas de los materiales compuestos resultantes.

Los resultados de la investigación se presentan como un compendio de seis publicaciones que ya han sido publicadas, aceptadas o enviadas.

1. INVESTIGATION OF NEEDLELESS ELECTROSPUN PAN NANOFIBER MATS, L. Sabantina, J. Rodríguez-Mirasol, T. Cordero, K. Finsterbusch, A. Ehrmann, AIP Conference Proceedings 1952, 020085 (2018), doi.org/10.1063/1.5032047

2. WATER VAPOR PERMEABILITY THROUGH PAN NANOFIBER MAT WITH VARYING MEMBRANE-LIKE AREAS, L. Sabantina, L. Hes, J. Rodríguez-Mirasol, T. Cordero, A. Ehrmann, accepted for publication in No. 1/2019 of FIBERS & TEXTILES in Eastern Europe

3. INVESTIGATION OF STABILIZATION PARAMETERS FOR PAN NANOFIBER MATS NEEDLELESS-ELECTROSPUN FROM DMSO, L. Sabantina, M. Klöcker, M. Wortmann, J. Rodríguez-Mirasol, T. Cordero, K. Finsterbusch, A. Ehrmann, (enviado)

4. DEVELOPMENT OF CARBON NANOFIBERS FOR INTEGRATION IN 3D PRINTING FILAMENTS, L. Sabantina, K. Finsterbusch, A. Ehrmann, J. Rodríguez-Mirasol, T. Cordero, Aachen-Dresden-Denkendorf International Textile Conference, Stuttgart, November 30-31, 2017

5. STABILIZATION OF ELECTROSPUN PAN/GELATIN NANOFIBER MATS FOR CARBONIZATION, L. Sabantina, D. Wehlage, M. Klöcker, A. Mamun, T. Grothe, J. Rodríguez-Mirasol, T. Cordero, K. Finsterbusch, A. Ehrmann, Special Issue "Functional Nanomaterials for Energy Applications", Journal of Nanomaterials, Volume 2018, Article ID 6131085, 12 pages, doi.org/10.1155/2018/6131085

6. FIXING PAN NANOFIBER MATS DURING STABILIZATION FOR CARBONIZATION AND CREATING NOVEL METAL/CARBON COMPOSITES, L. Sabantina, M. Ángel Rodríguez-Cano, M. Klöcker, F. J. García-Mateos, J. J. Ternero-Hidalgo, A. Mamun, F. Beermann, M. Schwakenberg, A.-L. Voigt, J. Rodríguez Mirasol, T. Cordero, A. Ehrmann, Polymers 10, 735 (2018), doi.org/10.3390/polym1007073

**Referencias**

1. T. Lin, X. Wang, 2014, Needleless electrospinning of nanofibers, technology and applications, Pan Stanfort Publishing Pte Ltd

2. J.F. Cooley, 1902, Apparatus for electrically dispersing fluids, US Patent Specification 692631

3. K.J. Pawlowski, C.P.Barnes, E.D. Boland, G.E.Wnek, G.L. Bowlin, 2004, Biomedical nanoscience: electrospinning basic concepts, applications, and classroom demonstration, Mater Res Soc Symp Proc, 827, 17-28

4. W.J. Morton, 19997, Method of dispersing fluids, US Patent Specification 705691

5. Y.K. Luu, K. Kim, B.S. Hsiao, B. Chu, M. Hadjiargyrou, 2003, Development of a nanostructured DNA delivery scaffold via electrospinning of PLGA and PLA-PEG block copolymers, J Control Release, 89, 341–353

6. T. Subbiah, G.S. Bhat, R.W. Tock, S. Parameswaran, S.S. Ramkumar, 2005, Electrospinning of nanofibers, J Appl Polym Sci, 96, 557–69

7. S. Ramakrishna, K. Fujihara, W.E. Teo, T. Yong, Z. Ma, R. Ramaseshan, 2006, Electrospun nanofibers: solving global issues, Mater Today, 9, 40–50

8.W. Cui, S. Zhou, X. Li, J. Weng, 2006, Drug-loaded biodegradable polymeric nanofibers prepared by electrospinning, Tissue Eng, 12, 1070

9. C.P. Barnes, S.A. Sell, D.C. Knapp, B.H. Walpoth, D.D. Brand, G.L. Bowlin, 2007, Preliminary investigation of electrospun collagen and polydioxanone for vascular tissue engineering applications, Int J Electrospun Nanofibers Appl, 1, 73–87

10. A. Welle, M. Kroger, M. Doring, K. Niederer, E. Pindel, S. Chronakis, 2007, Electrospun aliphatic polycarbonates as tailored tissue scaffold materials. Biomaterials, 28, 2211–9

11. N. Bhardwaj, S.C. Kundu, 2010, Electrospinning: A fascinating fiber fabrication technique, Biotechnology Advances, 28 (3), 325-347

12. A. Haider, S. Haider, I-K. Kang, 2015, A comprehensive review summarizing the effect of electrospinning parameters and potential applications of nanofibers in biomedical and biotechnology, Arabian Journal of Chemistry

13. D.J. Yang, L.-F. Zhang, L. Xu, C.-D. Xiong, J. Ding, Y.-Z. Wang, 2007, Fabrication and characterization of hydrophilic electrospun membranes made from the block copolymer of poly(ethylene glycol-co-lactide), J Biomed Mater Res, Part A, 82A (3), 680-688

14. M. Alaa, T.A. Osman, M.S. Toprak, M. Muhammed, A. Uheida, 2017, Surface functionalized composite nanofibers for efficient removal of arsenic from aqueous solutions, Chemosphere,180, 108-116

15. B. Duan, C. Dong, X. Yuan, K. Kangde Yao, 2004, Electrospinning of chitosan solutions in acetic acid with poly(ethylene oxide), Journal of Biomaterials Science, Polymer Edition, 15 (6), 795-803

16. P. Wang, L. Cheng, Y. Zhang, L. Zhang, 2017, Synthesis of SiC nanofibers with superior electromagnetic wave absorption performance by electrospinning, Journal of Alloys and Compounds, 716, 306-320

# Investigation Of Needleless Electrospun Pan Nanofiber Mats

Lilia Sabantina[1,2,a)] José Rodríguez Mirasol[2], Tomás Cordero[2], Karin Finsterbusch[1], and Andrea Ehrmann[3]

[1]*Niederrhein University of Applied Sciences, Faculty of Textile and Clothing Technology, 41065 Mönchengladbach, Germany.*
[2] *Universidad de Málaga, Andalucía Tech, Dpto. de Ingeniería Química, 29010 Málaga, Spain.*
[3] *Bielefeld University of Applied Sciences, Faculty of Engineering and Mathematics, 33619 Bielefeld, Germany.*

[a)] Corresponding author: lilia.sabantina@stud.hn.de

**Abstract:** Polyacrylonitrile (PAN) can be spun from a nontoxic solvent (DMSO, dimethyl sulfoxide) and is nevertheless waterproof, opposite to the biopolymers which are spinnable from aqueous solutions. This makes PAN an interesting material for electrospinning nanofiber mats which can be used for diverse biotechnological or medical applications, such as filters, cell growth, wound healing or tissue engineering. On the other hand, PAN is a typical base material for producing carbon nanofibers. Nevertheless, electrospinning PAN necessitates convenient spinning parameters to create nanofibers without too many membranes or agglomerations. Thus we have studied the influence of spinning parameters on the needleless electrospinning process of PAN dissolved in DMSO and the resulting nanofiber mats.

## INTRODUCTION

Electrospinning is a method to create mats from fine fibers, usually in the diameter range of some hundred nanometers. The process can be subdivided into electrospinning using a syringe to extrude the polymer which is spun, and needleless electrospinning. Both methods can be used to spin fibers from a molten polymer mass or from a polymer solution, opening this technology for a broad range of polymer materials.

In electrospinning from a solution, a suitable solvent has to be found to dissolve the desired polymer. This requirement often results in the problem that toxic, corrosive or other dangerous solvents have to be used which are hard to handle, especially in academic environments. Besides biopolymers, several of which can be spun from aqueous solutions [1,2], polyacrylonitrile (PAN) is of high interest since it is spinnable from dimethyl sulfoxide (DMSO). This solvent has to be handled with care because it increases penetration of other materials through the surface of the skin, but it does not cause problems in medical or biotechnological applications [3].

This is why PAN is often used for electrospinning [4,5], often to created nanofiber mats which are afterwards carbonized in order to create carbon nanofibers [5-8]. PAN can also be used with embedded inorganic components like ZnO or MgO [9-11]. In spite of the technological relevance of this material, only few articles about the dependence of the nanofiber mat morphology on the spinning and material parameters can be found [12-14], none of which deals with needleless electrospinning. Previous investigations, however, have already shown the large influence of the polymer solution as well as the spinning conditions on the resulting nanofiber mats, with some parameters apparently having stronger effects than it was found in a previous systematic investigation of needleless electrospinning poly(ethylenglycol) (PEG) [15]. This is why our article depicts the results of systematic variations of different spinning parameters and the resulting changes in nanofiber mat morphologies.

## ACKNOWLEDGMENTS

## REFERENCES

1. N. Grimmelsmann, S. V. Homburg, A. Ehrmann, IOP Conference Series: Materials Science and Engineering **213**, 012007(2017).
2. T. Grothe, C. Großerhode, T. Hauser, P. Kern, K. Stute, A. Ehrmann, Advances in Engineering Research **102**, 54-58 (2017).
3. C. Großerhode, D. Wehlage, T. Grothe, N. Grimmelsmann, S. Fuchs, J. Hartmann, P. Mazur, V. Reschke, H. Siemens, A. Rattenholl, S. V. Homburg, A. Ehrmann, AIMS Bioengineering **4**, 376-385 (2017).
4. B. Maddah, M. Soltaninezha, K. Adib, M. Hasanzadeh, Separation Science and Technology **52**, 700-711 (2017).
5. G. Panthi, S. J. Park, S. H. Chae, T. W. Kim, H. J. Chung, S. T. Hong, M. Park, H. Y. Kim, Journal of Industrial and Engineering Chemistry **45**, 277-286 (2017).
6. R. E. Neisiany, J. K. Y. Lee, S. N. Khorasani, S. Ramakrishna, Journal of Applied Polymer Science **134**, 44956 (2017).
7. G. H. Kim, S. H. Park, M. S. Birajdar, J. W. Lee, S. C. Hong, Journal of Industrial and Engineering Chemistry **52**, 211-217 (2017).
8. J. Y. Guo, Q. J. Niu, Y. C. Yuan, I. Maitlo, J. Nie, G. P. Ma, Applied Surface Science **416**, 118-123 (2017).
9. M. Kancheva, A. Toncheva, D. Paneva, N. Manolova, I. Rashkov, N. Markova, Journal of Inorganic and Organometallic Polymers and Materials **27**, 912-922 (2017).
10. F. E. C. Othman, N. Yusof, H. Hasbullah, J. Jaafar, A. F. Ismail, N. Abdullah, N. A. H. M. Nordin, F. Aziz, W. N. W. Salleh, Journal of Industrial and Engineering Chemistry **51**, 281-287 (2017).
11. I. Iatsunskyi, A. Vasylenko, R. Viter, M. Kempinski, G. Mowaczyk, S. Jurga, M. Bechelany, Applied Surface Science **411**, 494-501 (2017).
12. H. T. Niu, X. G. Wang, T. Lin, Journal of Engineered Fibers and Fabrics **7**, 17-22 (2012).
13. S. V. Lomos, K. Molnar, Express Polymer Letters **10**, 25-35 (2016).
14. J. N. Zhang, M. Y. Song, D. W. Li, Z. P. Yang, J. H. Cao, Y. Chen, Y. Xu, Q. F. Wei, Fibers and Polymers **17**, 1414-1420 (2016).
15. T. Grothe, J. Brikmann, H. Meissner, A. Ehrmann, Materials Science **23**, 342-349 (2017).
16. H. Fong, I. Chun, D. H. Reneker, Polymer **40**, 4585-4592 (1999).
17. Z.-M. Huang, Y.-Z. Zhang, M. Kotaki, S. Ramakrishna, Composites Science and Technology **63**: 2223-2253 (2003).
18. E. Kostakova, M. Seps, P. Pokorny, D. Lukas, eXPRESS Polymer Letters **8**, 554-564 (2014).

XXXII

B.2 WATER VAPOR PERMEABILITY THROUGH PAN NANOFIBER MAT WITH VARYING MEMBRANE-LIKE AREAS, L. Sabantina, L. Hes, J. Rodríguez-Mirasol, T. Cordero, A. Ehrmann, accepted for publication in No. 1/2019 of FIBRES & TEXTILES in Eastern Europe

**IBWCh** | Institute of Biopolymers and Chemical Fibres

24th August 2018

Lilia Sabantina
Bielefeld University of Applied Sciences,
Faculty of Engineering and Mathematics,
Working Group of Textile Technologies,
33619 Bielefeld, Germany

Dear Lilia Sabantina,

I am glad to inform you that your paper entitled "WATER VAPOR PERMEABILITY THROUGH PAN NANOFIBER MAT WITH VARYING MEMBRANE-LIKE AREAS", registered at **No.5128**, authors: Lilia Sabantina, Lubos Hes, José Rodríguez Mirasol, Tomás Cordero and Andrea Ehrmann, has been finally accepted for publication in issue **No. 1/2019** of *FIBRES & TEXTILES in Eastern Europe*.

I am looking forward to fruitful co-operation with you also in the future and encourage you to send us your scientific articles for publication in our journal.

Kind regards,

Emilia Jaszczurska-Niedźwiedzka
Editor-in-Chief
*FIBRES & TEXTILES in Eastern Europe*

UNIVERSIDAD DE MÁLAGA

B.3 INVESTIGATION OF STABILIZATION PARAMETERS FOR PAN NANOFIBER MATS NEEDLELESS-ELECTROSPUN FROM DMSO, L. Sabantina, M. Klöcker, M. Wortmann, J. Rodríguez-Mirasol, T. Cordero, K. Finsterbusch, A. Ehrmann, (submitted)

B.4 DEVELOPMENT OF CARBON NANOFIBERS FOR INTEGRATION IN 3D PRINTING FILAMENTS, L. Sabantina, K. Finsterbusch, A. Ehrmann, J. Rodríguez-Mirasol, T. Cordero, Aachen-Dresden-Denkendorf International Textile Conference, Stuttgart, November 30-31, 2017

## DEVELOPMENT OF CARBON NANOFIBERS FOR INTEGRATION IN 3D PRINTING FILAMENTS

Lilia Sabantina[1,2], Karin Finsterbusch[2], Andrea Ehrmann[3], José Rodríguez Mirasol[1], Tomás Cordero[1]

[1] *University of Málaga, Málaga (Spain)*
[2] *Niederrhein University of Applied Sciences, Moenchengladbach, (Germany)*
[3] *Bielefeld University of Applied Sciences, Bielefeld, (Germany)*

### Abstract

Nanotechnologies as well as additive manufacturing technologies are gaining increasing economic importance worldwide and have a great application potential in many industrial sectors such as automotive industry. New polymeric composites, so-called nanofiber-reinforced composites, combine the advantages of different materials. In this way, highly complex structures can be produced that are extremely light and stable at the same time. Furthermore the use of bio-based plastics in nanofiber reinforced sandwich composites provides the opportunity to reduce negative environmental impacts.

The aims of this project are development und evaluation of polyacrylonitrile (PAN) based nanofiber mats for the production of carbon nanofibers. After electrospinning the PAN with different solution and spinning parameters, the gained nanofiber mats are carbonized using a horizontal furnace in an N2 atmosphere at a controlled temperature. The resulting carbon nanofibers are evaluated by scanning electron microscopy (SEM).

The article will give an overview of the properties of these carbon nanofibers and an outlook to embedding them in poly(lactide acid) (PLA) or other 3D printing polymers.

### Introduction

Carbon nanofibers can be produced by carbonizing nanofibers of different precursors, e.g. lignin [1-3], polyacrylonitrile (PAN) [4-6], or PAN blended with biochar [7] or cellulose acetate [8].

The production of such submicron- or nano-fibers is usually done by electrospinning. PAN nanofibers are often prepared for the possible use as electrode materials [9-11], but also for biotechnological and other applications [12]. Their morphology and diameter – which are essential for the morphology and diameter of the carbon nanofibers gained from them – are influenced by diverse spinning and solution parameters, such as capillary diameter, collector-capillary distance, solution feed rate and voltage in needle-based electrospinning [13] or additionally the carriage speed and other parameters in diverse techniques of needleless electrospinning [14-17].

Another crucial factor for successful carbonization of PAN nanofibers is the previous stabilization process to avoid the degradation of the fibers [18]. For this, thermal treatment under slow heating up to 280 °C and following isothermal treatment at 280 °C for 2 h was found to be suitable [19], while temperatures higher than 300 °C caused combustion of the

Investigation of microalgae growth on electrospun nanofiber mats; AIMS Bioengineering 4, 376-385 (2017).

13. da Silva Vaz B., Vieira Costa J. A., de Morais M. G., Production of polymeric nanofibers with different conditions of the electrospinning process; Materia-Rio de Janeiro 22, E-11847 (2017).

14. Zhang J. N., Song M. Y., Li D. W., Yang Z. P., Cao J. H., Chen Y., Xu Y., Wei Q. F., Preparation of self-clustering highly oriented nanofibers by needleless electrospinning methods; Fibers and Polymers 17, 1414-1420 (2016).

15. Lomos S. V., Molnar K., Compressibility of carbon fabrics with needleless electrospun PAN nanofibrous interleaves; Express Polymer Letters 10, 25-35 (2016).

16. Niu H. T., Wang X. G., Lin T., Upward needleless electrospinning of nanofibers; Journal of Engineered Fibers and Fabrics 7, 17-22 (2012).

17. Sabantina L., Mirasol J. R., Cordero T., Finsterbusch K., Ehrmann A., Investigation of Needleless Electrospun PAN Nanofiber Mats; AIP Conference Series, accepted.

18. Molnár K., Szolnoki B., Toldy A., Mihály Vas L., Thermochemical stabilization and analysis of continuously electrospun nanofibers; Journal of Thermal Analysis and Calorimetry 117, 1123-1135 (2014).

19. Wu M. Y., Wang Q. Y., Li K. N., Wu Y. Q., Liu H. Q., Optimization of stabilization conditions for electrospun polyacrylonitrile nanofibers; Polymer Degradation and Stability 97, 1511-1159 (2012).

20. Arshad S. N., Naraghi M., Chasiotis I., Strong carbon nanofibers from electrospun polyacrylonitrile; Carbon 49, 1710–1719 (2011).

*Research Article*

# Stabilization of Electrospun PAN/Gelatin Nanofiber Mats for Carbonization

**Lilia Sabantina,**[1,2] **Daria Wehlage,**[1] **Michaela Klöcker,**[1] **Al Mamun,**[3] **Timo Grothe,**[1] **Francisco José García-Mateos,**[2] **José Rodríguez-Mirasol,**[2] **Tomás Cordero,**[2] **Karin Finsterbusch,**[3] **and Andrea Ehrmann** [1]

[1]*Bielefeld University of Applied Sciences, Faculty of Engineering and Mathematics, Bielefeld, Germany*
[2]*Universidad de Málaga, Andalucía Tech, Dpto. de Ingeniería Química, Málaga, Spain*
[3]*Niederrhein University of Applied Sciences, Mönchengladbach, Germany*

Correspondence should be addressed to Andrea Ehrmann; andrea.ehrmann@fh-bielefeld.de

Due to their electrical and mechanical properties, carbon nanofibers are of large interest for diverse applications, from batteries to solar cells to filters. They can be produced by electrospinning polyacrylonitrile (PAN), stabilizing the gained nanofiber mats, and afterwards, carbonizing them in inert gas. The electrospun base material and the stabilization process are crucial for the results of the carbonization process, defining the whole fiber morphology. While blending PAN with gelatin to gain highly porous nanofibers has been reported a few times in the literature, no attempts have been made yet to stabilize and carbonize these fibers. This paper reports on the first tests of stabilizing PAN/gelatin nanofibers, depicting the impact of different stabilization temperatures and heating rates on the chemical properties as well as the morphologies of the resulting nanofiber mats. Similar to stabilization of pure PAN, a stabilization temperature of 280°C seems suitable, while the heating rate does not significantly influence the chemical properties. Compared to stabilization of pure PAN nanofiber mats, approximately doubled heating rates can be used for PAN/gelatin blends without creating undesired conglutinations, making this base material more suitable for industrial processes.

## 1. Introduction

Functional nanofibers are used in a broad variety of applications, from nanofibrous membranes for filters [1] to substrates in tissue engineering [2, 3] to electrocatalysis [4], capacitors [5], and other applications based on the conductivity of the nanofibers [6]. Especially for batteries and other energy applications, often carbon nanofibers are used [7–11].

Such carbon nanofibers are often prepared via the electrospinning route, followed by stabilization and afterwards carbonization. Both steps influence the morphologies, the mechanical and electrical properties of the final carbon nanofibers significantly. While carbon nanofibers can be produced from a broad variety of materials [12–14], one of the most common materials for this purpose is polyacrylonitrile (PAN). PAN changes fiber diameters and mat morphologies significantly for varying spinning and solution parameters [15, 16], while the fibers themselves keep their flat, even surfaces.

In most applications, however, it is advantageous to further increase the surface : volume ratio of the nanofibers. This can be done by blending PAN with other polymers or inorganic material, a method which may also alter other physical properties, such as the conductivity. Increased crystallinity and conductivity were found, e.g., when PAN/pitch nanofibers were carbonized [17]. Blending PAN with cellulose acetate resulted in increased adsorption properties of the carbonized nanofibers [18]. Combined with diverse water-soluble polymers, only gelatin showed a significant influence on the PAN fiber diameters [19]. PAN/gelatin blends have also shown to create highly porous fibers by electrospinning [20]. Nevertheless, to the best of our knowledge,

[3] G. Potjewyd, S. Moxon, T. Wang, M. Domingos, and N. M. Hooper, "Tissue engineering 3D neurovascular units: a biomaterials and bioprinting perspective," *Trends in Biotechnology*, vol. 36, no. 4, pp. 457–472, 2018.

[4] H. Tang, W. Chen, J. Wang, T. Dugger, L. Cruz, and D. Kisailus, "Electrocatalytic N-doped graphitic nanofiber – metal/metal oxide nanoparticle composites," *Small*, vol. 14, no. 11, article 1703459, 2018.

[5] Y. Li and Y. Zheng, "Preparation and electrochemical properties of polyaniline/reduced graphene oxide composites," *Journal of Applied Polymer Science*, vol. 135, no. 16, article 46103, 2018.

[6] Y. Li, J. Ji, Y. Wang, R. Li, and W. H. Zhong, "Soy protein-treated nanofillers creating adaptive interfaces in nanocomposites with effectively improved conductivity," *Journal of Materials Science*, vol. 53, pp. 8653–8665, 2018.

[7] H. Wang, Y. Jiang, and A. Manthiram, "Long cycle life, low self-discharge sodium–selenium batteries with high selenium loading and suppressed polyselenide shuttling," *Advanced Energy Materials*, vol. 8, no. 7, article 1701953, 2018.

[8] S. Yao, J. Cui, J. Huang et al., "Rational assembly of hollow microporous carbon spheres as P hosts for long-life sodium-ion batteries," *Advanced Energy Materials*, vol. 8, no. 7, article 1702267, 2018.

[9] K. Wu, Y. Hu, Z. Shen et al., "Highly efficient and green fabrication of a modified C nanofiber interlayer for high-performance Li–S batteries," *Journal of Materials Chemistry A*, vol. 6, no. 6, pp. 2693–2699, 2018.

[10] X. Song, S. Wang, G. Chen et al., "Fe-N-doped carbon nanofiber and graphene modified separator for lithium-sulfur batteries," *Chemical Engineering Journal*, vol. 333, pp. 564–571, 2018.

[11] L. Zhu, L. You, P. Zhu, X. Shen, L. Yang, and K. Xiao, "High performance lithium–sulfur batteries with a sustainable and environmentally friendly carbon aerogel modified separator," *ACS Sustainable Chemistry & Engineering*, vol. 6, no. 1, pp. 248–257, 2018.

[12] Y. Zhao, Y. Liu, C. Tong et al., "Flexible lignin-derived electrospun carbon nanofiber mats as a highly efficient and binder-free counter electrode for dye-sensitized solar cells," *Journal of Materials Science*, vol. 53, no. 10, pp. 7637–7647, 2018.

[13] F. J. García-Mateos, R. Berenguer, M. J. Valero-Romero, J. Rodríguez-Mirasol, and T. Cordero, "Phosphorus functionalization for the rapid preparation of highly nanoporous submicron-diameter carbon fibers by electrospinning of lignin solutions," *Journal of Materials Chemistry A*, vol. 6, no. 3, pp. 1219–1233, 2018.

[14] W. Fang, S. Yang, T. Q. Yuan, A. Charlton, and R. C. Sun, "Effects of various surfactants on alkali lignin electrospinning ability and spun fibers," *Industrial & Engineering Chemistry Research*, vol. 56, no. 34, pp. 9551–9559, 2017.

[15] T. Grothe, D. Wehlage, T. Böhm, A. Remche, and A. Ehrmann, "Needleless electrospinning of PAN nanofibre mats," *Tekstilec*, vol. 60, no. 4, pp. 290–295, 2017.

[16] L. Sabantina, J. R. Mirasol, T. Cordero, K. Finsterbusch, and A. Ehrmann, "Investigation of needleless electrospun PAN nanofiber mats," in *AIP Conference Proceedings*, vol. 1952, article 020085, Secunderabad, India, 2018.

[17] C. Liu and K. Lafdi, "Fabrication and characterization of carbon nanofibers from polyacrylonitrile/pitch blends,"

[18] Y. W. Ju and G. Y. Oh, "Behavior of toluene adsorption on activated carbon nanofibers prepared by electrospinning of a polyacrylonitrile-cellulose acetate blending solution," *Korean Journal of Chemical Engineering*, vol. 34, no. 10, pp. 2731–2737, 2017.

[19] D. Wehlage, R. Böttjer, T. Grothe, and A. Ehrmann, "Electro-spinning water-soluble/insoluble polymer blends," *AIMS Materials Science*, vol. 5, no. 2, pp. 190–200, 2018.

[20] L. Yu and L. Gu, "Effects of microstructure, crosslinking density, temperature and exterior load on dynamic pH-response of hydrolyzed polyacrylonitrile-*blend*-gelatin hydro-gel fibers," *European Polymer Journal*, vol. 45, no. 6, pp. 1706–1715, 2009.

[21] A. Bigi, G. Cojazzi, S. Panzavolta, K. Rubini, and N. Roveri, "Mechanical and thermal properties of gelatin films at different degrees of glutaraldehyde crosslinking," *Biomaterials*, vol. 22, no. 8, pp. 763–768, 2001.

[22] E. Cipriani, M. Zanetti, P. Bracco, V. Brunella, M. P. Luda, and L. Costa, "Crosslinking and carbonization processes in PAN films and nanofibers," *Polymer Degradation and Stability*, vol. 123, pp. 178–188, 2016.

[23] K. Mólnar, B. Szolnoki, A. Toldy, and L. M. Vas, "Thermochemical stabilization and analysis of continuously electrospun nanofibers," *Journal of Thermal Analysis and Calorimetry*, vol. 117, no. 3, pp. 1123–1135, 2014.

[24] G. S. Al-Saidi, A. Al-Alawi, M. S. Rahman, and N. Guizani, "Fourier transform infrared (FTIR) spectroscopic study of extracted gelatin from shaari (*Lithrinus microdon*) skin: effects of extraction conditions," *International Food Research Journal*, vol. 19, pp. 1167–1173, 2012.

[25] L. Sabantina, M. Rodríguez-Cano, M. Klöcker et al., "Fixing PAN nanofiber mats during stabilization for carbonization and creating novel metal/carbon composites," *Polymers*, vol. 10, no. 7, p. 735, 2018.

[26] C. Peña, K. de la Caba, A. Eceiza, R. Ruseckaite, and I. Mondragon, "Enhancing water repellence and mechanical properties of gelatin films by tannin addition," *Bioresource Technology*, vol. 101, no. 17, pp. 6836–6842, 2010.

[27] S. Gautam, A. K. Dinda, and N. C. Mishra, "Fabrication and characterization of PCL/gelatin composite nanofibrous scaffold for tissue engineering applications by electrospinning method," *Materials Science and Engineering: C*, vol. 33, no. 3, pp. 1228–1235, 2013.

[28] S. N. Arshad, M. Naraghi, and I. Chasiotis, "Strong carbon nanofibers from electrospun polyacrylonitrile," *Carbon*, vol. 49, no. 5, pp. 1710–1719, 2011.

[29] C.-W. Park, W.-J. Youe, S.-Y. Han, Y. S. Kim, and S.-H. Lee, "Characteristics of carbon nanofibers produced from lignin/polyacrylonitrile (PAN)/kraft lignin-g-PAN copolymer blends electrospun nanofibers," *Holzforschung*, vol. 71, no. 9, pp. 743–750, 2017.

*Journal of Applied Polymer Science*, vol. 134, no. 42, article 45388, 2017.

XXXVIII

*polymers*

MDPI

*Communication*

# Fixing PAN Nanofiber Mats during Stabilization for Carbonization and Creating Novel Metal/Carbon Composites

Lilia Sabantina [1,2], Miguel Ángel Rodríguez-Cano [2], Michaela Klöcker [1], Francisco José García-Mateos [2], Juan José Ternero-Hidalgo [2], Al Mamun [3], Friederike Beermann [1], Mona Schwakenberg [1], Anna-Lena Voigt [1], José Rodríguez-Mirasol [2], Tomás Cordero [2] and Andrea Ehrmann [1,*]

[1] Faculty of Engineering and Mathematics, Bielefeld University of Applied Sciences, 33619 Bielefeld, Germany; lilia.sabantina@fh-bielefeld.de (L.S.); michaela.kloecker@fh-bielefeld.de (M.K.); friederike.beermann@fh-bielefeld.de (F.B.); mona.schwakenberg@fh-bielefeld.de (M.S.); anna-lena.voigt@fh-bielefeld.de (A.-L.V.)

[2] Departamento de Ingeniería Química, Campus de Teatinos s/n, Universidad de Málaga, Andalucía Tech, 29010 Málaga, Spain; marodriguez@uma.es (M.Á.R.-C.); garciamateos@uma.es (F.J.G.-M.); ternerohidalgo@uma.es (J.J.T.-H.); mirasol@uma.es (J.R.-M.); cordero@uma.es (T.C.)

[3] Faculty of Textile and Clothing Technology, Niederrhein University of Applied Sciences, 41065 Mönchengladbach, Germany; mamun26th@gmail.com

* Correspondence: andrea.ehrmann@fh-bielefeld.de; Tel.: +49-521-1067-0254

check for updates

**Abstract:** Polyacrylonitrile (PAN) is one of the materials most often used for carbonization. PAN nanofiber mats, created by electrospinning, are an especially interesting source to gain carbon nanofibers. A well-known problem in this process is fixing the PAN nanofiber mats during the stabilization process which is necessary to avoid contraction of the fibers, correlated with an undesired increase in the diameter and undesired bending. Fixing this issue typically results in breaks in the nanofiber mats if the tension is too high, or it is not strong enough to keep the fibers as straight as in the original state. This article suggests a novel method to overcome this problem by electrospinning on an aluminum substrate on which the nanofiber mat adheres rigidly, stabilizing the composite and carbonizing afterwards either with or without the aluminum substrate to gain either a pure carbon nanofiber mat or a metal/carbon composite.

**Keywords:** polyacrylonitrile; PAN; nanofiber mat; electrospinning; stabilization; dimension stability; carbonization

## 1. Introduction

Electrospinning can be used to create nanofiber, e.g., from polyacrylonitrile (PAN) which is a typical precursor of carbon nanofibers [1–3]. Such carbon nanofibers can be applied, e.g., to improve the mechanical properties of plastic materials by forming a composite with a polymer or a resin, the electrical properties of batteries and super-capacitors, etc. [4–7].

To gain carbon nanofibers, the first step is a stabilization process which is typically performed in air, resulting in cyclization and thermally stable aromatic ladder polymer formation [8] which increases the chemical and mechanical stability of the nanofiber mat and is essential before the carbonization step. The whole stabilization process also includes dehydrogenation, aromatization, oxidation, and crosslinking [9–11].

40. Yate, L.; Caicedo, J.C.; Hurtado Macias, A.; Espinoza-Beltrán, F.J.; Zambrano, G. Composition and mechanical properties of AlC, AlN and AlCN thin films obtained by r.f. magnetron sputtering. *Surf. Coat. Technol.* **2009**, *203*, 1904–1907. [CrossRef]

41. Ohsaki, T.; Yoshida, M.; Fukube, Y.; Nakamura, K. The properties of carbon fiber reinforced aluminum composites formed by the ion-plating process and vacuum hot pressing. *Thin Solid Films* **1977**, *45*, 563–568. [CrossRef]

42. Akbarzadeh, E.; Picas Barrachina, J.A.; Puig, M.B. Thixomixing as Novel Method for Fabrication Aluminum Composite with Carbon and Alumina Fibers. *Int. J. Chem. Mol. Nucl. Mater. Metall. Eng.* **2015**, *9*, 822–826.

XL

## DECLARATION

I hereby certify that this material, which I now submit for assessment on the program of study leading to the award of PhD,. is entirely my own work, that I have exercised reasonable care to ensure that the work is original, and does not to the best of my knowledge breach any law of copyright, and has not been taken from the work of others save and to the extent that such work has been cited and acknowledged within the text of my work.

*L. Sabantina*

Málaga,  November 2018

Lilia Sabantina